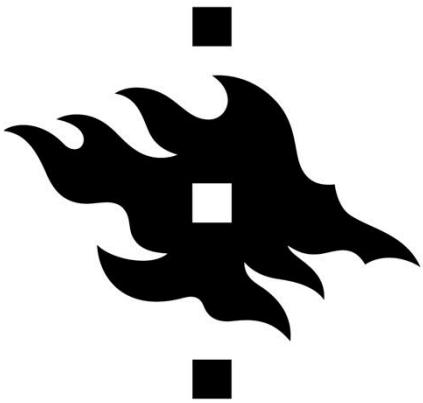

HELSINGIN YLIOPISTO
HELSINGFORS UNIVERSITET
UNIVERSITY OF HELSINKI

Photocatalytic N-Arylation of 3-Substituted Pyrrolidines and Comparison with Traditional Methods

Solja Säde

Master's thesis

University of Helsinki

Department of Chemistry

February 2021

HELSINGIN YLIOPISTO
HELSINGFORS UNIVERSITET
UNIVERSITY OF HELSINKI

MATEMAATTIS-LUONNONTIETEELLINEN TIEDEKUNTA
MATEMATISK-NATURVETENSKAPLIGA FAKULTETEN
FACULTY OF SCIENCE

Tiedekunta – Fakultet – Faculty	Koulutusohjelma – Utbildningsprogram – Degree programme
Faculty of Science	Master's Programme in Chemistry and Molecular Sciences

Opintosuunta – Studieinrikting – Study track

Organic chemistry

Tekijä – Författare – Author

Solja Säde

Työn nimi – Arbetets titel – Title

Photocatalytic N-Arylation of 3-Substituted Pyrrolidines and Comparison with Traditional Methods

Työn laji – Arbetets art – Level	Aika – Datum – Month and year	Sivumäärä – Sidoantal – Number of pages
Master's thesis	February 2021	110

Tiivistelmä – Referat – Abstract

Photocatalytic reactions utilize energy harnessed from light for the activation of a catalyst. In photoredox catalysis, an excited photocatalyst can take part in redox reactions with a substrate. The most common photocatalysts could be divided into three classes: metal catalysts, organic dyes, and heterogeneous semiconductors. These catalysts are often employed with a transition metal dual catalyst. The dual catalyst enables the cross-coupling of substrates, and the photocatalyst oxidizes or reduces the dual catalyst. Photocatalytic reactions can offer a milder alternative for the traditional C-N coupling reactions.

In the literature review section, the photocatalytic N-arylation of pyrrolidines was examined. The review found that pyrrolidines were successfully N-arylated with all of the catalyst types, and multiple variations on the substituents on the aryl halide. In the majority of the research, electron withdrawing groups (EWG) as substituents enhanced product yields, but electron donating groups (EDG) decreased yields. In an organic dye catalysed reaction, the effects of the substituents were opposite. In addition, the photocatalytic reactions were compared with traditional C-N coupling reactions, such as the Buchwald-Hartwig reaction, Ullmann-type reactions nucleophilic aromatic substitution and the Chan-Lam reaction. These reactions often had harsh reaction conditions.

The photocatalytic N-arylation of 3-substituted pyrrolidines was examined in the experimental part of this thesis. The objectives of this study were to investigate the use of photoredox methodologies for the C-N coupling of 3-substituted pyrrolidines to arenes and examine the scope and limitations of the reaction and the effects of substituents. In addition, the aim was to optimize the reaction conditions for multiple parameters and for each product separately, apply the reaction on a flow chemistry appliance, and execute scale-up reactions on both photoreactors. The study found 3-substituted pyrrolidines to be successfully coupled with aryl halides with great variation in the substituents of both starting materials. With optimization, the reactions with lower product yields were able to be improved significantly. The reaction was successfully upscaled, but the adaptation on the flow reactor requires further optimization. Photocatalytic C-N coupling reactions offer a promising alternative for traditional reactions.

Avainsanat – Nyckelord – Keywords

Photocatalysis, Photoredox catalysis, C-N coupling, N-arylation, photochemistry, pyrrolidine

Säilytyspaikka – Förvaringställe – Where deposited

HELDA - Digital Repository of the University of Helsinki

Muita tietoja – Övriga uppgifter – Additional information

TABLE OF CONTENTS

ACKNOWLEDGEMENTS

I wish to express my appreciation for the Orion Corporation for the opportunity to conduct my master's thesis research in their facilities and under their guidance. I am especially grateful for all the help and knowledge received from my instructor, Pekka Pietikäinen, PhD. His enthusiasm inspired me, and I thoroughly enjoyed working with him. In addition, I want to thank the staff of the Medicine Design function for their endless readiness to instruct me when needed, and the company and support they offered during my time at Orion.

I highly appreciate the guidance and valuable insights my supervisor Professor Timo Repo from the University of Helsinki gave me. He was encouraging and understanding, and he directed me on the right path with my thesis when I had doubts.

Furthermore, I want to thank my family and friends for their support and patience, and Eerika Haajanen for spell checking my thesis even though it was boring.

LIST OF ABBREVIATIONS

PC	Photocatalyst
SET	Single electron transfer
EnT	Energy transfer
MLCT	Metal to ligand charge transfer
HOMO	Highest occupied molecular orbital
LUMO	Lowest unoccupied molecular orbital
ISC	Intersystem crossing
NCS	*N*-chlorosuccinimide
PET	Photoinduced electron transfer
VB	Valence band
CB	Conduction band
DABCO	1,4-Diazabicyclo[2.2.2]octane
DBU	1,8-Diazabicyclo[5.4.0]undec-7-ene
DMA	Dimethylacetamide
ACN	Acetonitrile
THF	Tetrahydrofuran
DCM	Dichloromethane
PBI	Perylene bisimide
NP	Nanoparticle
HPB	Hexaphenylbenzene
DMSO	Dimethyl sulfoxide
CSS	Central switching station
EWG	Electron withdrawing group
EDG	Electron donating group
NMR	Nuclear magnetic resonance
MTBD	7-Methyl-1,5,7-triazabicyclo[4.4.0]dec-5-ene
LC-MS	Liquid chromatography-mass spectrometry

GC-MS	Gas chromatography-mass spectrometry
HSQC	Heteronuclear single quantum coherence
NP-FC	Normal-phase flash chromatography
RP-FC	Reversed-phase flash chromatography

LITERATURE REVIEW

1. Introduction

C–N bond formation plays an integral part in the pharmaceutical and agricultural industries, material science research, and synthesis of dyes.[1] The most frequently used reactions in medicinal chemistry are aminations[2], and therefore new and improved reaction alternatives are always welcome. Although classical C–N couplings, such as the Buchwald-Hartwig, Ullmann, S_NAr and Chan-Lam reactions, have been developed to milder conditions in recent years, still heating to approximately 100 °C for prolonged periods on time is usually necessary.[3,4] Due to the harsh reaction conditions of classical C–N coupling reactions, photoredox catalysis can offer complimentary solutions.

The easiest way to harness the photonic energy of visible light in a controlled manner is to use photocatalysts (PCs).[5] Photocatalyzed reactions occur commonly either through photoredox catalysis, which is based on single electron transfer (SET) events, or energy transfer (EnT), which is based on the transfer of the excitation.[6] Photoredox catalysis is the more frequently employed method, and therefore it will obtain a greater focus in this research.

There have been multiple variations on light-mediated catalysis in the past, but the rise of photoredox catalysis has been evident. Great progress has been achieved in the last ten years as the amount of studies has increased rapidly.[6] The use of visible light instead of higher energy radiation such as ultraviolet light prevents unwanted reactivity to other reagents than the photocatalyst. Visible light sources such as LED lights are also safer and thus preferable in laboratory use. Due to the use of a catalyst, photochemical reactions commonly require less reactive, and therefore typically less harmful compounds compared to traditional reactions.[7] In addition, photoredox catalyzed reactions are oftentimes conducted in room temperature. All of these benefits explain the rising interest in photoredox catalysis.

Photoredox chemistry enables demanding chemical transformations without harsh reaction conditions, especially combined with transition metal catalysis.[8] Transition metal catalysis without photocatalysis often requires strong reducing agents or bases, an inert gas atmosphere (Ar, N_2) to perform the reaction in, and high temperatures. Transition metal catalysis with

photocatalysis (aka metallaphotoredox catalysis) solves these problems, and succeeds in performing the needed reaction without demanding reaction conditions.[5]

In the development of a lead compound in the pharmaceutical industry, small heterocycles are often used for the exploration of the chemical space around the molecule[9-12] and therefore this research will attempt to broaden the knowledge surrounding pyrrolidines and their reactivity. The research of photocatalytic cross-coupling of aryl halides with cyclic aliphatic amines has increased simultaneously with the increase of research in photoredox catalysis. Majority of the studies utilized piperidine, and a minority also pyrrolidine. Substituent effects in aryl halides were examined, but only one study included a 3-substituted pyrrolidine to its substrate scope. A 3-substituted pyrrolidine will add value as a building block due to the possibility of continuing the reaction easily in both ends of the molecule.

This research will review the current methods of photocatalytic C–N cross-coupling of arenes and pyrrolidines and study the substrate scope and limitations of these reactions for 3-substituted pyrrolidines, as displayed in **Scheme 1**.

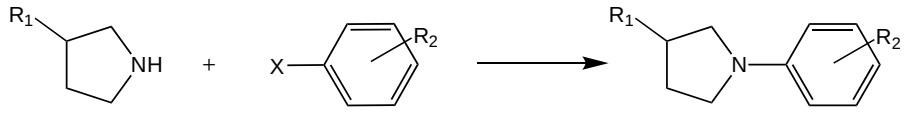

Scheme 1. *The N-arylation of a 3-substituted pyrrolidine.*

1.1. Photoexcitation of the catalyst

To gain the full benefits of photoredox catalysts, it is important to understand the theory behind their reactivity. This knowledge will help in the modification of ligands when adapting it to a specific reaction.

When a PC is radiated with visible light, it absorbs a photon, and a high energy excited state (*PC) is formed. The generally preferred wavelength for higher energy visible light is around 400-475 nm.[13] $Ru(bpy)_3Cl_2$ absorbs energy at a maximum of 452 nm, and a common light source for photochemical reactions is the blue LED light at 450 nm. Organic dyes generally absorb light on a lower energy level (Eosin Y at 522 nm) and therefore they can apply less energy to a catalyzed reaction than the transition metal PC can.[13]

After absorbing the photon, the PC is excited to a singlet excited state (S_1), as pictured in **Scheme 2**. In a common photocatalyst, which consists of a metal atom and polypyridyl ligands, an electron is moved to the π-orbital (system) of the ligand from the non-bonding metal-centered orbital. This is described as metal to ligand charge transfer (MLCT).[14] When MLCT occurs for a metal complex photocatalyst, an electron from the highest occupied molecular orbital (HOMO) of the metal transfers to the lowest unoccupied molecular orbital (LUMO) of the ligand.[15]

After the MLCT, intersystem crossing (ISC) can change the spin of the excited electron leading the singlet excited state to change to a triplet state (T_1). The triplet excited state is desirable due to its long lifetime.[13] A longer lifetime before deactivation increases the reactivity of the catalyst.

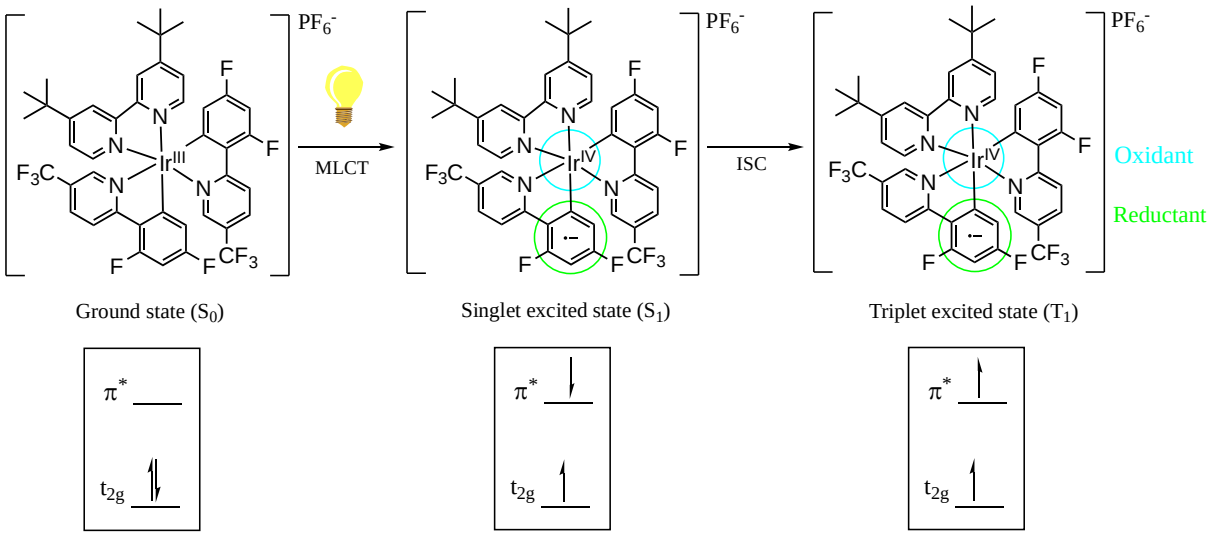

Scheme 2. *The photoexcitation of an iridium photocatalyst. This scheme is an adaptation from McAtee et al.*[16]

During the favorable triplet state the photocatalyst has oxidative and reductive potential due to the vacant metal center orbital and the high-energy electron that is located at the π* orbital of the ligand. The metal center has a low-energy vacancy open to accept an electron and therefore act as an oxidant. The ligand has a high-energy electron, which it can donate, and therefore act as a reductant.[14]

In MLCT in Ir^{3+} and Ru^{3+} ground state complexes, the metal center usually oxidizes, and the ligand is reduced. Therefore, the combinations of metals and ligands affect the reduction potentials, and the potentials can be adjusted by varying combinations. The ability for the metal to oxidize depends on the properties of the ligand, especially on the electronegativity of it. If the ligand is more electron donating, the metal will oxidize easier, because the electron density of the metal increases, and therefore it is easier for the metal to let go of an electron. This is regarding the oxidation which occurs in the MLCT. The oxidative power of the catalyst towards other substrates increases when the ligand is more electron withdrawing due to the increased capability of the metal center to receive an electron from the substrate.[13]

1.2. Oxidative and reductive quenching cycles

Oxidative and reductive quenching cycles demonstrate how the photocatalyst interacts with other molecules. In an oxidative or reductive quenching cycle the PC can oxidize and reduce, and the order defines if the cycle is called oxidative or reductive. In an oxidative quenching cycle the PC is oxidized first, and in a reductive quenching cycle the PC is reduced first. The oxidative and reductive quenching cycles are opposite events.

A reductive quenching cycle begins with the light source exciting the PC, as displayed in **Scheme 3**. The excited PC ([cat]*) then interacts with a substrate, and the substrate oxidizes as the PC is reduced. The PC is then oxidized to its original state by another substrate. This substrate is reduced while the PC is oxidized.[7]

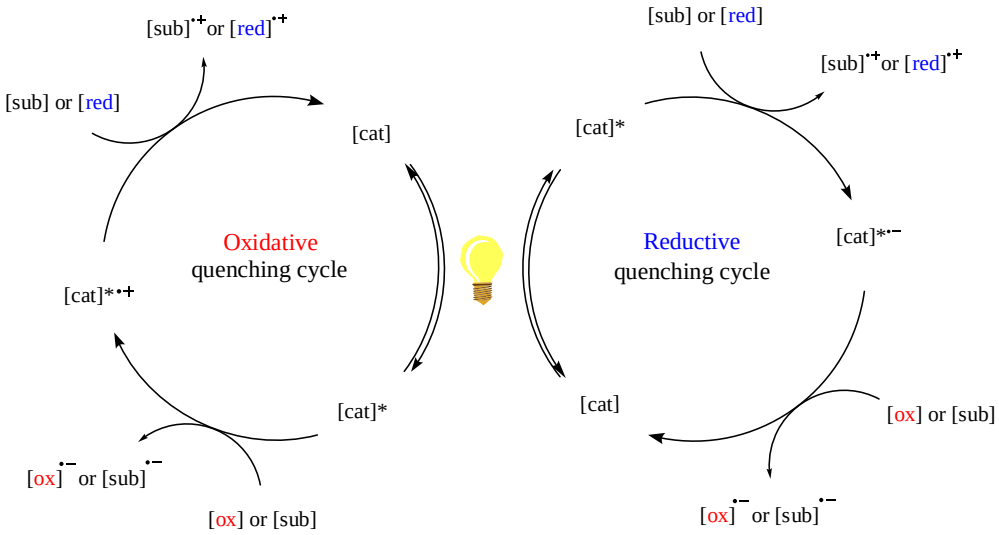

Scheme 3. *The reductive and oxidative quenching cycles of photocatalysts. This scheme is an adaptation from Bogdos et al.*[7]

The intention of the catalyst in the reaction is to oxidize or reduce the substrates it interacts with. If only one oxidation or reduction is needed for the reaction, a sacrificial substrate can be used for the second redox reaction. Sacrificial electron donors include amines and ascorbic acid, and sacrificial electron acceptors include for example peroxodisulfate and oxygen from air. The

sacrificial substrates can be used to acquire a ground state oxidation/reduction for the actual substrate.[17]

If the reaction does not require a sacrificial substrate as both of the redox reactions are needed for the completion of the main reaction, the reaction is redox-neutral.[17] In addition to redox-neutral, the reaction can be classified as net reductive or net oxidative according to the reaction of the substrate.[7]

Because the catalyst returns to its original oxidation state after the cycle, the catalyst is regenerated during the cycle, and therefore it can be used again in the same reaction. This decreases the amount of the catalyst that is necessary for the reaction, which is both economically and environmentally favourable.[14]

2. Photocatalysts

The most typically used photocatalysts include metal complexes, organic dyes and heterogeneous semiconductors. In **Figure 1**, common organic dyes and metal catalysts are depicted.

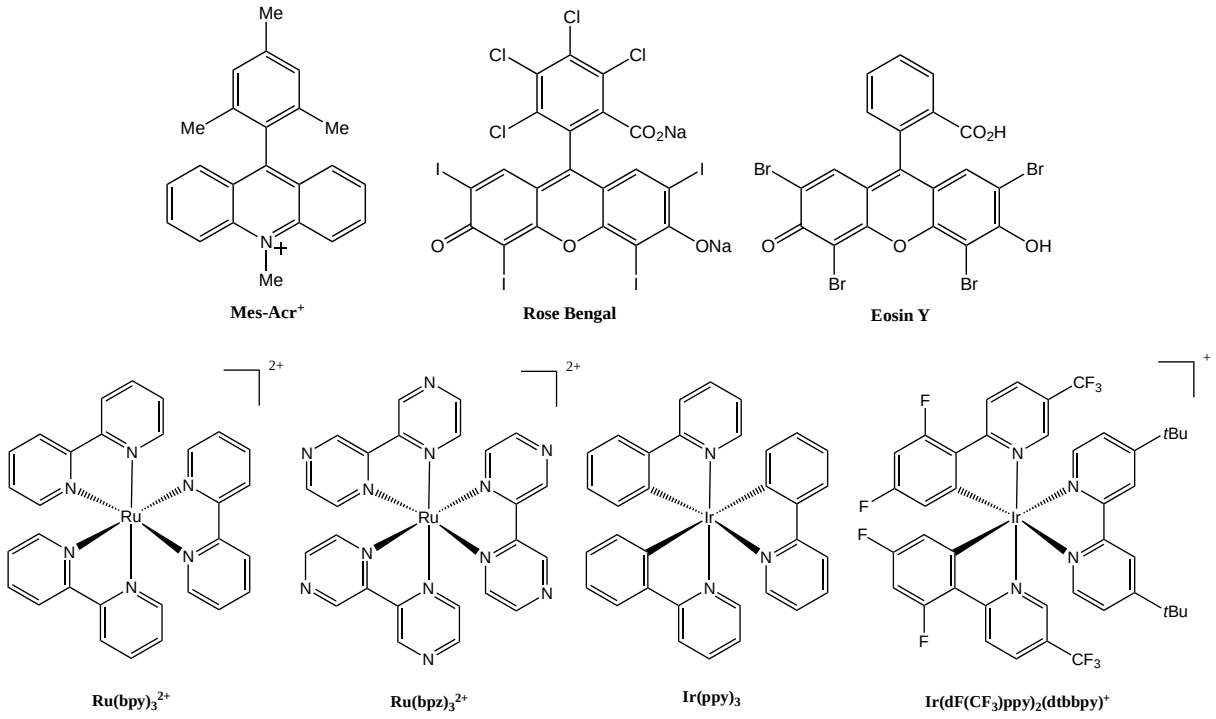

Figure 1. *Common organic dyes and transition metal polypyridyl photocatalysts.*

In addition, these photocatalysts are often employed with a transition metal dual catalyst. The most commonly used metal complexes are iridium and ruthenium polypyridyl complexes, and these catalysts have significantly broadened the scope of photocatalytic reactions in recent years.[6] In accordance with their name, organic dyes have previously been used as colorants.[18] Nowadays their usage has expanded far beyond their original purpose, for example to a broad variety of organic reaction catalysis. Heterogeneous semiconductors are utilized in the environmental treatment industry in a large scale, but they have also found their place in organic synthesis with photoredox catalysis.[19] Transition metal dual catalysts have been

employed with all of the forementioned photocatalyst types, and they have been proven to play an essential role in the development and research of new reactions.[6]

2.1. Metal complexes

Metal complexes, especially ruthenium and iridium polypyridyl complexes, are widely used due to their photostability, long excited lifetime, strong absorption and the possibility to change the properties of the catalyst by changing the ligand.[5] The most common transition metal complexes used for photocatalysis are ruthenium and iridium complexes. However, new research on other photoactive coordination compounds is currently being conducted. These metals include Cr, Mn, Fe, Co, Ni, Cu, Zn, Zr, Mo, W and Ce. The different parameters to vary are for example the ligand and the oxidation state of the metal.[20]

Although metal complexes are widely used, they are not free from disadvantages. The complexes can be toxic, difficult to remove during purification, and unsuitable for strongly acidic or basic reaction conditions.[7,21]

A metal complex catalyst was utilized in a C–N coupling reaction by Svejstrup *et al.* in 2017.[22] Compared to many other C–N coupling reactions, this methodology relies on the activation of nitrogen instead of a halogen leaving group. The proposed mechanistic alternatives are displayed in **Scheme 4**. An electron deficient O-aryl hydroxylamine **1** is protonated by a strong acid $HClO_4$ to generate an ammonium salt **2**. A SET event reduces **2** to form **3**, an electrophilic piperidinium radical, after which a carbon radical **4** is generated with polarized radical amination. The formation of **5**, the protonated product, has three different mechanistic proposals. **4** can close the photoredox cycle with an oxidative SET event or it can oxidize due to the electron relay cycle, a "dark" pathway. The third option is a propagative SET event with **2** for the formation of **5**. After the formation of the protonated product, a basic work-up was executed for the extraction of the product.[22] **Scheme 5** displays the reaction conditions and the pyrrolidine product.

The reaction utilized a ruthenium photocatalyst, which was established to be necessary. However, control experiments exposed the lack of need for the blue LED irradiation for the formation of the product. The radiation of the reaction increased yields consistently, but the existence of a "dark" pathway is proposed.[22] The hypothesis is that the catalyst can reduce the

substrate and act as a radical-chain initiator/electron-relay catalyst without visible-light excitation. A theory is postulated that **2** is a powerful oxidant after the protonation from **1**, and it might lead to the oxidation of ruthenium. This proposition was supported by UV/Vis spectroscopy studies exhibiting the oxidized Ru catalyst.

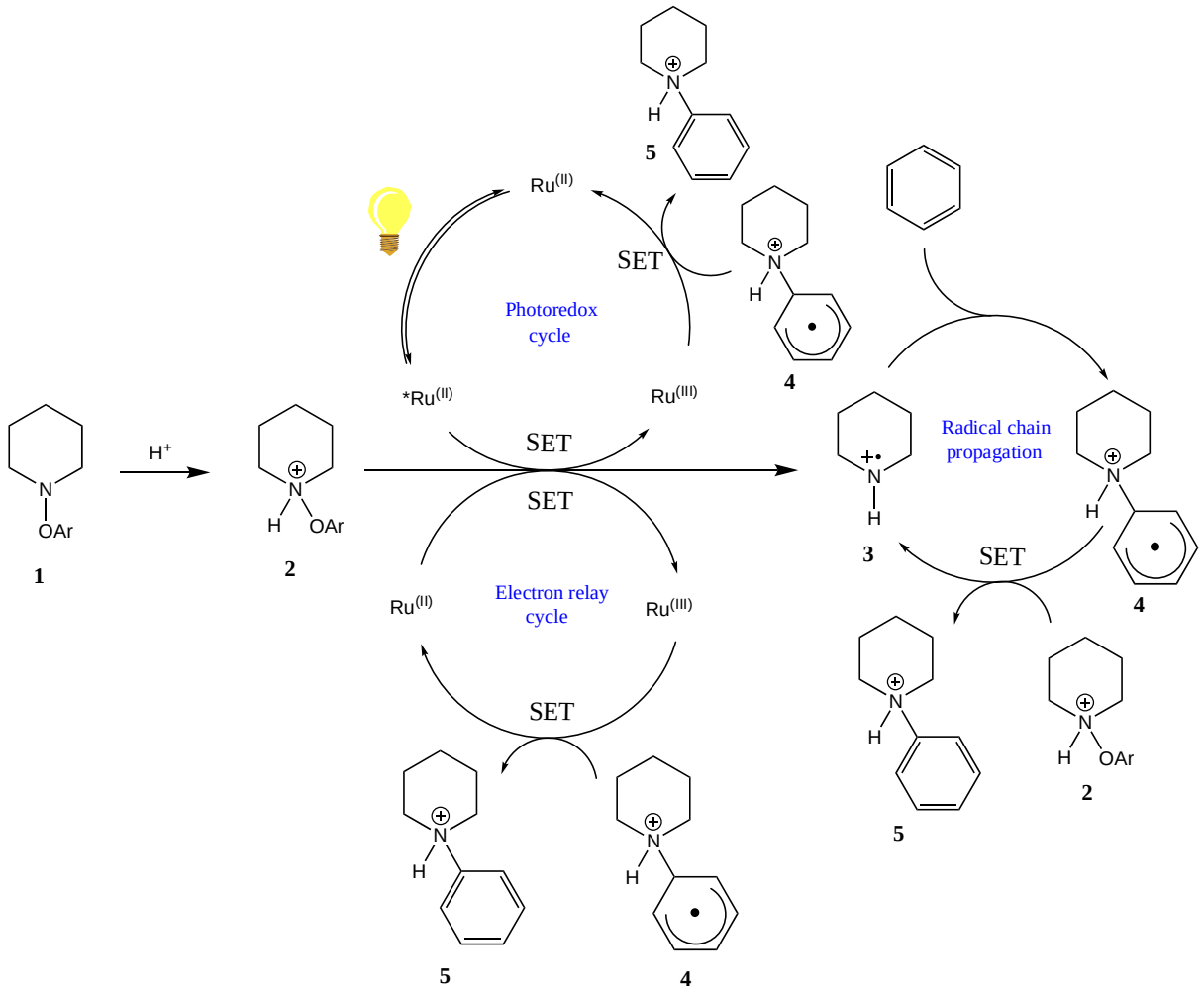

Scheme 4. *The proposition for mechanistic pathways for the formation of the product. This scheme is an adaptation from Svejstrup et al.*[22]

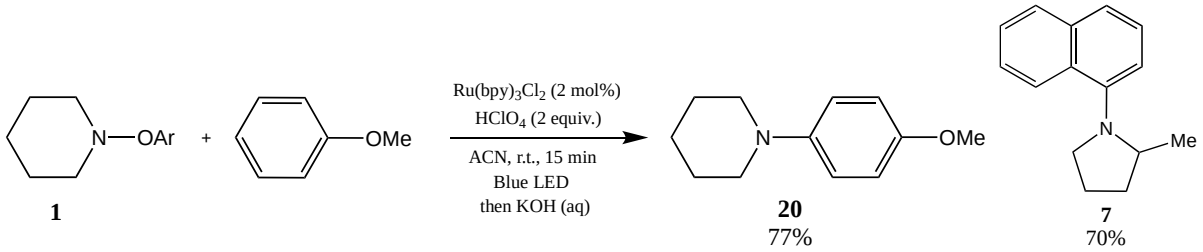

1 **20** 77% **7** 70%

Scheme 5. *The nitrogen radical process C–N coupling reaction and a pyrrolidine product **7**.*

In 2019 Ruffoni *et al.* developed a method for the amination of arenes.[12] This method, depicted in **Scheme** 6, uses chlorination of **8** with *N*-chlorosuccinimide (NCS) to obtain an *N*-chloroammonium species **9**, which is protonated to form **10** under acidic conditions. A SET event then reduces the species to produce a highly electrophilic aminium radical **11**. After this the arene is added by radical addition to the aminium radical to generate **12**. This addition is regioselective and works with a variety of different amines. The regioselectivity can be explained by the arene's natural nucleophilicity, which determines the site of the amination similarly as in electrophilic aromatic substitutions. Another SET event now oxidizes the species forming **13**, and the photocatalyst reduces to form its original state. After deprotonation, the desired aryl amine **14** is now formed. A basic work-up produced the final product **6**. For the verification of the reaction mechanism, cyclic voltammetry was used.

Similarly to the forementioned research by Svejstrup *et al.*, this methodology is based on the activation of nitrogen. In most classical and modern C–N cross-coupling reactions a halide or a pseudohalide is used to obtain an electrophilic site on the reacting arene. This reaction pathway was suppressed by Ruffoni *et al.* by creating acidic conditions, and combining it with the use of a PC, and therefore a radical process proceeded. These conditions are displayed in **Scheme 7**.

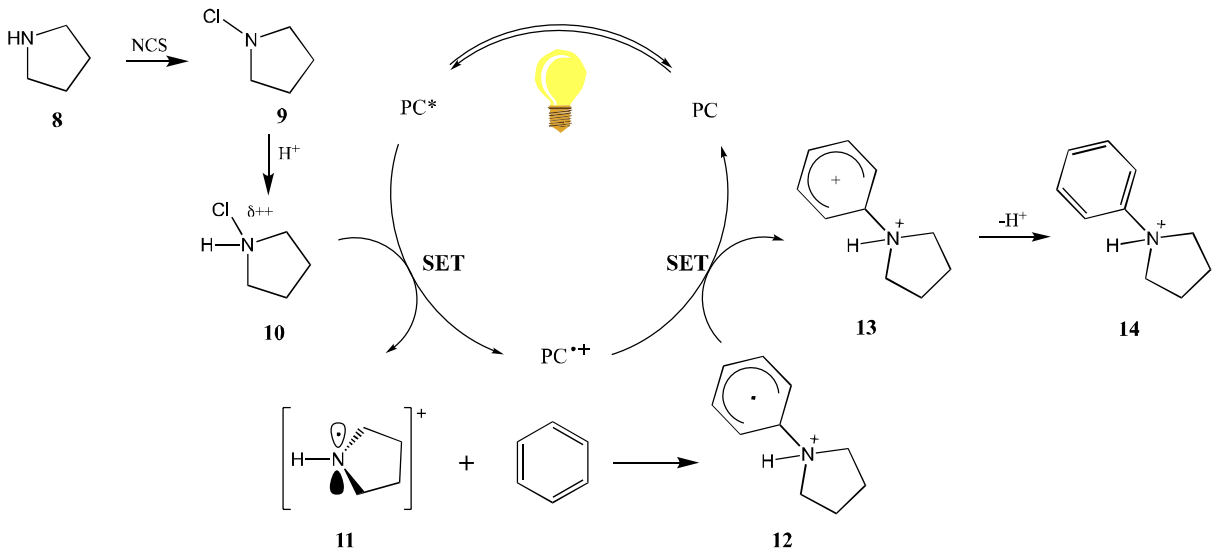

Scheme 6. *The mechanistic pathway proposal for an NCS assisted C–N coupling. This scheme is an adaptation from Ruffoni et al.*[12]

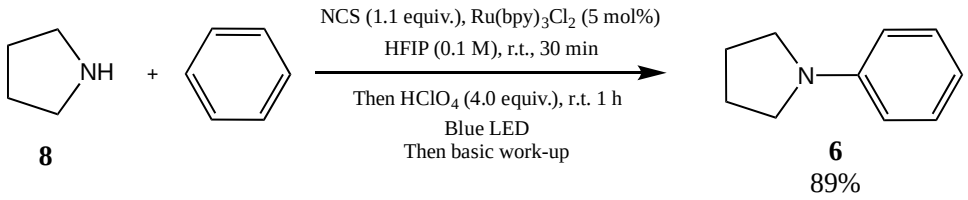

Scheme 7.*The synthesis of 1-phenylpyrrolidine with a ruthenium photocatalyst.*

2.2. Transition metal dual catalysis

In 2007, the first use of visible light, a photocatalyst and a transition metal catalyst was executed, when Osawa *et al.* combined visible light with a ruthenium photocatalyst and the Sonogashira reaction, which uses a palladium catalyst.[23] Traditionally C–N coupling reactions have mostly been based on transition metal catalysis. Palladium and copper catalysts have been represented in multiple reactions, but other metals also have their variation on this topic. However, these reactions often require a prolonged reaction time with an elevated temperature, and photoredox catalysis can be utilized to avoid these conditions.[5]

Photoredox catalysis and transition metal catalysis combined creates a dual catalytic process, which is called metallaphotoredox catalysis. Metallaphotoredox catalysis usually includes a cross-coupling reaction. In metallaphotoredox catalysis the cross-coupling reaction is responsible for the bond formation of the desired molecules, and the photocatalyst is responsible for the oxidation and reduction of the transition metal.[5]

Nickel is a common transition metal catalyst for metallaphotoredox catalysis. In a cross-coupling reaction nickel has a great capacity for oxidative addition, but a decreased capacity for reductive elimination. This can be modified with the help of a photocatalyst. In **Scheme 8**, a simplified mechanism for the dual catalysis reaction is presented. First, an aryl halide **29** is added to the Ni(II) complex by oxidative addition. The desired nucleophile **30** then replaces the halide in the complex, forming the complex **31**. In this complex Ni is at an oxidative state II and is relatively stable. The excited photocatalyst is reduced whilst oxidizing the Ni(II) complex to form a high-valent Ni(III). Due to this oxidation, the Ni complex is now less stable, and therefore more prone to go through reductive elimination, and form the desired product **33**. After this the Ni complex is left at an oxidation state of I, and the PC is its reduced form. A SET event then oxidizes the photocatalyst and reduces the Ni complex bringing the Ni complex and the photocatalyst to their starting states.[5]

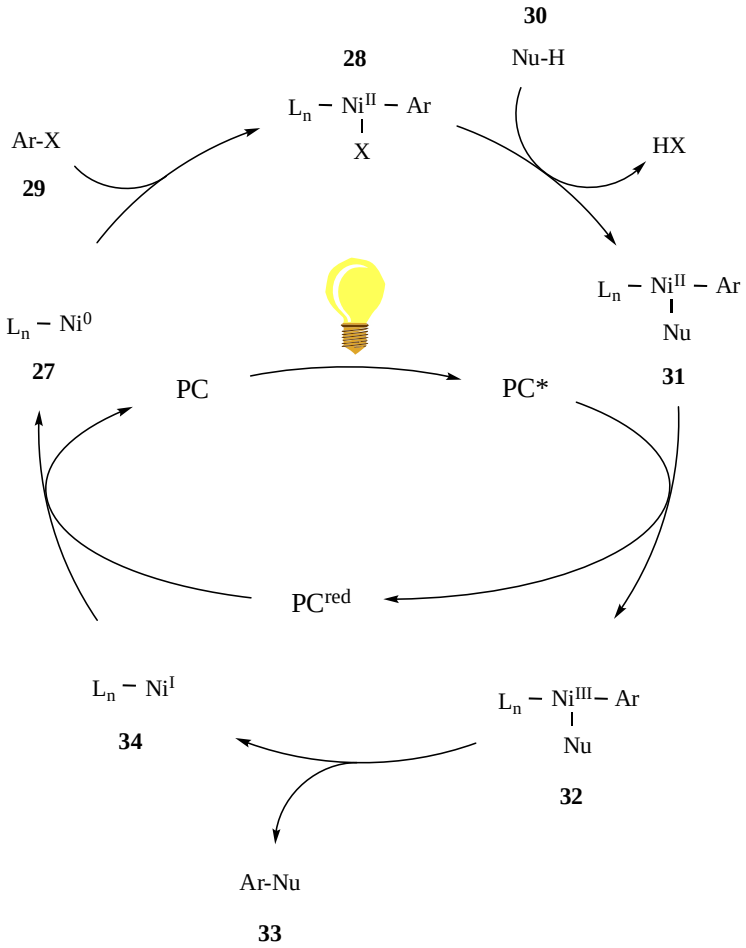

Scheme 8. *A mechanistic presentation of dual catalytic cycles: the transition metal catalytic cycle and the photocatalytic cycle combined. This scheme is an adaptation from Cavedon et al.*[5]

The destabilization of the Ni complex by the photocatalyst is a key factor which drives the reaction forward and through reductive elimination. Buchwald-Hartwig type reactions combated this issue by designing ligands that destabilized the Ni centre enough for the reaction to go through reductive elimination. Metallaphotoredox catalysis solves this issue without alteration of the ligands, but by changing the oxidation state of nickel.[6] Common Ni catalysts are carcinogenic and toxic, and lucrative alternatives include copper salts, which show promising results.[24] Corcoran *et al.* utilized Ni(II)-halide salts in a metallaphotoredox reaction successfully without ligands.[25]

Because the two catalytic cycles are dependent on each other, the generation of large amounts of highly reactive species is hindered.[6] In addition, the lower temperatures and the absence of a strong separate oxidant enable the substrate scope to be broadened, and the tolerance for different functional groups to be enhanced.[14]

Copper and palladium photocatalyzed C–N coupling reactions have been shown to work sufficiently[26,27], and the Chan-Lam reaction has been enhanced by photocatalysis. Its substrate scope has been expanded and efficiency increased. In these studies it was hypothesized that the ability to access higher oxidation states for the metal (Cu(III) and Pd(III/IV)) was enhancing the C–N bond formation.[6]

In 2016 Corcoran *et al.* reported a metallaphotoredox catalysis methodology with a nickel(II)-halide salt as the transition metal catalyst[25]. They worked in collaboration with Merck laboratories, who had developed a testing mechanism to broaden the substrate scope; the chemistry informer plate.[14] The testing mechanism is essentially a screening method, and here used to test the photocatalytic reaction conditions at coupling amines with pharmaceutically important organic species. These reaction conditions, displayed in **Scheme 10** and **Figure 2**, have later proven to be very adaptable to a variety of reactions. The reaction mechanism in **Scheme 9** depicts the destabilization of the nickel center with the photocatalyst and the modification of the Ni oxidation state. Therefore, the need to design intricate ligands to the transition metal catalyst was unnecessary. The SET event enabled a facile reductive elimination.

Substituent effects in the arene were examined. Electron withdrawing groups displayed better turnover and yield for the reaction compared to electron donating groups. The amount of the catalyst was varied, and the disadvantage and hindrance caused by electron donating groups as substituents could be compensated by decreasing the amount of the photocatalyst to 0.002 mol% from the substrate amount.[25,28]

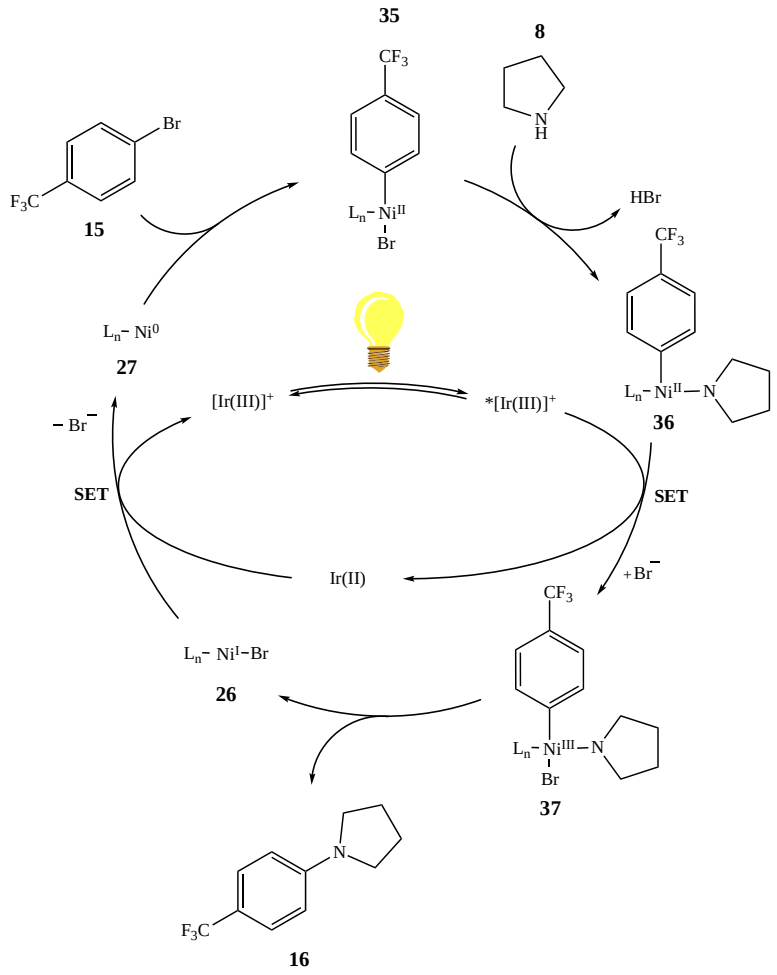

Scheme 9. *The reaction mechanism for a metallaphotoredox catalyzed arylation of pyrrolidine. This scheme is an adaptation from Corcoran et al.*[25]

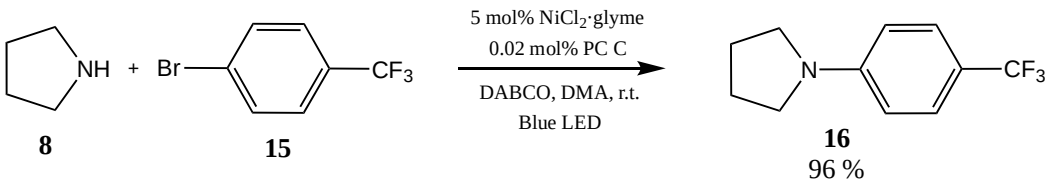

Scheme 10. *A dual catalyzed C–N coupling.*

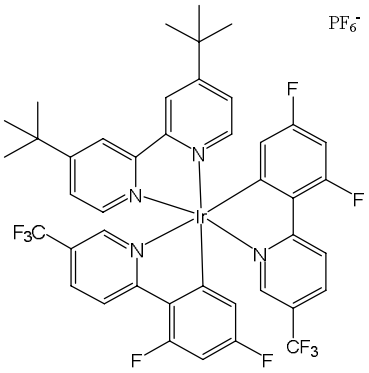

Figure 2. *Photocatalyst C: Ir[dF(CF$_3$)ppy]$_2$(dtbbpy)PF$_6$.*

2.3. Organic dyes

The majority of organic dyes, also known as organic photocatalysts, are aromatic and highly conjugated systems.[29] Based on reviewed literature, the most used organic dyes are Eosin Y, methylene blue, Rose Bengal and MesAcr, displayed in **Figure 3**. All of these, except MesAcr, are capable of both oxidation and reduction. MesAcr is only capable of strongly oxidizing other substrates.[7]

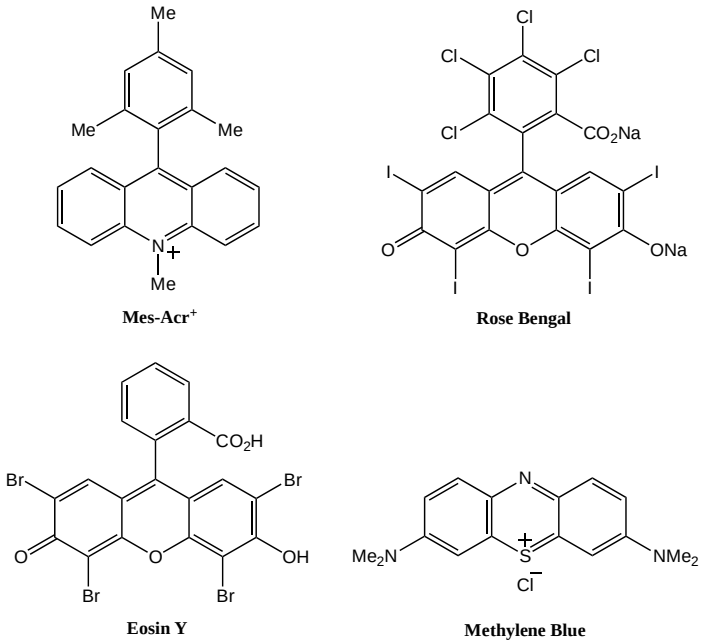

Figure 3. *The most common organic photocatalysts in the review literature.*

For a long period of time the ability of organic chromophores for photoinduced electron transfer (PET) has been recognized, but the research into photoredox chemistry has focused mainly on transition metal catalysts.[30] As the desire for environmentally friendly solutions rises, the interest for metal free catalysts increases the amount of research into organic catalysts.

In addition to the decreased toxicity, organic dyes are also easier to remove during purification, when compared with transition metal complexes.[7] However, organic dyes are less photostable[5], and their full potential has most likely not been reached due to the lack of research. The photophysical properties of for example Eosin Y change significantly when the pH of the reaction solution is changed. Some catalysts, such as acridinium, quinolinium and triarylpyryliums have low tolerance for certain nucleophiles including phosphates, acetates, amines and cyanide ions.[30-32]

Du *et al.* compared organic photoredox catalysts to more traditional metal catalysts.[8] They examined the electrochemical and photophysical properties of multiple catalysts, but the ones used for aryl amination were PC A: N,N-5,10di(2-naphthalene)-5,10-dihydrophenazine, and PC B: 3,7-(4-biphenyl)-1-naphthalene-10-phenoxazine, depicted in **Figure 4**. The reactions utilized dual catalysis with organic photoredox catalyst and a nickel catalyst. In the literature no arylation reactions of pyrrolidines were executed with organic dyes and without a transition metal dual catalyst.

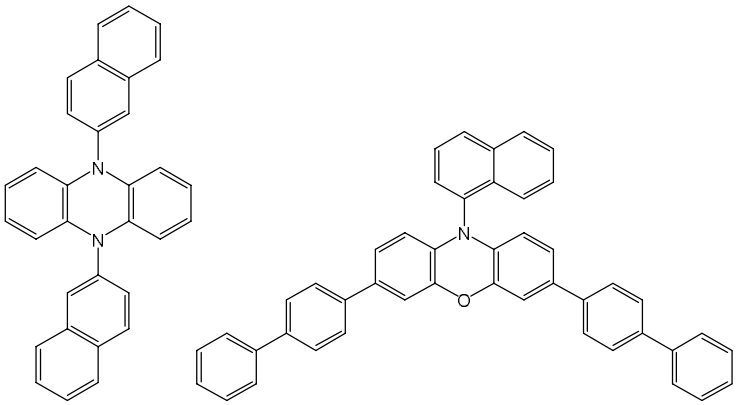

Figure 4. *Photocatalysts A and B. PC A: N,N-5,10di(2-naphthalene)-5,10-dihydrophenazine, and PC B: 3,7-(4-biphenyl)-1-naphthalene-10-phenoxazine.*

These photocatalysts gave the desired products, pyrrolidines coupled with arenes, in good to excellent yields. The research compared its organic dye reactions to the metallaphotoredox reaction by Corcoran *et al.* in 2016.[25] The reaction conditions utilized by Du *et al*., displayed in **Scheme 11**, are similar to those of Corcoran *et al.*, excluding the catalyst and its amount, the wavelength of the LED and the reaction time. The reactions were also able to be executed with radiation from sunlight without decreasing yields.

It is worthy to notice, that with these reaction conditions, the substitution of the arene has an opposite effect to that in the majority of articles with metal catalysts. An electron withdrawing group (EWG) in the *para*-position of the arene, e.g. CF_3, commonly increases the turnover of the reaction, and an electron donating group (EDG), e.g. MeO, commonly decreases the turnover. In this reaction the results, as displayed in **Figure** 5, are opposite. The catalysts A and B are reported to undergo an intramolecular charge transfer (CT), from the electron-rich core of phenazine as the donor, to the electron-poor *N*-substituent 2-naphtyl for PC A. A long-lived triplet excited state is also achieved, and it is competitive with iridium and ruthenium catalysts in lifetime. The authors do not postulate on the surprizing preferance of EDG substituents, but due to the similar reaction conditions with the research from Corcoran *et al.*, the catalyst could be a possible cause for this disparity.

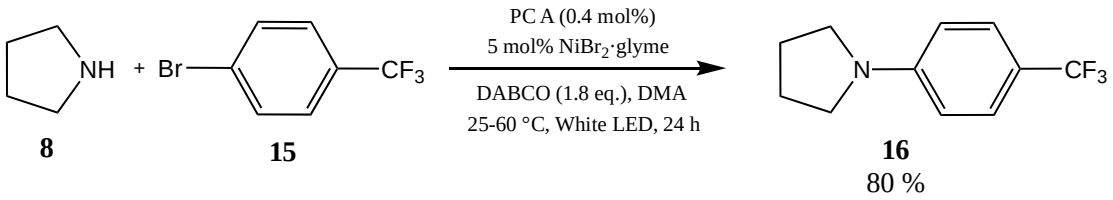

8 **15** **16** 80 %

Scheme 11. *The reaction scheme for an organic dye photocatalyzed reaction.*

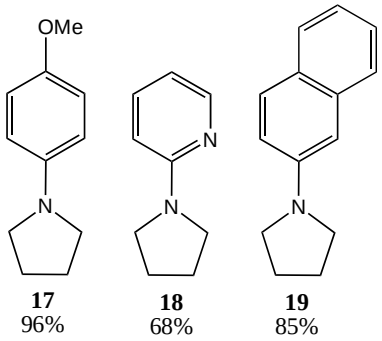

17 96% **18** 68% **19** 85%

Figure 5. *The pyrrolidine-including substrate scope of the reaction.*

2.4. Heterogeneous semiconductors

Heterogeneous semiconductors have been a powerful tool for the environmental treatment industry for a long time, but they have yet not gained the same appreciation in organic synthesis. Photodisinfection, solar-energy conversion and environmental cleaning are major applications of heterogeneous semiconductors. The most common heterogeneous semiconductors include CdS, TiO_2, ZnO, SnO_2, CdTe, WO_3 and $SrTiO_3$.[19]

The utilization of heterogeneous semiconductors in organic photoredox catalysis has increased due to its easy preparation, good recyclability and good stability.[5] Organic dyes and transition metal photocatalysts suffer from a lack of stability in strongly acidic or basic conditions, and their use is restricted with strong nucleophiles and electrophiles.[21]

Figure 6 displays the excitation of heterogeneous semiconductors. Upon light absorption by the heterogeneous semiconductor, an electron is excited from the valence band (VB) to the conduction band (CB) forming an electron-hole pair. When these electron-hole pairs reach the surface separately, redox centers for external substrates are formed. Reduction and oxidation

are possible for two different substrates (A and D in **Figure 6**). Upon collision of the electron and the hole, recombination occurs.[21]

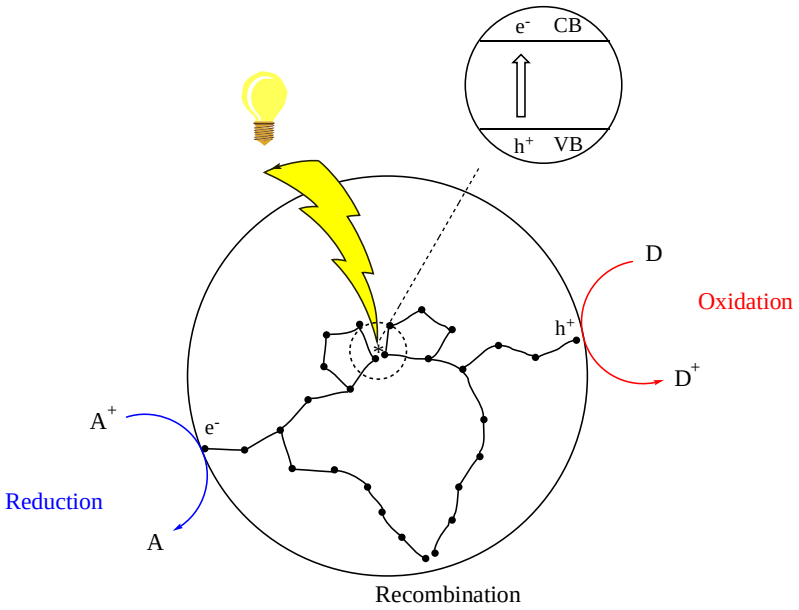

Figure 6. *Activation of a semiconductor catalyst via a visible light source and creation of an electron hole pair. D: electron donor, A: electron acceptor, e^-: electron, h^+: hole, VB: valence band, CB: conduction band. The movement of the electron hole pair is depicted with black dots and lines. This scheme is an adaptation from Friedmann et al.*[33]

Ghosh *et al.* published a new methodology for the use of mesoporous graphitic carbon nitride (mpg-CN) as an organic semiconductor in 2019.[21] The advantages of this method include the catalysts recyclability for at least four times when the catalyst is recovered by centrifugation, and the tolerance of strong nucleophiles and reactive radicals.

Here, mpg-CN was used together with a nickel dual catalyst in an amination reaction of an aryl halide as in **Scheme 12**. Four different pyrrolidine products, displayed in **Figure 7**, were reported with good to excellent yields. However, all of the products constituted of electron-poor arenes, and no results are represented to show applicability to electron rich arenes. A reaction executed with morpholine and bromobenzene yielded only 26 % of product, while similar reactions with electron withdrawing substituents, such as CO_2Et, COMe, CN and CF_3, yielded over 80 %.

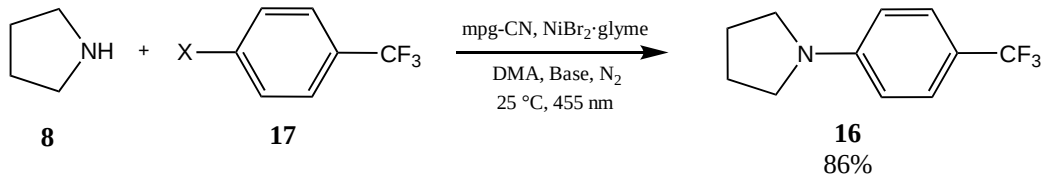

8 **17** **16** 86%

Scheme 12. *An mpg-CN catalyzed arylation of pyrrolidine.*

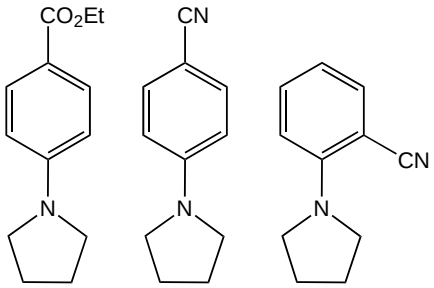

21 92% **22** 91% **22b** 84%

Figure 7. *The pyrrolidine-including substrate scope of the reaction.*

Liu *et al.* developed a heterogeneous semiconductor photoredox application combined with nickel dual catalyst in 2019.[34] Cadmium sulfide was used with $NiCl_2 \cdot 6\ H_2O$ for C–N and C–O coupling reactions. The optimized conditions were similar to previous ones in literature[25] excluding the catalyst, but a surprising deviance was found when it was noticed that 1,4-diazabicyclo[2.2.2]octane (DABCO) hindered the reaction completely. In addition, 1,8-diazabicyclo[5.4.0]undec-7-ene (DBU) and raising the temperature had a positive effect on the aryl bromide conversion. In addition, a variety of solvents were examined, and dimethyl acetamide (DMA) was discovered to be the most suitable, while acetonitrile (ACN) decreased yields, and tetrahydrofuran (THF), chloroform ($CHCl_3$) and dichloromethane (DCM) hindered the reaction.

A relatively broad range of substituents for the aryl halide were examined, and multiple primary and secondary amines were successfully used. However, it was observed that electron-neutral or electron-rich aryl halides did not generate the product. The reaction conditions and products are depicted in **Scheme 14** and **Figure 8**.

CdS is a cheap and readily available catalyst which can be recycled and reused up to ten times. The reaction conditions are mild, and scalability up to at least 20 mmol is possible. A

disadvantage compared to other photoredox reactions is that the reaction time is considerably longer; 24 h. In addition, with the contact of air, the reaction is completely hindered.

Scheme 13 represents the proposed mechanism for the dual catalytic reaction. **23** is generated after oxidative addition from **27**, and a ligand change forms the Ni(II) intermediate complex **24**. As the photocatalyst CdS is excited, an electron-hole pair is formed. The oxidizing holes in the VB take part in a SET event, which generates the oxidized Ni(III) complex **25**. This complex is less stable than **24**, and therefore it proceeds to reductive elimination, which generates the product. After this the resulting Ni(I) complex **26** is reduced by the electron in the CB of the catalyst, to form the Ni(0) catalyst **27** in its original state.[34]

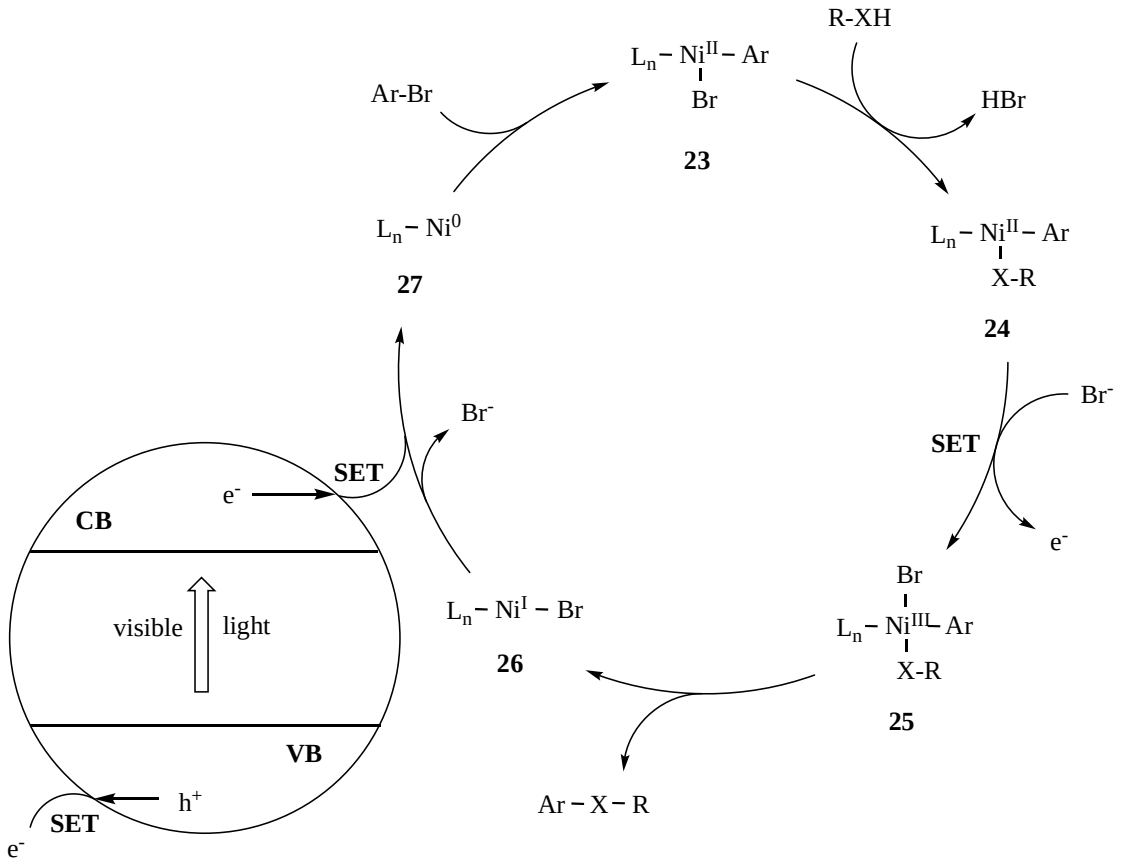

Scheme 13. *A mechanistic proposal for a cadmium sulfide catalyzed aryl amination. This scheme is an adaptation from Liu et al.[34]*

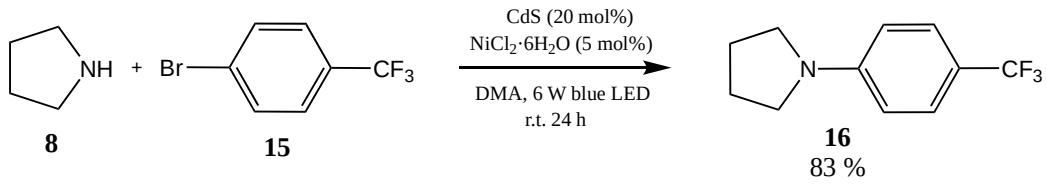

8 **15** **16**
83 %

Scheme 14. *A heterogeneous semoconductor photocatalyzed arylation of pyrrolidine.*

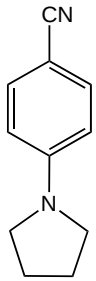

22
98%

Figure 8. *The pyrrolidine-including substrate scope of the reaction.*

3. Additional methodologies

3.1. Photocatalyst free reactions

A photoredox catalysis reaction without a supplementary photocatalyst was developed by Lim *et al.* in 2018.[35] This method utilized photoexcitation with a 365 nm LED of a nickel-amine complex that formed in the reaction. To examine the mechanism of the reaction, which is displayed in **Scheme 15**, density functional theory (DFT) calculations were employed. These calculations suggested a mechanism, where an amino radical is formed after the photoexcitation of the nickel-amine complex.

This reaction functions without the addition of an extra base, as the amine acts as the reagent, the base and a ligand in nickel-complexes. For this, the amine had to be added in larger quantities (3.5 equivalents). However, for aromatic amines an addition of quinuclidine was necessary. The advantages of this methodology include the absence of a photocatalyst and a base, room temperature conditions, and the tolerance for air. The removal of base can broaden the substrate scope. The reaction conditions for the pyrrolidine product are displayed in **Scheme 16**.

Aryl halides with para-positioned electron withdrawing substituents reacted considerably better than aryl halides with no substituents or electron donating substituents. In similar reaction conditions a nitrile substituent yielded 86% of product, when no substituent (hydrogen) yielded 53%, and methoxy 7%. Interestingly the results of the electron-neutral aryl bromides and electron-rich aryl bromides could be enhanced by changing the leaving group bromide to iodide. The previously mentioned reaction with no substitute and 53 % yield could be elevated to 66 %, and the use of 4-iodoanisole increased the yield to 26 %. Also in the case of pyridine the yield increased by 11 % when the halide was changed from bromide to iodide.[35] However, when the substituent was electron withdrawing, the replacement of bromide with iodide only declined the yield. 4-Bromobenzotrifluoride yielded 87 %, while 4-iodobenzotrifluoride yielded 70 %. A similar reaction with 4-chlorobenzotrifluoride was also conducted, but this reaction yielded only 18 % of product, and the reaction time increased from 3 hours to 15 hours.

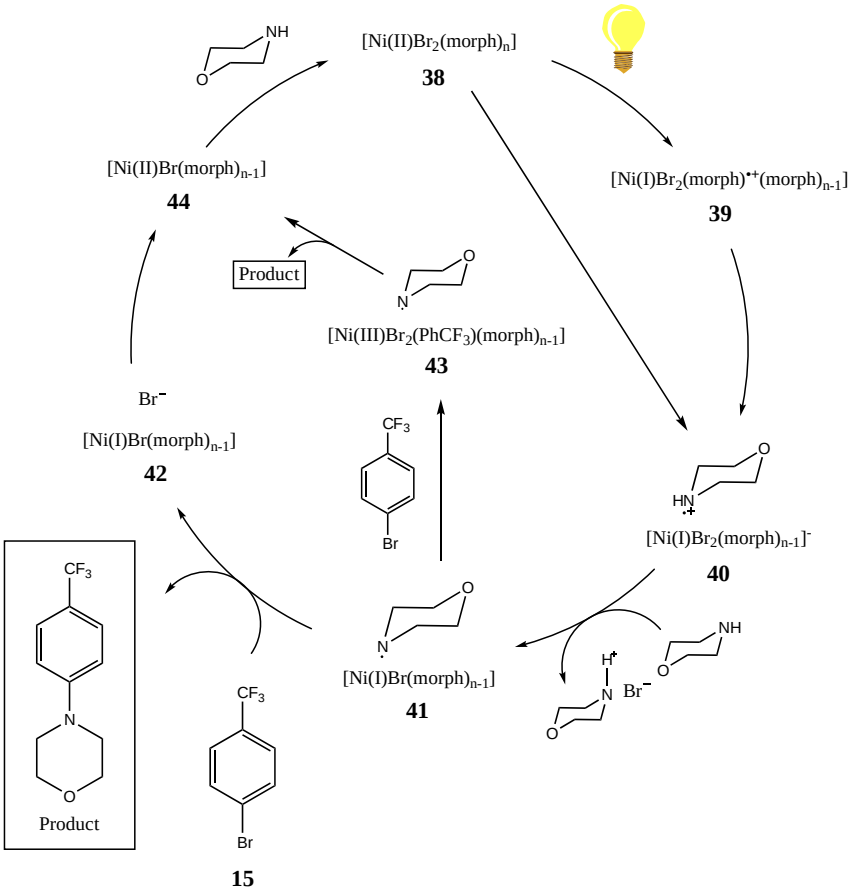

Scheme 15. *Proposed reaction mechanism for a morpholine product. Density functional calculations (DFT) were used for the determination of the reaction mechanism. This scheme is an adaptation from Lim et al.*[35]

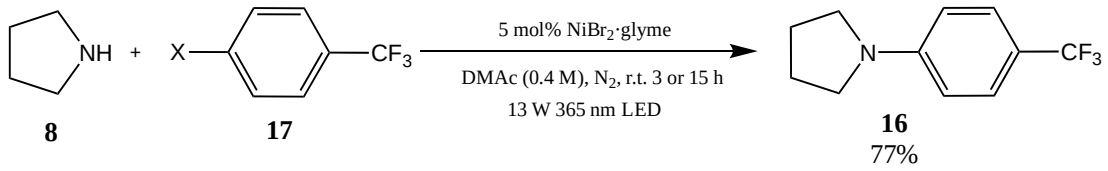

8 **17** **16**
77%

Scheme 16. *A light-induced C–N coupling reaction without a photocatalyst.*

3.2. Nanoparticle catalysts

In 2016 Kaur *et al.* developed a triazole-appended perylene bisimide (PBI) based supramolecular aggregates that functioned as the reactors for copper nanoparticle (CuNP) generation.[36] The PBI based derivative was oxidized to triazole *N*-oxide derivatives in a reduction process, where the CuNPs were generated *in situ.* These aggregates and CuNPs were found to easily harvest the energy of visible light together, and therefore act well as catalysts for the C(sp^2)–H alkylation and amination of arenes.

Compared to earlier studies[37-41] of the preparation of CuNPs, this method is advantageous due to it not requiring reducing agents, its reduced reaction time and a reusable catalyst. This reaction can also be favoured due to its mild conditions, depicted in **Scheme 17**, which include visible light irradiation, mixed aqueous media, no heating, and no need for inert conditions.[36]

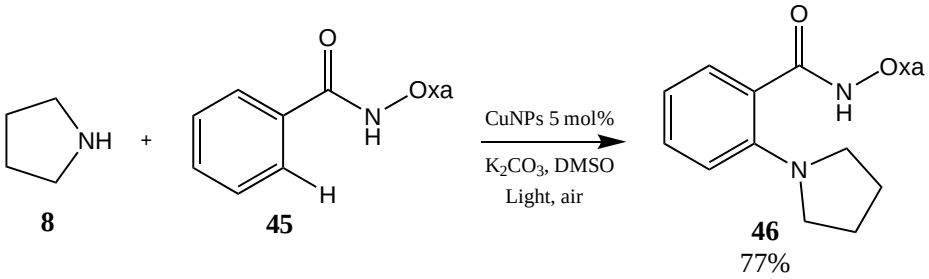

8 **45** **46**
77%

Scheme 17. *A copper nanoparticle catalyzed arylation of pyrrolidine.*

In 2018 Singh *et al.* developed a C–N coupling methodology based on ultrafine hybrid Cu_2O-Fe_2O_3 nanoparticles (NPs)[42]. An essential part of this methodology was the stabilization of the nanoparticles by hexaphenylbenzene (HPB) -based supramolecular assemblies. Due to the fact that this catalyst is recyclable as a “dip-strip”, and that this methodology does not require

heating, strong bases, inert atmosphere or strictly organic solvents, it is deemed more environmentally friendly and efficient. The reaction conditions and products are displayed in **Scheme 19** and **Figure 9**. An Ullmann-Goldberg type coupling can be excecuted in a greener way with this photoinduced NP catalysis.

A mechanism was proposed for the radical coupling reaction catalyzed by the Cu_2O-Fe_2O_3 nanoparticles, and it is displayed in **Scheme 18**.

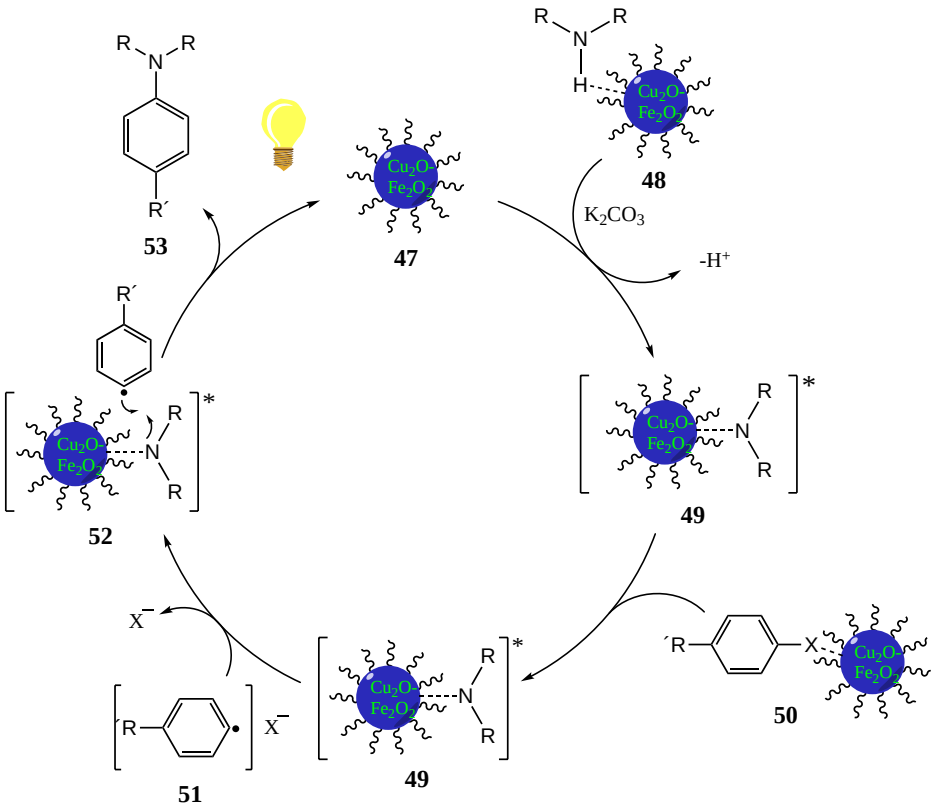

Scheme 18. *A proposed mechanism for a Cu_2O-Fe_2O_3 nanoparticle catalyzed C–N coupling. This scheme is an adaptation from Singh et al.*[42]

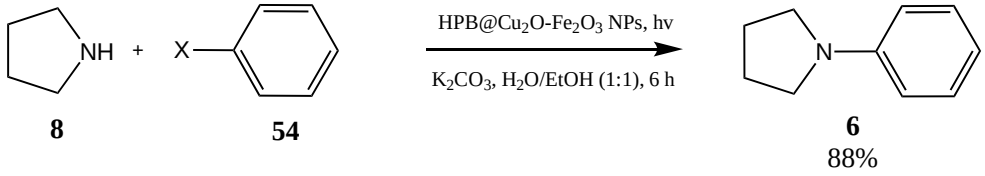

Scheme 19. *The reaction scheme for the synthesis of 1-phenylpyrrolidine.*

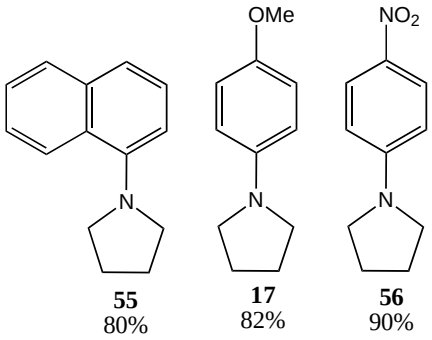

Figure 9. *The pyrrolidine-including substrate scope of the reaction.*

3.3. Flow chemistry photoredox reactions

Park *et al.* applied flow chemistry technology to the photocatalytic dual catalysis of aryl amines in 2020.[43] The reaction conditions were based on their previous article[25] with Corcoran and Merck laboratories, but they now optimized the conditions for flow. The reaction setup was applied to a Vapourtec E-series integrated flow chemistry appliance, which included a built-in UV-150 photochemical reactor. Several LED light sources were evaluated, but a 450 nm was selected after optimization.

The optimization of reaction conditions, displayed in **Scheme 20**, conducted on the flow system led to a few changes. When DMA was used as a solvent, precipitate formed, which clogged the flow system. Therefore, it was replaced with dimethyl sulfoxide (DMSO), which hindered the formation of salts and precipitate. $Ir[dF(CF)_3ppy]_2(dtbbpy)PF_6$ photocatalyst was used at first, and increases in product yield were noticed when the amount of catalyst was decreased (from 0.02 mol% to 0.002 mol% of the amount of the substrate). This was postulated to occur because of a decrease in competitive protodehalogenation.[43] However, experiments with $Ru(bpy)_3(PF_6)_2$ succeeded to gain higher yields. The ruthenium catalyst is favourable also because of its considerably lower price.

Reaction scale up succeeded significantly better in a flow system compared to batch reaction. An amination reaction conducted in 50 mmol scale yielded 41 % of product in a flow system, and 9 % in a batch reaction. Corresponding results in 10 mmol scale were 42 % for flow, and

32 % for a batch reaction. From these results it is evident that the scalability of the reaction is immensely greater in a flow system.

The pyrrolidine products are displayed in **Figure 10**. A slight hindrance in the reaction to electron-rich aryl halides can be noticed, but in a much lesser effect. A reaction of pyrrolidine with 4-bromobenzotrifluoride had a yield of 97 %, but a similar reaction with 4-bromoanisole yielded 80 % of product.[43] A difference in the reaction times must be pointed out, 10 min versus 60 min, but regardless this setup exceeds others when it comes to amination of electron-rich aryl halides.

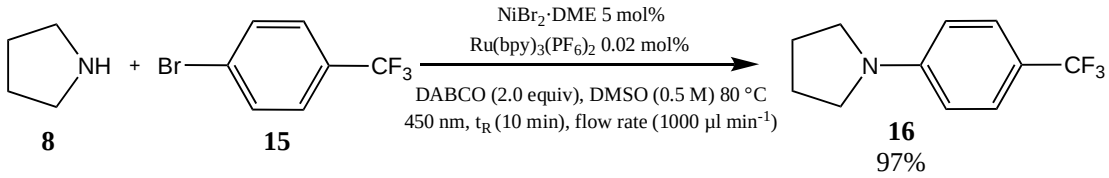

8 **15** **16** 97%

Scheme 20. *The arylation of pyrrolidine applied on a flow chemistry appliance.*

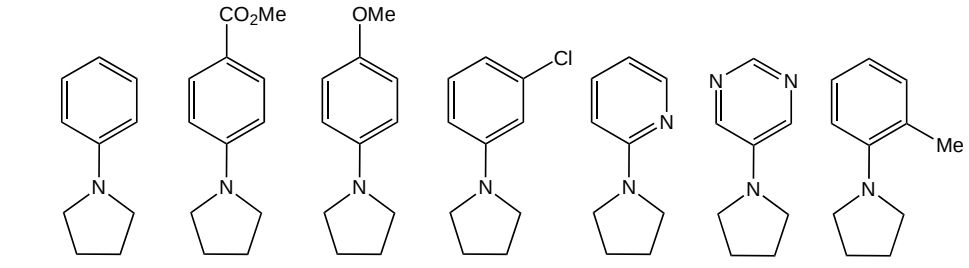

6 90% (30 min, 333 µl min^{-1}) **57** 87% **17** 80% (60 min, 167 µl min^{-1}) **59** 94% **18** 82% (30 min, 333 µl min^{-1}) **60** 98% **58** 75% (60 min, 167 µl min^{-1})

Figure 10. *The pyrrolidine-including substrate scope of the reaction.*

Harper *et al.* developed a photocatalytic flow chemistry reactor[44], and successfully upscaled the reaction previously presented by Corcoran *et al.*[25] Their continuous stirred tank reactor (CSTR) used high-power diode lasers and a continuous flow and achieved a kg/day pace in production. They observed that the intensity of the light source is proportional to the rate of the reaction universally, and therefore they experimented with multiple different powered light sources from 6 W to 26.1 W, and resulted in choosing the 26.1 W. The reaction conditions are depicted in **Scheme 21** and **Figure 11**.

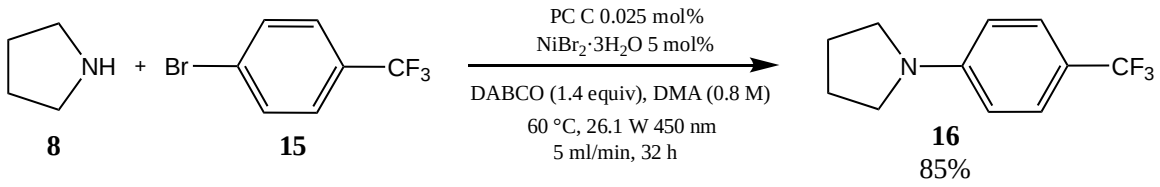

8 **15** **16**
85%

Scheme 21. *C–N coupling on a continuous stirred tank reactor.*

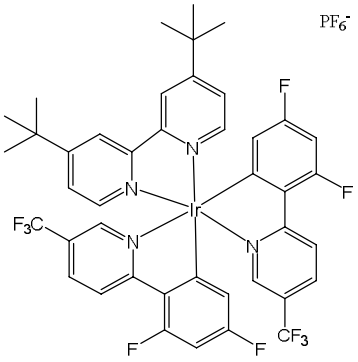

Figure 11. *Photocatalyst C: Ir[dF(CF$_3$)ppy]$_2$(dtbbpy)PF$_6$.*

Automated radial synthesis of small molecules was developed by Chatterjee *et al.* in 2020.[45] A 3-substituted pyrrolidine was included in the substrate scope among other pyrrolidines. A radial synthesis platform consists of multiple flow modules that can be connected and used sequentially, but not simultaneously. These modules are set up around a central switching station (CSS), which can perform both the reactions and the inline analytics. Multistep radial synthesis enables the variation of methods, including flow rates, residence times, temperatures and other conditions. Linear and convergent syntheses are a possibility as well as the storage of intermediates waiting a sequential reaction.[45]

Apart from the light wavelength, reaction conditions similar to Corcoran *et al.*[25] were utilized for the C–N coupling reaction, and three varying aryl pyrrolidines were obtained. The reaction conditions are displayed in **Scheme 22**. The yield for 1-(4-(trifluoromethyl)phenyl)pyrrolidine was significantly lower than other publications have accomplished[25], but this decrease might be a consequence from the alteration to the light source. The majority of studies utilize a 450 nm light source instead of a 420 nm source.

The substrate scope displayed in **Figure 12** included 1-(4-bromophenyl)pyrrolidine and (*S*)-1-(4-(trifluoromethyl)phenyl)pyrrolidin-3-ol. The latter is the only arene coupled 3-substituted pyrrolidine product produced with photoredox catalysis in literature to the best knowledge of the author.

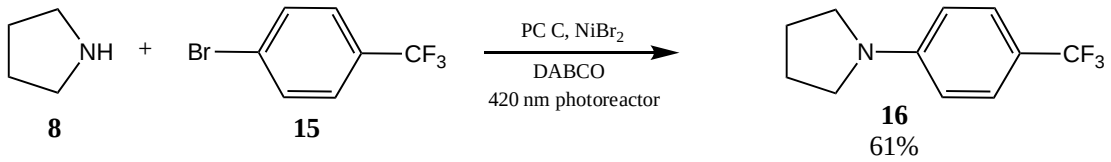

8 **15** **16**
61%

Scheme 22. *The synthesis of 1-(4-(trifluoromethyl)phenyl)pyrrolidine on a radial synthesis platform.*

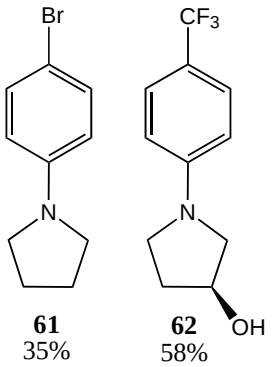

61 35%
62 58%

Figure 12. *The pyrrolidine-including substrate scope of the reaction.*

4. Light sources

Photocatalyzed reactions have evolved as the understanding and possibilities of new catalysts and lamps have emerged. Previous alternatives have included for example mercury lamps of different pressures and UV-light emitting lamps. Nowadays the preferred options are undoubtedly light-emitting diodes, LEDs. LEDs are advantageous due to their ability to emit light on a specific wavelength, instead of a spectrum of light. A broad range of visible light is often unfavourable, as it is not as powerful on the desired wavelength, and it can cause undesired reactivity with higher energy radiation than the catalyst absorbs, for example. $Ru(bpy)_3Cl_2$ has its maximum absorption of energy at 452 nm[13], and most iridium polypyridyl complexes fall on the same region, and hence the most common light source used is a 450 nm blue LED. As **Table 1** displays, nearly all studies in this review utilized LEDs, and 2/3 utilized specifically blue LEDs.

Table 1. The lamp types of the photoredox catalyzed reactions, and the wavelengths the lamps emit.

Reference	**Lamp**	**Wavelength (nm)**
Svejstrup *et al.*[22]	LED	450, Blue
Ruffoni *et al.*[12]	LED	450
Corcoran *et al.*[25]	LED	450
Du *et al.*[8]	LED	White
Ghosh *et al.I*[21]	LED	455
Liu *et al.*[34]	LED	450
Lim *et al.*[35]	LED	365
Kaur *et al.*[36]	60 W tungsten filament bulb	Visible light
Singh *et al.*[42]	60 W tungsten filament bulb	Visible light
Park *et al.*[43]	LED	450
Harper *et al.*[44]	LED	450
Chatterjee *et al.*[45]	LED	420

5. Traditional methods of C–N coupling

The preparation of aromatic amines has typically involved either the Buchwald-Hartwig coupling reaction, nucleophilic aromatic substitution (S_NAr), an Ullmann-type reaction or the Chan-Lam coupling reaction.[17] In **Scheme 23**, a general reaction scheme and their typical leaving groups are displayed.

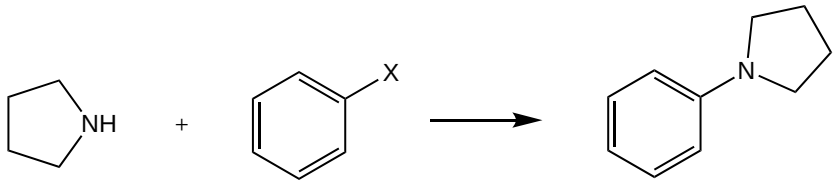

Scheme 23. *A general reaction scheme of the arylation of pyrrolidine.*

X= F: S_NAr

X=Br, I: Buchwald-Hartwig, Ullmann

X= $B(OH)_2$: Chan-Lam

Due to the extensive amount of traditional C–N coupling reactions between pyrrolidines and aryl halides, not all of them are addressed here. **Figure 13** displays two products, 1-phenylpyrrolidine and 1-(4-(trifluoromethyl)phenyl)pyrrolidine, that were chosen for the analyses for their published syntheses.

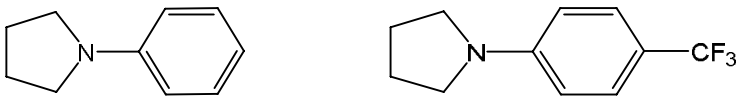

Figure 13. *1-Phenylpyrrolidine and 1-(4-(trifluoromethyl)phenyl)pyrrolidine.*

5.1. Buchwald-Hartwig

Masanori *et al.* developed a C(sp^2)–N bond formation reaction with a palladium catalyst in 1983.[46] Buchwald and Hartwig improved this methodology in 1994[47,48] and removed the use of toxic aminostannanes in their extended work in 1995.[49,50] These publications laid the groundwork for the Buchwald-Hartwig amination reaction.[51]

The Buchwald-Hartwig amination reaction commonly employs a palladium catalyst with ligands, a base, a solvent and heating, as displayed in **Scheme 24**. Numerous adaptations have been developed since 1995, and the Buchwald-Hartwig reaction is considered to have a large substrate scope and to be more generally applicable than Ullmann type reactions or S_NAR.[52]

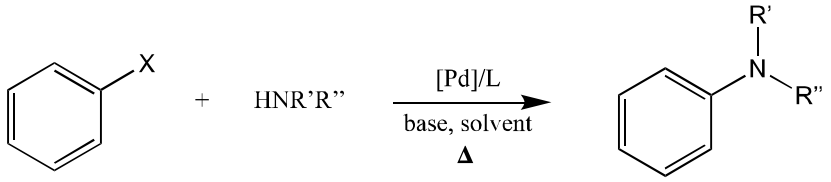

Scheme 24. *A general Buchwald-Hartwig reaction scheme.*

However, regardless of the advancements in the reaction conditions, the reaction still requires elevated temperatures, inert conditions, long reaction times and a high loading of the palladium catalyst in order to achieve good yields.[42] The reactions displayed in **Table 2** clearly demonstrate that most of the reactions still require temperatures of at least 80 °C, and reaction times of several hours.

The displayed reactions include a variety of novel palladium catalysts, but only one of the reactions can be performed at room temperature. Majority of the reactions also require a strong base. Even with new applications, no universal method with mild reaction conditions has been developed.[51]

Table 2. Buchwald-Hartwig type reactions for the synthesis of 1-phenylpyrrolidine and 1-(4-(trifluoromethyl)phenyl)pyrrolidine.

Reference	Catalyst	Base	Solvent	Temperature (°C)	Time (h)	Yield (%)
Veisi *et al.*[53]	Pd nanoparticles on MWCNTs	K_2CO_3	DMF	100	8 h	96
Veisi *et al.*[54]	Fe3O4@PDA@Pd(II)	Cs_2CO_3	DMF	100	10 h	95
Nirmala *et al.*[55]	Organonickel complex	t-BuOK	Dioxane	90	4 h	98
Topchiy *et al.*[56]	Pd(OAc)2, RuPhos	NaOBu-t	-	110	12 h	97
Zhou *et al.*[57]	[SiCCSi]NiBr2	t-BuOK	Dioxane	100	25 h	95 (GC)
Moghaddam *et al.*[58]	Nickel Ferrite NPs	t-BuOK	H2O	60	20 min	89
Zarnaghash *et al.*[59]	Pd-PFMN	K_2CO_3	-	120	24 h	91
Wheaton *et al.*[60]	NHC/P ligand with Pd	NaOBu-t	DME	rt	2 h	90
Prabhu and Ramesh[61]	Pd(II) thiosemicarbazone complex	K_2CO_3	s-BuOH	100	24 h	91
Cheng *et al.*[62]	Chitosan-Pd	t-BuOK	DMSO	100	12 h	84 (GC)
Kim *et al.*[63]	NHC-Pd-Phosphorus ligand	t-BuOK	DME	80	1 h	84
Sarvestani and Azadi[64]	Pd-NPs on GO-Chit	t-BuOK	DMF	100	12 h	89
Subramaniyan *et al.*[65]	Pd (II) carbene complex	NaHMDS	PhMe/THF	100	5 h	89
Fareghi-Alamdari *et al.*[66]	PFG-Pd	NaOBu-t	PhMe	110	15 h	88
Nirmala *et al.*[67]	Ni(II) dicarbene complex	t-BuOK	Dioxane	90	4 h	74
Huang *et al.*[68]	NHC-Pd(II)-Ox	K_2CO_3	Dioxane	90	1 h	62

5.2. Nucleophilic aromatic substitution (S_NAr)

In nucleophilic aromatic substitution a leaving group (usually a halide) is replaced by a nucleophile, as depicted in **Scheme 25**. S_NAr is a fundamental reaction in organic chemistry, but it is defeated in applicability and modern usage to palladium and copper catalyzed reactions. In the over 200 reactions examined for the synthesis of 1-phenylpyrrolidine and 1-(4-(trifluoromethyl)phenyl)pyrrolidine, only one reaction utilized S_NAr, and that article was from 1962. However, this does not mean S_NAr would be completely unused in these reactions due to the possibility of some Ullmann reactions proceeding through the S_NAr mechanism.[69]

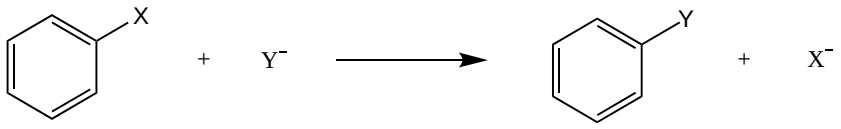

Scheme 25. *A general nucleophilic aromatic substitution reaction scheme.*

5.3. Ullmann-type reactions

Ullmann-type reactions for coupling nucleophilic nitrogen and hydrogen species with arenes were developed by Ullmann and Goldberg in the beginning of the 20th century, decades before similar reactions with other metals (for example palladium and nickel).[70,71] For a long period of time the reactions had not encountered significant improvements. In 2001 some improvement was achieved, and it led to the modification of the catalyst, and lowered reaction temperatures (from 210 ºC to ~100 ºC).[69] A benefit of the Ullmann reaction is the utilization of copper instead of the more expensive and toxic palladium in the Buchwald-Hartwig reaction.[69] A general Ullmann-type reaction scheme is depicted in **Scheme 26**.

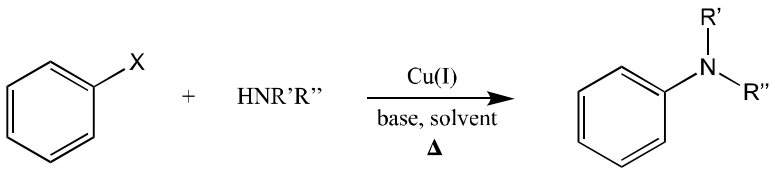

Scheme 26. *A general Ullmann-type reaction scheme.*

From **Table 3** it is apparent that the reaction conditions require elevated temperatures combined with a prolonged reaction time, even with the latest developments. The average reaction temperature is approximately 80 °C, and the average reaction time is above 25 hours.

Table 3. Ullmann type reactions for the synthesis of 1-phenylpyrrolidine and 1-(4-(trifluoromethyl)phenyl)pyrrolidine.

Reference	**Catalyst**	**Base**	**Solvent**	**Temperature (°C)**	**Time (h)**	**Yield (%)**
Wang *et al.*[72]	CuI, acid ligand	K_3PO_4	DMSO/H2O	25	24-30	94
Lo *et al.*[73]	CuI	TBPM	DMSO	rt	24	94
Cano *et al.*[74]	-	KOH	DMSO	120	72	99
Jia *et al.*[75]	CuI	K_2CO_3	DMF	130	48	92
Farahat *et al.*[76]	CuMeSal	K_2CO_3	DMSO	110	3	90
Zhou *et al.*[77]	CuI, NH2-G-NH2	KOH	DMSO	80	20	76
Sung *et al.*[78]	CuI	K_2CO_3	d-DMSO	80	18	68 (NMR)
Nemati and Elhampour[79]	Fe3O4@TiO2/Cu2O	KOH	DMSO	100	2,7	73
Deldaele and Evano[80]	CuI, L-proline ligand	-	DMSO	rt	17	56
Hwang *et al.*[81]	CuI	K_3PO_4	IPA	90	24	52

5.4. Chan-Lam

The Chan-Lam coupling reaction for C–N bond formation was developed simultaneously in 1998 by Chan, Evans and Lam in independent studies.[82-85] The reaction is a cross-coupling between aryl boronate derivatives and nitrogen containing substrates catalyzed by a copper catalyst as displayed in **Scheme 27**. The Chan-Lam reaction has multiple advantages especially compared to Buchwald-Hartwig and Ullman-type reactions. The Chan-Lam reaction can be conducted under air and in room temperature, and the copper catalyst is inexpensive compared to other metal catalysts.[82]

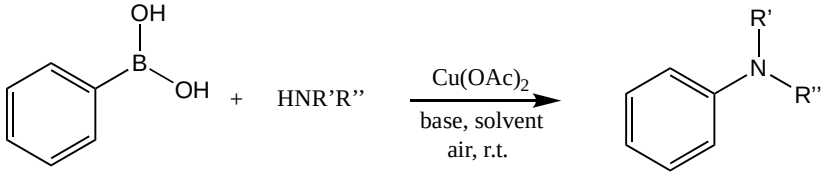

Scheme 27. *A general Chan-Lam reaction scheme.*

As the lack of results in **Table 4** indicates, a disadvantage with the Chan-Lam reaction is the deficiency in studies, results and therefore substrate scope and adaptations. This inadequacy is decreasing with time and new research, but due to the current situation, the reaction lacks reliability that comes with a larger amount of data.

Table 4. Chan-Evans-Lam type reactions for the synthesis of 1-phenylpyrrolidine and 1-(4-(trifluoromethyl)phenyl)pyrrolidine.

Reference	Catalyst	Base	Solvent	Temperature (°C)	Time (h)	Yield (%)
Hardouin Duparc *et al.*[86]	Iminoarylsulfonate Cu(II) complex	-	MeOH	rt	2	100 (GC/MS)
Hardouin Duparc and Schaper[87]	Sulfonato-imino Cu(II) complex	-	MeOH	rt	2	100 (GC/MS)

6. Aims of the present study

The aims of the present study were to broaden the substrate scope and knowledge from previous studies of photoredox C–N coupling of pyrrolidines and arenes. This included the use of photoredox methodologies for the C–N coupling of 3-substituted pyrrolidines to arenes (**Scheme 28**), examining the scope and limitations of the reaction and effect of substituents on pyrrolidine and the aryl halide. In addition, the aim was to optimize the reaction conditions for multiple parameters and for each product separately, apply the reaction on a flow chemistry appliance, and execute scale-up reactions on the photoreactor and the flow appliance.

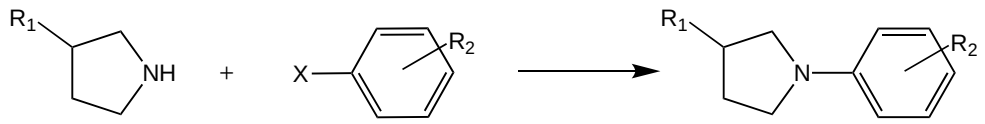

Scheme 28.*The general reaction scheme of the C–N coupling of 3-substituted pyrrolidines to arenes.*

7. Summary

Photoredox chemistry has evolved significantly over the last decade, and the amount of ongoing research is increasing rapidly. The ability to create radicals in mild conditions and with readily available reagents has previously been a challenge in organic chemistry. The unique possibility of having a catalyst that can be a strong oxidant and a strong reductant simultaneously enables special reaction conditions that are rare in other fields of organic chemistry.

Pyrrolidines were successfully coupled with arenes using photoredox catalytic methods, and one 3-substituted pyrrolidine was included as well. This review presented versatile alternatives for traditional C–N coupling, and adaptations of a variety of reaction conditions and appliances. The combination of transition metal catalysts and photocatalysts is a powerful tool for multiple photoredox reactions, and it works readily with carbon-heteroatom cross-coupling. Transitional metal dual catalysts have been utilized extensively with iridium and ruthenium catalysts, but also with organic dyes and heterogeneous semiconductors. The examination of “dark” cycles

in reaction mechanisms demonstrates the lack of verified knowledge in photoredox chemistry and proves the need for further research. In addition, the reasons between the varying results with EWG and EDG substituents with organic and metal catalysts lack an explanation.

Photoredox chemistry offers a competitive alternative to traditional C–N coupling reactions. Photochemical reactions are often employed in milder reaction conditions and in significantly faster reaction times. The substrate scope of photoredox reactions cannot yet compete with those of traditional reactions, but with time the scope will broaden. Applications of photocatalytic Ullmann and Chan-Lam reactions have been developed, and hopefully more fusions of these methodologies will be explored in the future.

EXPERIMENTAL PART

8. Introduction

The experimental research was conducted at Orion Corporation in the Global Medicine function from November 2019 to May 2020.

The goal of the research was to use photoredox methodologies for C–N coupling of 3-substituted pyrrolidines to arenes. The C–N coupling reaction is an essential reaction in the pharmaceutical industry, and a new option to improve from the traditional methods would be tremendously useful. Numerous previous studies have succeeded in the C–N coupling reaction of pyrrolidines and arenes with photoredox catalysis, but only one has included a 3-substituted pyrrolidine. By the time the experimental laboratory work of this research was finished, no research had been published including the C–N arylation of 3-substituted pyrrolidines. After this, one example was introduced by Chatterjee *et al.*[45]

After examining the C–N coupling of 3-substituted pyrrolidines to arenes, the scope and limitations of the reaction were analyzed. The effect of substituents on pyrrolidine and the aryl halide were determined, and the reaction conditions were optimized for multiple parameters. In addition, the reaction was applied on a flow chemistry appliance, and scale-up reactions were executed on the photoreactor and the flow appliance. 3-substituted pyrrolidines are valuable building blocks in the pharmaceutical industry, as heterocycles are often used in the synthesis of pharmacologically active compounds. Therefore, it was essential to include pyrrolidines with substituents such as -CN, -NHBoc, and -COOMe, which would enable sequential reactions onwards from the substituent, and facilitate a broader range of synthesis possibilities.

The majority of the photoredox C–N coupling reaction studies have utilized electron-deficient arenes successfully in their reactions, and a minority also included electron-rich arenes. A plethora of studies also utilize a transition metal catalyst such as NiX_2 to combine these two catalytic cycles as metallaphotoredox catalysis. In addition, several alternative methodologies have been employed such as heterogeneous semiconductors and flow chemistry applications. This research adapted these methods and broadened the substrate scope of earlier studies. The parameters investigated and their corresponding chapters are listed in **Table 5**.

Table 5. The research matrix and areas of optimization.

Chapter	Subject of optimization	Variable
9.1	Pyrrolidine	12 different pyrrolidines
9.2	Aryl halide	12 different aryl halides
9.3.1	Leaving group	Br, I, Cl
9.3.2	Photocatalyst	Ir, Ru, CdS, 0.06 and 0.02 mol% for Ru
9.3.3	Base	DABCO, DBU, MTBD
9.3.4	Dual catalyst	$NiBr_2$·glyme, $NiCl_2$·$6H_2O$
9.3.5	Solvent	DMA, ACN, DMSO
9.3.6	Light wavelength	450 nm, 365 nm
9.3.7	Radiation intensity	50%, 100%
9.4	Reaction scale-up	
9.5	Flow chemistry	

9. Results and discussion

9.1. C–N coupling of 3-substituted pyrrolidines

The experimental research was commenced by replicating Corcoran's photoredox reaction from a previous article[25] depicted in **Scheme 29**. This reaction successfully coupled 1-bromo-4-(trifluoromethyl)benzene and pyrrolidine with an iridium photocatalyst and a nickel transition metal catalyst with DABCO as the base. A Penn PhD Photoreactor M2 was utilized for the photocatalyzed reactions.

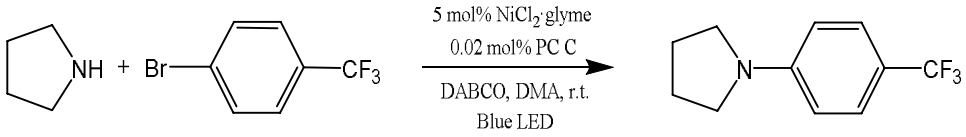

Scheme 29. *The reaction conditions from Corcoran et al.*[25]

After successfully replicating the forementioned reaction, the research for 3-substituted pyrrolidines was commenced. The reaction conditions were unaltered apart from the pyrrolidine. The reaction was assumed to follow a dual catalytic cycle reaction mechanism, similar to the one proposed by Corcoran *et al.*[25] For the first round of reactions, 11 different 3-substituted pyrrolidines were coupled with 1-bromo-4-(trifluoromethyl)benzene. The results are displayed in **Scheme 30**, including the nuclear magnetic resonance (NMR) yield of the product and the purified yield in brackets.

The substrate scope of pyrrolidines included both electron withdrawing substituents and electron donating substituents for the purpose of determining possible impacts. For example products **5**, **7** and **12** were chosen due to the possibility of sequential reactions from the substituent side. This aspect was considered essential for the future applications of this reaction due to pyrrolidine's usability as a building block in pharmaceutical compounds.

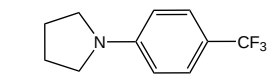

1

75 (70) %

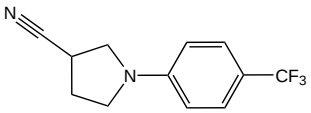

12

74 (65) %

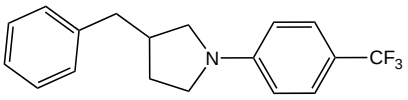

2

84 (66) %

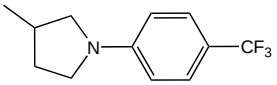

4

50 (28) %

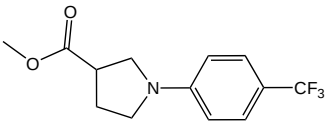

5

58 (40) %

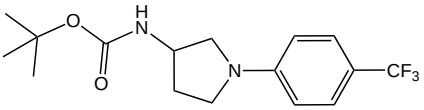

7

66 (50) %

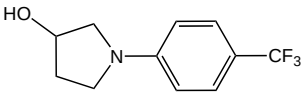

3

28 (22) %

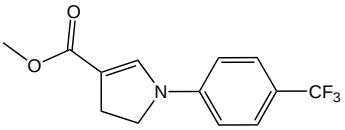

6

(5) %

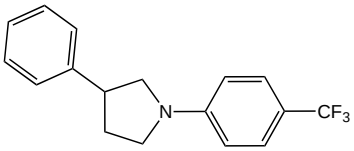

11

85 (65) %

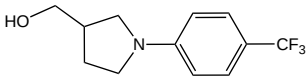

9

83 (64) %

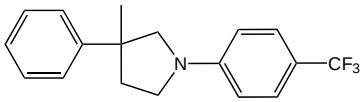

8

75 (60) %

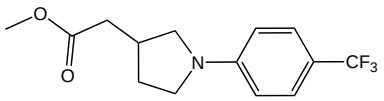

10

41 (21) %

Scheme 30. *The substrate scope for the first round of reactions describing the quantitative NMR yields, and the isolated yields in parentheses. The reaction conditions are described in* ***Scheme 29****.*

From the results on **Scheme 30** it was clear that the photoredox C–N coupling reaction was applicable for 3-substituted pyrrolidines. The only pyrrolidine which did not produce any product was pyrrolidin-3-one (not displayed on **Scheme 30**). Some of the products in **Scheme 30** show poor yields, but with optimization they were improved. In the reaction displayed in **Scheme 31**, the low yield of product **6** is explained by it being a side product of product **5**.

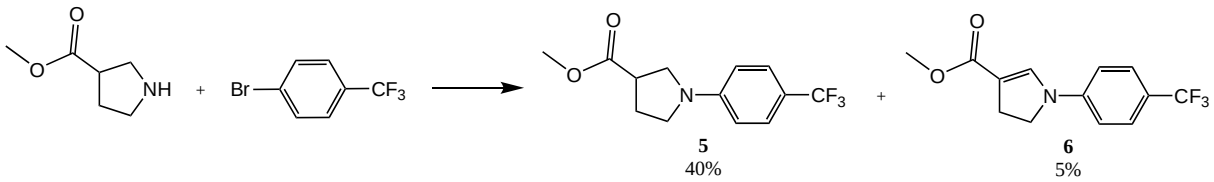

Scheme 31. *The reaction resulting in products **5** and **6** and their yields.*

Reactivity in the alpha-position of nitrogen was hypothesized, but only the formation of a double bond after a deprotonation was observed. A product (**6**) following this event was isolated with a poor yield, and the location of the double bond was confirmed with ^{13}C NMR measurements. This undesired reactivity occurred in most reactions after prolonged irradiation with 450 nm light.

The results of the substrates seem to indicate that EWGs react with greater ease, but no clear separation between EWGs and EDGs can be observed. Since only one product with a 3-substituted pyrrolidine has been published in the literature, no supporting or differing results can be used to verify this hypothesis. Additional substrates and repetitions of the reactions are needed for confirming any conclusion.

9.2. Aryl halide substituent effects

The effects of the aryl halide substituents were explored next. The effects of *ortho-*, *meta-* and *para*-substitution to the reactivity were studied with multiple compounds, and the impact of electron withdrawing groups (EWGs) as substituents compared to electron donating groups (EDGs) was also analyzed. Two pyridine products were also obtained. **Scheme 32** displays the substrate scope for aryl halide substituents.

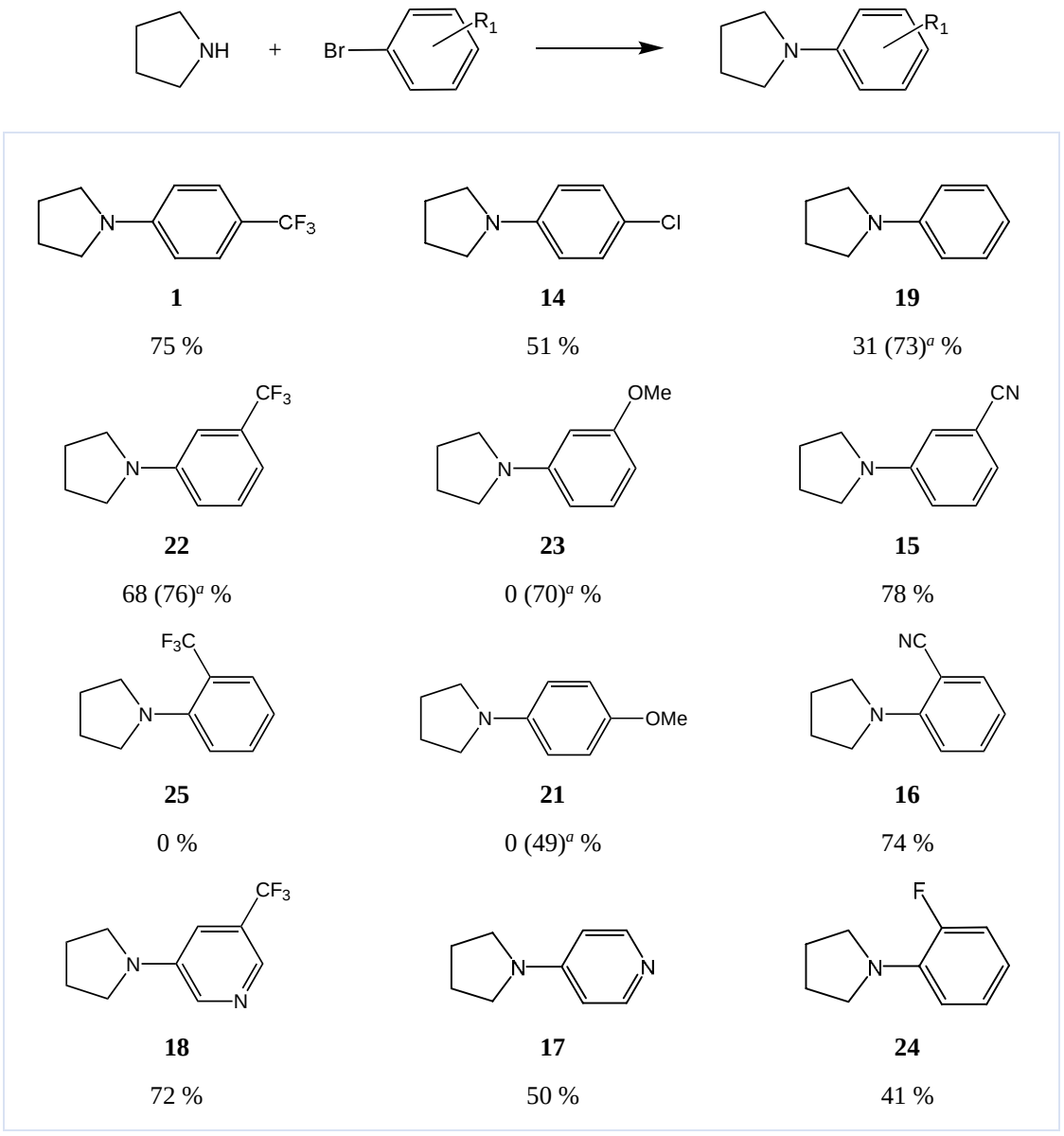

Scheme 32. *The substrate scope for aryl halide substituents describing the quantitative NMR yields for the products. a) an aryl iodide was used instead of an aryl bromide. The reaction conditions are described in* ***Scheme 29****.*

The results in ***Scheme 32*** indicate that multiple different substituents in aryl halides can be employed without hindering the reaction. In the original reaction conditions by Corcoran *et al*.[25] an aryl bromide is used. The results in **Scheme 32** show that EWGs as substituents function well with a bromide as the leaving group, contrary to bromide with EDGs.

Multiple reactions with varying pyrrolidine substituents were conducted with 2-bromobenzotrifluoride. As displayed by product **25**, no reaction occurred. Presumably steric effects hindered the reaction, because good yields were obtained with *meta* and *para* trifluoromethyl substituted arenes, as well as smaller fluoro ja nitrile groups in *ortho* position. Park *et al.*[43] also mention the lowered reactivity for sterically hindered arenes. Due to electronic effects, EDGs in *meta*-position performed better than in *ortho*- or *para*-position. EWGs in *meta*-position conversely performed worse than EWGs in *ortho*- or *para*-position.

Similarly to the substrate scope in pyrrolidines, a trend is observed towards the superior functionality of EWG substituted aryl halides. The scale of reactivity can be observed when comparing products **1**, **14**, **19** and **21**. From stronger EWGs to weaker EWGs and an EDG: CF_3 > Cl > H > MeO, and their yields 75 > 51 > 31 > 0 correlate. Again, this research is not comprehensive, but data from other studies utilizing Ir or Ru catalysts supports this conclusion.[35,43] Park *et al.*[43] synthesized multiple pyrrolidine products with similar reaction conditions (excluding a flow reactor setup), and compared EWG and EDG including products. The product yields of for example 4-bromobenzotrifluoride (97 %) and 4-bromoanisole (80 %) differ slightly, but 4-bromoanisole required 6 times longer reaction time to achieve this yield.

Pyridine products **17** and **18** were obtained in relatively good yields, and showed improvement compared to products **19** and **22**. A variety of 3-substituted pyrrolidines were also coupled with differently substituted aryl halides, and the results followed the forementioned trends in reactivity.

9.3. Optimization of reaction conditions

Optimization of reaction conditions was conducted to improve poorly performing reactions, and to explore better options in general. The optimized parameters were the aryl halide leaving group, the photocatalyst, the amount of photocatalyst for ruthenium catalysts, the base, the dual catalyst, the solvent, the light source (wavelength), and the radiation intensity. The reaction time varied with each reaction and was optimized for each one separately based on liquid chromatography-mass spectrometry (LC-MS) or gas chromatography-mass spectrometry (GC-MS) reaction monitoring.

9.3.1. Aryl halide leaving group

The leaving group originally employed for all reactions was bromide, in accordance with the majority of recent literature. After the poor performance of some reactions, an iodide leaving group was introduced. As displayed on **Scheme 32**, three aryl halides with EDG substituents performed significantly better with iodide as the leaving group instead of bromide. Other reactions conducted with 4-iodobenzotrifluoride and various 3-substituted pyrrolidines were for example 3-pyrrolidinol, 3-methylpyrrolidine and 3-(tert-butoxycarbonylamino)pyrrolidine, displayed in **Scheme 33**. With these reactions the improvement in quantitative ^{1}H NMR yields was minor, less than 10 %. Some of these reactions were improved later on with the combination of iodide and a ruthenium catalyst.

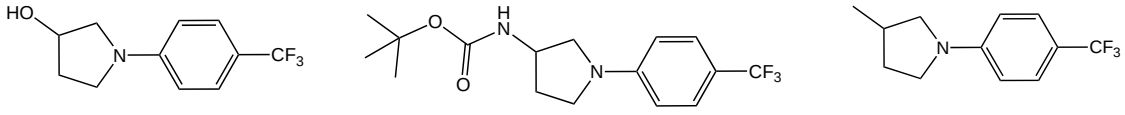

3 28 → 31%

7 66 → 66%

4 50 → 58%

Scheme 33. *The qNMR yields of products 3, 7 and 4 for the reactions with Br → I leaving groups.*

The drastic improvement with the methoxy substituent and the lack of any substituent has also been observed by Lim *et al.*[35] They reported an increase in yields for electron rich and electron neutral aryl halides when the bromide leaving group was replaced with iodide. However, these reactions were conducted with morpholine, not pyrrolidine, but similar results could indicate a benefit of using iodide with EDGs.

The selectivity between chloride and bromide was explored with the utilization of 4-bromochlorobenzene. The reaction coupled selectively with bromide, as depicted in **Scheme 34**.

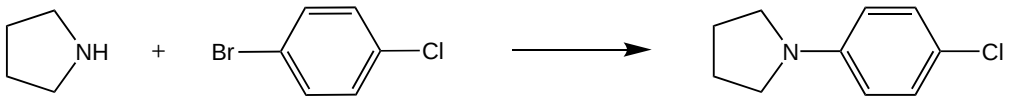

Scheme 34. *A selective C–N coupling reaction with coupling from bromide.*

9.3.2. Photocatalyst

The reactions were first executed with an iridium catalyst (PC C), and later optimization possibilities were explored with a ruthenium catalyst (PC D) and CdS. PC C and PC D are displayed in **Figure 14**.

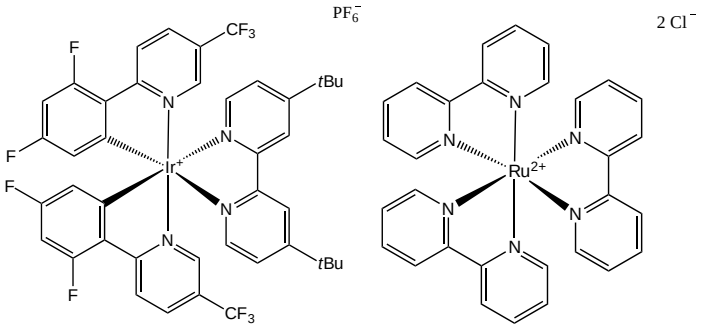

Figure 14. *Photocatalyst C: Ir[dF(CF$_3$)ppy]$_2$(dtbbpy)PF$_6$ and photocatalyst D:tris(2,2-bipyridyl)ruthenium(II)chloridehexahydrate.*

The iridium catalyst proved to be a generally well-functioning catalyst for most reactions. For the majority of reactions conducted, it provided the best yields. The ruthenium catalyst performed worse than the Ir catalyst in some cases, but was able to offer a significant improvement in others. **Table 6** displays the optimization for 1-(4-(trifluoromethyl)phenyl)pyrrolidin-3-ol (**3**), a pyrrolidine product with a hydroxyl group substituent. **Table 6** showcases the increase in yield due to a change to a Ru catalyst. The change from the Ir catalyst to a Ru catalyst increases the yield by 25%. It is worthy to notice, that when Br was changed to I with the Ir catalyst, the increase in yield was only 3%. However, when a Ru catalyst was used, and the same change from Br to I was made, an increase of 18% was observed.

Table 6. The optimization of the synthesis of 1-(4-(trifluoromethyl)phenyl)pyrrolidin-3-ol (**3**).

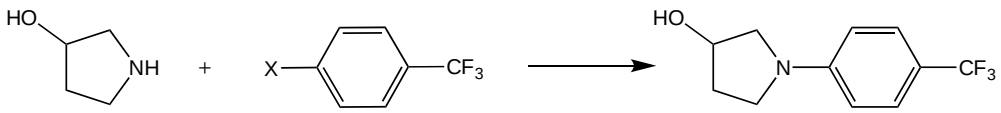

PC	X	Yield (%)
Ir	Br	28
Ir	I	31
Ru	Br	53
Ru	I	71

A possible explanation could arise from the compatible properties of iodide and Ru catalyst. Iodide is a better leaving group than bromide, and the Ru catalyst reacts faster to its maximum conversion than the Ir catalyst as depicted in **Chart 1**. The combination of a fast leaving group and a fast catalyst could lead to a higher yield. However, Ru and I were not the preferrable combination for all reactions, and there was not a clear distinction between electron-withdrawing and electron-donating groups, so a definitive hypothesis cannot be established.

Chart 1. The rate of reactions depicted on **Table 6.**

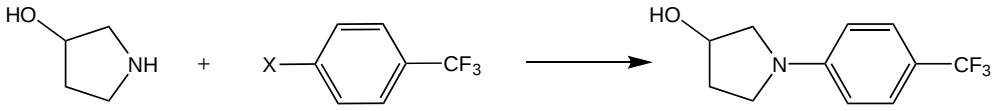

A reaction with cadmium sulphide was executed following the conditions from Liu *et al.*[34] 4-Bromobenzotrifluoride (1 equiv.) and pyrrolidine (2 equiv.) were coupled utilizing CdS (0.2 equiv.), Ni(II)$Cl_2 \cdot 6H_2O$ (0.05 equiv.) and DMA. The reaction time reported from Liu *et al.* was 24 h. After 18 hours the reaction came to a halt with an LC-MS conversion of 87%. The quantitative NMR yield was 67%. The reaction worked, but it was significantly slower and did not exceed the yields of the reference reactions with Ir or Ru photocatalysts.

Changing the amount of the ruthenium catalyst was examined with 0.06 mol% and 0.02 mol%. Most of the reactions were executed with a 0.06 mol% ruthenium catalyst. Two reactions were completed with 0.02 mol%, the couplings of pyrrolidine and methyl 2-(pyrrolidine-3-yl)acetate with 4-bromobenzotrifluoride. The coupling of methyl 2-(pyrrolidine-3-yl)acetate with 4-bromobenzotrifluoride yielded the same result as with 0.06 mol% catalyst loading. The reaction of pyrrolidine with 4-bromobenzotrifluoride yielded a slightly higher amount of product, 82%, than with 0.06 mol%, 77%. However, this increase is not significant enough to draw conclusions from the impact of the catalyst loading. A valuable addition to this research would

have been to test the decreased catalyst loading with an EDG substituent, since Park *et al.*[43] reported of the improved yields due to diminished competitive protodehalogenation. The small rise in the yield of 1-(4-(trifluoromethyl)phenyl)pyrrolidine (**1**) could be an implication of this event.

9.3.3. Base

1,4-Diazabicyclo[2.2.2]octane (DABCO) was employed as the base originally due to its frequent use in the literature. 7-Methyl-1,5,7-triazabicyclo[4.4.0]dec-5-ene (MTBD)[25] and DBU[34] were also explored for optimization of reactions.

DBU was applied with 1.8 equiv. similarly to DABCO in earlier reactions. A reaction with pyrrolidine and 4-bromobenzotrifluoride was conducted, but no product or other reactivity was observed. Liu *et al.* utilized DBU for the C–N coupling of primary amines and some secondary amines, but not pyrrolidine.[34] With those reactions, DBU increased yields. The reactions were conducted with a CdS photocatalyst and a transition metal dual catalyst. Interestingly, DABCO inhibited the reactions between aryl halides and pyrrolidine. Reactions with pyrrolidine succeeded without a base.

MTBD was examined with 1.8 equiv. in a reaction between pyrrolidine and 4-bromoanisole without any observed reactivity. Corcoran *et al.* tested the differences in functionality of DABCO and MTBD, and utilized MTBD especially with amine hydrogen chloride salts.[25] These comparison tests displayed a preference towards MTBD, but were only conducted on primary amines. Some reactions were conducted with only MTBD and not DABCO, and these included secondary amines. Pyrrolidines were not included in these tests. MTDB was also reported to reduce protodehalogenation. The results between Corcoran *et al.* and this research cannot be reliably compared due to the lack of similar reaction conditions. In addition to the disparity in amines, Corcoran *et al.* followed a stricter method in creating a nitrogen atmosphere and radiated the reaction for 24 hours.

9.3.4. Dual catalyst

Two different transition metal dual catalysts were employed for these reactions. For the majority of the reactions $NiBr_2$·glyme was utilized, but as an alternative $NiCl_2·6H_2O$ was examined. 3-Phenylpyrrolidine and pyrrolidine were reacted using $NiCl_2·6H_2O$ with varying results. The reaction with pyrrolidine resulted in a 16% increase in yield, contrary to a decrease of 25% for 3-phenylpyrrolidine. No reason for the disparity can be postulated with such a limited number of reactions.

Corcoran *et al.*[25] employed $NiBr_2$·glyme for most of their reactions, but examined the use of $Ni(cod)_2$ and $NiBr_2·3H_2O$ as well. The use of $Ni(cod)_2$ resulted in the exact same yield for the product, 95%, as $NiBr_2$·glyme. $NiBr_2·3H_2O$ was utilized with the flow chemistry appliance, as was $NiBr_2$·glyme, however as the residence time and concentration of the catalyst were also altered, no comparison of the catalyst efficiency can be made.

Liu *et al.*[34] used $NiCl_2·6H_2O$ and $NiCl_2$·glyme for optimization reactions. $NiCl_2·6H_2O$ afforded a 3% better yield for the product, thus no significant difference was observed between the catalysts. Lim *et al.*[35] compared different Ni catalysts in optimization reactions with morpholine. All of the compared catalysts, $NiBr_2·3H_2O$, $NiBr_2$·glyme and $NiCl_2·6H_2O$, resulted in a 95% yield.

9.3.5. Solvent

DMA, ACN and DMSO were examined as solvents for these reactions. DMA is used in the majority of photoredox literature, excluding flow reactor reactions. Two reactions with ACN were executed, the syntheses of 1-(4-(trifluoromethyl)phenyl)pyrrolidine (**1**) and (1-(4-(trifluoromethyl)phenyl)pyrrolidin-3-yl)methanol (**9**). These reactions suffered a decrease in yield of 20-30%. A synthesis of 1-(4-(trifluoromethyl)phenyl)pyrrolidine (**1**) was conducted also with DMSO as a solvent for the application of the reaction to the flow chemistry reactor. DMA was unusable on flow due to the formation of precipitation during the reaction, which would clog the appliance. In DMSO no precipitation formed, but the yield of the reaction was 17% lower than with DMA.

Corcoran *et al.*[25] examined the use of ACN as well as DMA, but resulted in the use of DMA due to slightly higher yields (9%). Liu *et al.*[34] used DMA, ACN, THF, DCM and $CHCl_3$ for the

optimization of the solvent. The reaction with DMA afforded an 83% product yield, ACN 58%, and the rest hindered the reaction completely. Park *et al.*[43] initially utilized DMA in their reactions, but swiftly changed to DMSO, due to precipitation forming in the reaction with DMA, and clogging the flow chemistry appliance.

9.3.6. Light wavelength

For all of the reactions excluding one, 450 nm LED light source was utilized. 450 nm is the most common light source used in photoredox chemistry literature, as it is optimal for iridium and ruthenium catalysts. A 365 nm LED light source was utilized for a repetition of a reaction from Lim *et al.*[35] For this reaction, only pyrrolidine (3.5 equiv.), 4-bromobenzotrifluoride (1 equiv.), $NiBr_2$·glyme (0.05 equiv.), and DMA were used. No product formed in the reaction.

9.3.7. Radiation intensity

For all of the reactions excluding one, radiation intensity of 100% from the Penn PhD photoreactor M2 was utilized. For the synthesis of methyl 2-(1-(4-(trifluoromethyl)phenyl)pyrrolidine-3-yl)acetate (**10**) intensity of 50% was also examined. The decrease in radiation intensity led to a decrease of 15% in yield, a longer reaction time, a lower LC-MS conversion and an increased formation of the deprotonated side product.

9.4. Reaction scale-up

A scale-up reaction to 2 mmol scale was conducted on the Penn PhD Photoreactor M2 appliance. The reaction successfully coupled 4-bromochlorobenzene and pyrrolidine-3-carbonitrile with DABCO, a nickel catalyst, an iridium photocatalyst, DMA and 450 nm light source. A 40 ml reaction vial was used for the scale-up. The reaction progressed at approximately the same pace as the 0.5 mmol scale reaction, i.e. came to a halt at 82% LC-MS conversion after 220 minutes (2 mmol) versus 250 minutes (0.5 mmol). 60 mg of the internal standard trimethoxybenzene was added for the quantitative NMR measurement, and the work-up was executed on a 30 ml scale. A 63% qNMR yield was obtained, slightly greater than 57%

for the 0.5 mmol scale reaction. The product was purified with flash chromatography (A: heptane, B: EtOAc, gradient 0-50 % eluent B). The product was obtained as a white solid, with a purified yield of 48%, 0,197 g. The 0.5 mmol scale reaction yielded 41% of purified product. The purity of the isolated product was determined with a chromatographic purity measurement, and it was 97%. The scale-up on the Penn PhD Photoreactor M2 appliance succeeded exceptionally well with no indication of loss of radiated surface due to a larger vial and an increased reaction volume.

9.5. Flow chemistry

The starting reaction coupling 1-bromo-4-(trifluoromethyl)benzene and pyrrolidine was implemented on a flow chemistry platform, displayed in **Figure 14**, to study the function of the photochemical reactor, and to research scale-up possibilities.

Figure 14. *A Vapourtec R-Series Integrated Flow chemistry system RS-200.*

To inhibit the blockage of the flow chemistry system, the reaction was completed with DMSO as a solvent, because formation of precipitation had been observed earlier with DMA. Park *et al.*[43] encountered the problem in their research in 2020, and proposed that the clogging of their reactor occurred due to DABCO-containing salts formed in DMA.

The reaction conditions from Corcoran *et al.*[25] excluding the solvent were applied on the flow appliance, with flow system settings implemented from Park *et al.*[43] These included starting materials of pyrrolidine and 1-bromo-4-(trifluoromethyl)benzene, DABCO as the base, an iridium photocatalyst (PC C), a $NiBr_2$ transition metal catalyst, and DMSO as the solvent. The reaction mixture was inserted to the system via a needle under nitrogen atmosphere. The flow rate was 1 ml/min, and the residence time in the photoreactor 10 minutes. The pressure remained under 4 bar in all of the reactions, and the temperature varied between 35-45 °C. The lamp power was set between 50-100 % in each reaction, but no significant relevance in the product yield was observed.

The reactions were conducted on a 0.500 mmol scale excluding the scale-up, which was quadrupled to a 2 mmol scale. One reaction was conducted with 3-pyrrolidinemethanol instead of pyrrolidine, and one with a ruthenium photocatalyst (tris(2,2'-bipyridyl)dichlororuthenium(II) hexahydrate) instead of an iridium PC. The maximum qNMR product yield was 21% and obtained with the scale-up reaction.

A significant amount of undesired reactivity occurred in the flow chemistry platform, and the hypothesis is that the light source was not optimal for these types of reactions. The light source in the flow chemistry system was a 150-Watt reactor with a medium pressure mercury lamp equipped with a Vapourtec wavelength filter type 3 – red, which filters out light excluding wavelengths from 300 to 2000 nm. The optimal wavelength for the reactions would have been 450 nm, and therefore radiating with 300-2000 nm does not acquire the optimal results. The yields for the reactions were poor, although the products were identifiable. A future improvement for this reaction would be likely if the appropriate light sources were obtained. The results from Park *et al.*[43] support this proposal, since they successfully completed the same reaction with a 450 nm LED photoreactor.

10. Conclusions

The coupling of 3-substituted pyrrolidines with aryl halides via photoredox catalysis was successful, and the optimization of the reactions improved the results. 24 products were synthesized and characterized, and a scale-up reaction was executed successfully. The adaptation of reactions on the flow chemistry reactor did not provide the desired results, as the light source used was not optimal.

As only one product including a 3-substituted pyrrolidine was reported in literature[45], this research broadened the substrate scope with 10 new substituents and multiple new combinations of 3-substituted pyrrolidines and aryl halides. The substituents on aryl halides had been examined previously in the literature, and the results of this research are in coherence.

Both electron withdrawing and electron donating groups functioned adequately as substituents on pyrrolidine. Variation in yields was observed, but with optimization most of the products were obtained in good to excellent yields. Substituents on aryl halides presented a preference towards EWGs in *para*-, or *ortho*-positions due to electronic effects. The yields of electron-rich or electron-neutral arenes were improved significantly with optimization.

Optimization of reaction conditions was executed on the poorly performing reactions. The optimized parameters were the aryl halide leaving group, the photocatalyst, the amount of photocatalyst for ruthenium catalysts, the base, the dual catalyst, the solvent, the light source (wavelength), and the radiation intensity. The most substantial improvements were obtained with the change of the leaving group from bromide to iodide, and the photocatalyst from an iridium catalyst to a ruthenium catalyst. The preferred combination of a leaving group and a photocatalyst had to be examined for each product separately due to a lack of a definitive correlation between product properties and yields with certain reaction conditions. However, with most products, good results were obtained with iodide and EDG substituents, and ruthenium and EDG substituents either combined or separately. The improvement of EDG substituent including reactions with iodide as the leaving group were reported in literature previously[35], but the combination of a ruthenium catalyst and an iodide leaving group were not, according to the best knowledge of the author.

The reliability of the results is increased on the subject matters that are coherent with literature, but other results, especially if inconsistent, would require further research and repetitions to gain a similar level of reliability. In retrospect, more alternatives of photocatalysts, especially

organic dyes, should have been examined. The screening of reaction conditions could have included a reaction without radiation, for the analysis of possible “dark” cycle reactions. The decrease in catalyst loading should have been experimented with EDG substituents for the examination of protodehalogenation. In addition, the additional 450 nm LED reactor should have been ordered in the beginning of this project for the successful use of the flow chemistry appliance.

If this research were to be continued, the substrate scope could be broadened, and the forementioned suggestions could be implemented. In addition, the temperature and fan speed could be optimized, and further applications and scale-up reactions on the flow reactor could be executed. The mechanistic studies of different catalysts could also shed a light on the disparity in reactivity.

11. Methods

11.1. Analysis Methods

The Penn PhD Photoreactor M2 was used for the photoredox reaction setup. LED lights of 365 nm and 450 nm were utilized, a clear reaction vial of 4 ml with a screw cap was set 6 mm above the light source with a 2 ml reaction vial holder and covered with an 8 ml reflector cone. The reaction was stirred with a magnet 500 rpm, and the fan speed was 3500 rpm.

The reaction monitoring was conducted using a liquid chromatography-mass spectrometry setup. The setup included Waters Acquity UPLC system, Waters Acquity UPLC PDA and Waters SQ Detector 2 with cone voltage 20. The solvents ACN:H_2O (5:95) + 0.1% HCOOH and ACN:H_2O (95:5) + 0.1% HCOOH were used for the acidic method, and ACN:H_2O (5:95) + 0.01% NH_4OH and ACN:H_2O (95:5) + 0.01% NH_4OH for the basic method. The injection volume was 1 µl, and the run time was 3 minutes. The chromatographic purity measurement was executed on the same appliance with 15 mM KH_2PO_4 pH 2.2/ACN as the eluent with a gradient method. The injection volume was 1 µl, and the run time was 5 minutes.

An alternative reaction monitoring method with gas chromatography-mass spectrometry was applied when LC-MS was not suitable. Shimadzu GCMS-QP2020 NX gas chromatograph mass spectrometer was equipped with Shimadzu AOC-20i Plus auto injector.

Bruker Avance III HD 400 MHz was used for structure verification and quantitative NMR measurements. For most of the targets, ^{1}H, ^{13}C and ^{1}H–^{13}C heteronuclear single quantum coherence (HSQC) NMR spectra were acquired. Deuterated chloroform ($CDCl_3$-*d*) was used as a solvent, and its residual peak is at 7.26 ppm. For the quantitative NMR alternative parameters were applied for more accurate results. A pulse of 45° and relaxation delay of 30 seconds were applied.

A Vapourtec R-Series Integrated Flow chemistry system RS-200 with R2S+ and R2C+ pumping systems, and a UV-150 photochemical reactor performed the flow chemistry experiments. A 150-Watt reactor with a medium pressure mercury lamp was used with a Vapourtec wavelength filter type 3 – red, which filters out light excluding wavelengths from 300 to 2000 nm. The product was collected in fractions automatically by Gilson FC203B fraction collector.

The purification of products was conducted with normal phase flash chromatography (NP-FC) using Combiflash Rf 200 or reversed phase flash chromatography (RP-FC) using Combiflash Rf+ by Teledyne ISCO. For the NP-FC 12 or 24 g RediSepRf Silica columns were used, and for the RP-FC 15,5 or 30 g RediSepRf C18 Gold columns were used.

11.2. Quantitative NMR Spectroscopy

Quantitative NMR spectroscopy measurements were used obtain an estimate of the amount of product in the crude product. 1,3,5-trimethoxybenzene was used as the internal standard. A particular set of parameters were applied for the quantitative NMR measurements. A pulse of 45° and relaxation delay of 30 seconds were applied.

The internal standard was added to each reaction mixture after the reaction was completed, and before starting the work-up. Approximately 30 mg of the internal standard was added to each reaction. The work-up was conducted as mentioned below, and the loss of product due to the work-up would be comparable to the loss of the internal standard. The integrals of the aromatic protons of the internal standard, and the aromatic protons of the product were used for the calculation of the concentration of the product. The concentrations of the products were calculated according to equation 1.

$$c(NMR) = \frac{m_{is} * M_{cp} * I_{cp} * N_{is} * c_{is}}{m_{cp} * M_{is} * I_{is} * N_{cp} * 10}$$

$$Quantitative\ yield = \frac{c(NMR) * m_{cp}}{m_{ty}}$$

c_{is} = concentration of the internal standard (0,99)

m_{is} = mass of the internal standard

I_{is} = integral of the internal standard

N_{is} = number of protons of the internal standard

M_{is} = molecule weight of the internal standard

m_{cp} = mass of the crude product

I_{cp} = integral of the crude product

N_{cp} = number of protons of the crude product

M_{cp} = molecule weight of the crude product

M_{ty}=theoretical yield of the product

11.3. General Methods

11.3.1. General method A

In a 4 ml vial aryl bromide (0.500 mmol, 1 equiv.), amine (0.750 mmol, 1.5 equiv.), DABCO (0.900 mmol, 1.8 equiv.) and degassed DMA (1 ml) were added and stirred. The photocatalyst (4,4'-Di-t-butyl-2,2'-bipyridine)bis[3,5-difluoro-2-(5-trifluoromethyl-2-pyridinyl-kN)phenyl-kC]iridium(III) hexafluorophosphate (0.100 µmol, 0.0002 equiv.) was diluted in DMA (50 µl), and the dilution was added to the reaction mixture. A dual catalyst nickel(II) bromide ethylene dimethyl ether complex (0.025 mmol, 0.05 equiv.) was diluted in DMA (1 ml), and the dilution was added to the reaction mixture. The reaction was performed under a nitrogen atmosphere with a Penn PhD m2 photoreactor (blue LED, 450 nm) at room temperature, with LC-MS or GC-MS reaction monitoring.

Before the work-up 30 mg of trimethoxybenzene as the internal standard was added. The reaction mixture and the internal standard combined were diluted with EtOAc (10 ml) and water (10 ml). The water phase was then extracted with EtOAc (3 x 10 ml), after which the organic phases were combined and washed with water (30 ml) and then dried over Na_2SO_3. The crude product was dried overnight *in vacuo*. The products were purified with a variety of methods using flash chromatography on a Combiflash setup by Teledyne ISCO.

11.3.2. General method B

General method B was identical with general method A with these exceptions:

The aryl bromide was replaced with an aryl iodide, and the photocatalyst was changed to (tris(2,2-bipyridyl)ruthenium(II)chloridehexahydrate (0.300 µmol, 0.0006 equiv.) diluted in DMA (50 µl).

11.3.3. General method C

General method C was identical with general method A with these exceptions:

The aryl bromide was replaced with an aryl iodide.

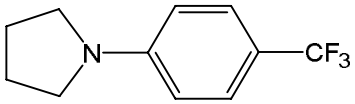

1-(4-(trifluoromethyl)phenyl)pyrrolidine (1)

The reaction was executed following general method A, with the exception of nickel(II) chloride hexahydrate used instead of nickel(II) bromide ethylene glycol dimethyl ether complex. The aryl halide used was 1-bromo-4-(trifluoromethyl)benzene, and the amine was pyrrolidine. The reaction came to a halt at 94 % LC-MS conversion after 15 minutes. The quantitative NMR yield was 91 %. Another reaction to obtain the same product was done with general method A. The quantitative NMR yield for this reaction was 75 %. The product was purified with flash chromatography (heptane). The product was obtained as a white solid, with a purified yield of 70 %, 0,076 g.

^{1}H NMR (400 MHz, Chloroform-*d*): δ ppm 1.97–2.08 (m, 4 H) 3.25–3.37 (m, 4 H) 6.54 (d, *J*=8.62 Hz, 2 H) 7.43 (d, *J*=8.15 Hz, 2 H).

^{13}C NMR (101 MHz, Chloroform-*d*): δ ppm 25.5, 47.5, 110.8, 116.6 (q, *J*=32.6 Hz), 126.4 (q, *J*=3.7 Hz) 126.7 (q, *J*=270.3 Hz) 149.7.

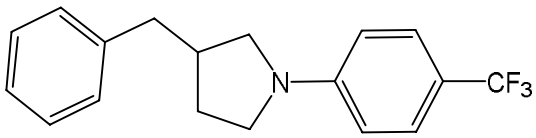

3-benzyl-1-(4-(trifluoromethyl)phenyl)pyrrolidine (2)

The reaction was executed following general method A. The aryl halide used was 1-bromo-4-(trifluoromethyl)benzene, and the amine was 3-benzylpyrrolidine. The reaction came to a halt at 92 % LC-MS conversion after 30 minutes. The quantitative NMR yield was 84 %. The product was purified with flash chromatography (A: heptane, B: heptane:EtOAc 9:1, gradient 0-100 % eluent B). The product was obtained as a white solid, with a purified yield of 66 %, 0,101 g.

^{1}H NMR (400 MHz, Chloroform-*d*): δ ppm 1.71–1.84 (m, 1 H) 2.07–2.18 (m, 1 H) 2.56–2.68 (m, 1 H) 2.73–2.80 (m, 2 H) 3.04 (dd, *J*=8.46 Hz, 1 H) 3.27–3.34 (m, 1 H) 3.38–3.45 (m, 2 H) 6.50 (d, *J*=8.68 Hz, 2 H) 7.13–7.28 (m, 3 H) 7.30–7.33 (m, 2 H) 7.41 (d, *J*=8.44, 2 H).

^{13}C NMR: δ ppm 31.3, 39.6, 40.5, 47.2, 52.8, 110.7, 116.8 (q, *J*=32.5 Hz) 125.3 (q, J=269.8 Hz) 126.3, 126.4 (q, *J*=3.6 Hz) 126.6, 128.5, 128.7, 129.3, 140.4, 149.7.

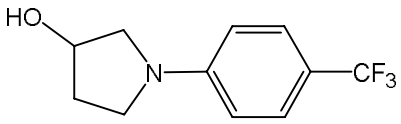

1-(4-(trifluoromethyl)phenyl)pyrrolidin-3-ol (3)

The reaction was executed following general method B. The aryl halide used was 1-iodo-4-(trifluoromethyl)benzene, and the amine was 3-pyrrolidinol. The reaction came to a halt at 80 % LC-MS conversion after 10 minutes. The yield obtained with quantitative NMR from this reaction was 71 %. Another reaction to obtain the same product was done with general method A. The quantitative NMR yield for this reaction was 28 %. The product was purified with flash chromatography (A: heptane, B: EtOAc, gradient 0-100 % eluent B). The product was obtained as a white solid, with a purified yield of 22 %, 0,025 g.

^{1}H NMR (400 MHz, Chloroform-*d*): 1.78 (br s, 1 H) 2.03–2.22 (m, 2 H) 3.29 (d, *J*=10.64 Hz, 1 H) 3.39 (td, *J*=8.91, 3.27 Hz, 1 H) 3.48–3.57 (m, 2 H) 4.62 (br s, 1 H) 6.54 (d, *J*=8.74 Hz, 2 H) 7.44 (d, *J*=8.44 Hz, 2 H).

^{13}C NMR: 34.3, 45.6, 56.3, 71.3, 111.2, 117.5 (q, *J*=32.7 Hz) 125.4 (q, *J*=270.2 Hz) 126.6 (q, *J*=3.7 Hz) 126.8, 129.5, 149.8.

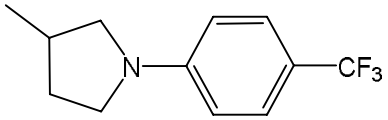

3-methyl-1-(4-(trifluoromethyl)phenyl)pyrrolidine (4)

The reaction was executed following general method C. The aryl halide used was 1-iodo-4-(trifluoromethyl)benzene, and the amine was 3-methylpyrrolidine HCl. Because of the HCl salt, the amount of the base was doubled to 1.8 equiv. The reaction came to a halt at 88 % LC-MS conversion after 90 minutes. The yield obtained with quantitative NMR from this reaction was 58 %. Another reaction to obtain the same product was done with general method A. The quantitative NMR yield for this reaction was 50 %. The product was purified with flash chromatography (A: heptane, B: heptane:EtOAc 9:1, gradient 0-100 % eluent B). Some internal standard was left after the purification, so the reaction was repeated without the internal standard. The product was obtained as a white solid, with a purified yield of 28 %, 0,033 g.

^{1}H NMR (400 MHz, Chloroform-*d*): 1.14 (d, *J*=6.66 Hz, 3 H) 1.60–1.69 (m, 1 H) 2.11–2.19 (m, 1 H) 2.34 –2.47 (m, 1 H) 2.85–2.91 (m, 1 H) 3.28–3.49 (m, 3 H) 6.51 (d, *J*=8.62 Hz, 2 H) 7.42 (d, *J*=8.11 Hz, 2 H).

^{13}C NMR: 18.4, 33.5, 33.6, 47.6, 55.0, 110.8, 116.8 (q, *J*=32.3 Hz) 119.5, 125.6 (q, *J*=269.9 Hz) 126.6 (q, *J*=3.7 Hz) 149.9.

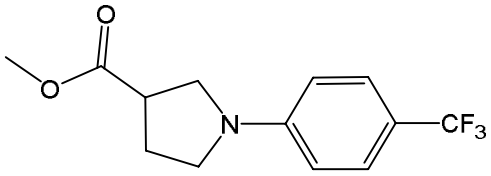

Methyl 1-(4-(trifluoromethyl)phenyl)pyrrolidine-3-carboxylate (5)

The reaction was executed following general method A. The aryl halide used was 1-bromo-4-(trifluoromethyl)benzene, and the amine was methyl pyrrolidine-3-carboxylate hydrochloride. The reaction came to a halt at 91 % LC-MS conversion after 160 minutes. The reaction was monitored with GC-MS. The quantitative NMR yield was 58 %. The product was purified with flash chromatography (A: heptane, B: EtOAc, gradient 0-50 % eluent B). The product was obtained as a white solid, with a purified yield of 40 %, 0,055 g.

^{1}H NMR (400 MHz, Chloroform-*d*): 2.25–2.38 (m, 2 H) 3.17–3.31 (m, 1 H) 3.34–3.50 (m, 2 H) 3.52–3.64 (m, 2 H) 3.74 (s, 3 H) 6.55 (d, *J*=8.62 Hz, 2 H) 7.44 (d, *J*=8.10 Hz, 2 H).

^{13}C NMR: 28.7, 43.1, 47.2, 50.1, 52.4, 111.3, 117.7 (q, *J*=32.1 Hz) 125.4 (q, *J*=271.1 Hz) 126.6 (q, *J*=3.6 HZ).

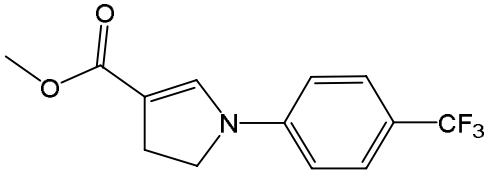

Methyl 1-(4-(trifluoromethyl)phenyl)-4,5-dihydro-1*H*-pyrrole-3-carboxylate (6)

This product was obtained as a side product of the reaction for methyl 1-(4-(trifluoromethyl)phenyl)pyrrolidine-3-carboxylate. The reaction conditions followed general method A. The aryl halide used was 1-bromo-4-(trifluoromethyl)benzene, and the amine was methyl pyrrolidine-3-carboxylate hydrochloride. The reaction time and conversion were not determined due to the original product peak overlapping the side product peak. In subsequent GC-MS monitored reactions the side product was produced in 1:10 compared to the original product. The product was purified with flash chromatography (A: heptane, B: EtOAc, gradient 0-50 % eluent B). The product was obtained as a white solid with a purified yield of 5 %, 0,0073 g. The structure of the side product was confirmed with ^{1}H and ^{13}C NMR spectroscopy.

^{1}H NMR (400 MHz, Chloroform-*d*): 2.93–3.03 (m, 2 H) 3.75 (s, 3 H) 3.97 (dd, *J*=10.48, 9.26 Hz, 2 H) 6.91 (d, *J*=8.16 Hz, 2 H) 7.53 (d, *J*=8.13 Hz, 2 H) 7.72 (t, *J*=1.56 Hz, 1 H).

^{13}C NMR: 27.0, 27.1, 49.5, 51.1, 109.2, 113.3, 122.3 (q, *J*=32.9 Hz) 124.4 (q, *J*=271.3 Hz) 126.8 (q, *J*=3.6 Hz) 128.5, 140.9, 144.1, 166.2.

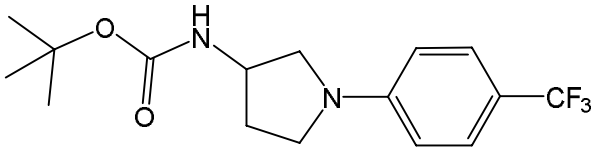

***tert*-Butyl (1-(4-(trifluoromethyl)phenyl)pyrrolidin-3-yl)carbamate (7)**

The reaction was executed following general method B. The aryl halide used was 1-iodo-4-(trifluoromethyl)benzene, and the amine was 3-(tert-butoxycarbonylamino)pyrrolidine. The reaction came to a halt at 88 % LC-MS conversion after 15 minutes. The yield obtained with quantitative NMR from this reaction was 69 %. Another reaction to obtain the same product was done with general method A. The quantitative NMR yield for this reaction was 66 %. The reaction time for this variation was 70 minutes. This product was purified with flash chromatography (A: heptane, B: MTBE, gradient 0-50 % eluent B). The product was obtained as a white solid, with a purified yield of 50 %, 0,083 g.

^{1}H NMR (400 MHz, Chloroform-*d*): 1.45 (s, 9 H) 1.92–2.02 (m, 1 H) 2.24–2.35 (m, 1 H) 3.14–3.23 (m, 1 H) 3.32 - 3.49 (m, 2 H) 3.56–3.64 (m, 1 H) 4.37 (br s, 1 H) 4.71 (br s, 1 H) 6.54 (d, *J*=8.62 Hz, 2 H) 7.44 (d, *J*=8.13 Hz, 2 H).

^{13}C NMR: 28.6, 31.9, 45.9, 50.6, 53.9, 80.1, 111.2, 117.8 (q, *J*=32.6 Hz) 125.4 (q, *J*=269.8 Hz) 126.7 (q, *J*=4.0 Hz) 129.4, 149.6, 155.5.

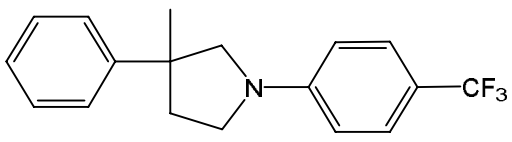

3-methyl-3-phenyl-1-(4-(trifluoromethyl)phenyl)pyrrolidine (8)

The reaction was executed following general method A. The aryl halide used was 1-bromo-4-(trifluoromethyl)benzene, and the amine was 3-methyl-3-phenylpyrrolidine. The reaction came

to a halt at 91 % LC-MS conversion after 30 minutes. The quantitative NMR yield was 75 %. The product was purified with flash chromatography (A: heptane, B: heptane:EtOAc 9:1, gradient 0-100 % eluent B). Some internal standard was left after the purification, so the reaction was repeated without the internal standard. The product was obtained as a white solid, with a purified yield of 60 %, 0,046 g.

^{1}H NMR (400 MHz, Chloroform-*d*): 1.43 (s, 3 H) 2.17–2.39 (m, 2 H) 3.38–3.64 (m, 4 H) 6.58 (d, *J*=8.68 Hz, 2 H) 7.20–7.39 (m, 5 H) 7.46 (d, *J*=8.38 Hz, 2 H).

^{13}C NMR: 28.0, 37.7, 45.7, 46.6, 59.3, 110.7, 117.0 (q, *J*=32.7 Hz) 125.3 (q, *J*=270.6 Hz) 125.6, 126.40, 126.44, 126.48, 126.51, 128.6, 147.3, 149.6.

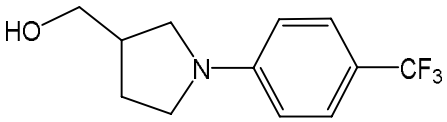

(1-(4-(trifluoromethyl)phenyl)pyrrolidin-3-yl)methanol (9)

The reaction was executed following general method A. The aryl halide used was 1-bromo-4-(trifluoromethyl)benzene, and the amine was 3-pyrrolidinemethanol. The reaction came to a halt at 97 % LC-MS conversion after 30 minutes. The quantitative NMR yield was 83 %. The product was purified with flash chromatography (A: heptane, B: EtOAc, gradient 0-100 % eluent B). The product was obtained as a white solid, with a purified yield of 64 %, 0,079 g.

^{1}H NMR (400 MHz, Chloroform-*d*): 1.52 (m, 1 H) 1.80–1.92 (m, 1 H) 2.12–2.22 (m, 1 H) 2.53–2.66 (m, 1 H) 3.13–3.20 (m, 1 H) 3.29–3.52 (m, 3 H) 3.62–3.77 (m, 2 H) 6.55 (d, *J*=8.68 Hz, 2 H) 7.42–7.46 (m, 2 H).

^{13}C NMR: 27.8, 40.9, 47.0, 50.4, 64.9, 110.9, 117.0 (q, *J*=32.7 Hz) 125.3 (q, *J*=269.3 Hz) 126.4 (q, *J*=3.7 Hz) 149.7.

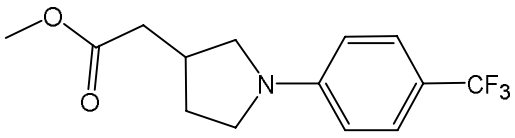

Methyl 2-(1-(4-(trifluoromethyl)phenyl)pyrrolidine-3-yl)acetate (10)

The reaction was executed following general method B. The aryl halide used was 1-iodo-4-(trifluoromethyl)benzene, and the amine was methyl 2-(pyrrolidine-3-yl)acetate hydrochloride. The reaction came to a halt at 86 % GC-MS conversion after 20 minutes. The reaction was monitored with GC-MS. The yield obtained with quantitative NMR from this reaction was 90 %. Another reaction to obtain the same product was done with general method A. The reaction time for this variation was 70 minutes. The quantitative NMR yield was 41 %. The product was purified with flash chromatography (A: heptane, B: heptane:EtOAc 9:1, gradient 0-100 % eluent B). The product was obtained as a white solid, with a purified yield of 21 %, 0,030 g.

^{1}H NMR (400 MHz, Chloroform-*d*): 1.69–1.80 (m, 1 H) 2.21–2.31 (m, 1 H) 2.51 (m, 2 H) 2.69–2.83 (m, 1 H) 2.97–3.06 (m, 1 H) 3.29–3.46 (m, 2 H) 3.54–3.62 (m, 1 H) 3.71 (s, 3 H) 6.53 (d, *J*=8.62 Hz, 2 H) 7.38–7.49 (m, 2 H).

^{13}C NMR: 31.5, 35.2, 38.0, 47.2, 52.0, 53.1, 111.0, 117.3 (q, *J*=32.6 Hz) 125.5 (q, *J*=269.9 Hz) 126.6 (q, *J*=3.6 Hz) 149.7, 172.9.

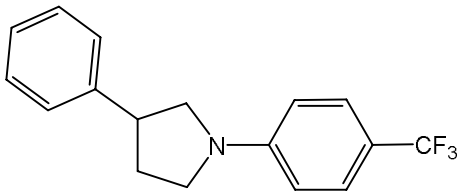

3-phenyl-1-(4-(trifluoromethyl)phenyl)pyrrolidine (11)

The reaction was executed following general method A. The aryl halide used was 1-bromo-4-(trifluoromethyl)benzene, and the amine was 3-phenylpyrrolidine. The reaction came to a halt at 99 % LC-MS conversion after 50 minutes. The quantitative NMR yield was 85 %. The product was purified with flash chromatography (A: heptane, B: heptane:EtOAc 9:1, gradient 0-100 % eluent B). Some internal standard was left after the purification, so the reaction was repeated without the internal standard. The product was obtained as a white solid, with a purified yield of 65 %, 0,095 g.

^{1}H NMR (400 MHz, Chloroform-*d*): 2.08–2.23 (m, 1 H) 2.39–2.49 (m, 1 H) 3.36–3.59 (m, 4 H) 3.69–3.82 (m, 1 H) 6.58 (d, *J*=8.62 Hz, 2 H) 7.21–7.48 (m, 7 H).

^{13}C NMR: 33.3, 44.2, 47.7, 54.5, 111.0, 117.3 (q, *J*=32.2 Hz) 120.0, 125.50 (q, *J*=270.5 Hz) 125.51, 126.7 (q, *J*=3.8 Hz) 127.1, 127.3, 128.7, 128.9, 142.2, 149.7.

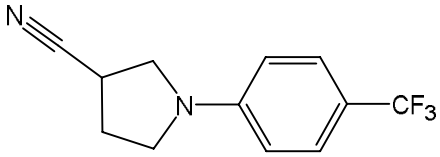

1-(4-(trifluoromethyl)phenyl)pyrrolidine-3-carbonitrile (12)

The reaction was executed following general method A. The aryl halide used was 1-bromo-4-(trifluoromethyl)benzene, and the amine was pyrrolidine-3-carbonitrile. The reaction came to a halt at 88 % LC-MS conversion after 50 minutes. The quantitative NMR yield was 74 %. The product was purified with flash chromatography (A: heptane, B: EtOAc, gradient 0-100 % eluent B). The product was obtained as a white solid, with a purified yield of 65 %, 0,078 g.

^{1}H NMR (400 MHz, Chloroform-*d*): 2.34–2.50 (m, 2 H) 3.21–3.35 (m, 1 H) 3.41–3.48 (m, 1 H) 3.50–3.71 (m, 3 H) 6.57 (d, *J*=8.62 Hz, 2 H) 7.48 (d, *J*=8.10 Hz, 2 H).

^{13}C NMR: 28.4, 30.0, 46.6, 50.9, 111.62, 118.9 (q, *J*=32.7 Hz) 120.35, 125.2 (q, *J*=270.1 Hz) 126.81 (q, *J*=3.7 Hz) 148.9.

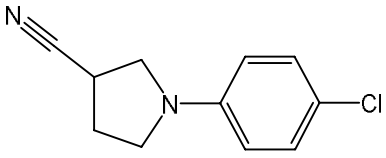

1-(4-chlorophenyl)pyrrolidine-3-carbonitrile (13)

The reaction was executed following general method A. The aryl halide used was 4-bromochlorobenzene, and the amine was pyrrolidine-3-carbonitrile. The reaction came to a halt at 72 % LC-MS conversion after 190 minutes. The quantitative NMR yield was 57 %. The product was purified with flash chromatography (A: heptane, B: EtOAc, gradient 0-50 % eluent B). The product was obtained as a white solid, with a purified yield of 41 %, 0,043 g. This reaction was upscaled to 2 mmol scale, an increase of 1,5 mmol. Similar reaction conditions

were applied. The product was obtained as a white solid, with quantitative NMR yield of 63 %, and a purified yield of 48 %, 0,197 g. The purity of the product was determined by a chromatographic purity measurement.

^{1}H NMR (400 MHz, Chloroform-*d*): 2.32–2.48 (m, 2 H) 3.20–3.32 (m, 1 H) 3.36–3.42 (m, 1 H) 3.46–3.65 (m, 3 H) 6.42–6.54 (m, 2 H) 7.14–7.25 (m, 2 H).

^{13}C NMR: 28.4, 30.0, 46.9, 51.2, 113.4, 115.3, 120.7, 122.3, 129.3, 129.8, 145.5.

HPLC purity: 97 %

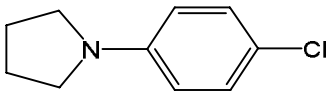

1-(4-chlorophenyl)pyrrolidine (14)

The reaction was executed following general method A. The aryl halide used was 4-bromochlorobenzene, and the amine was pyrrolidine. The reaction came to a halt at 84 % LC-MS conversion after 20 minutes. The quantitative NMR yield was 51 %. The product was purified with reversed phase flash chromatography (A: NH_4OH/water, B: ACN, gradient 0-100 % eluent B). An issue with the chromatography or the collection of fragments occurred, and therefore no reliable yield for the purified product can be presented. A 1H NMR spectrum was obtained successfully. The product was obtained as a white solid.

^{1}H NMR (400 MHz, Chloroform-*d*): 1.93–2.08 (m, 4 H) 3.18–3.29 (m, 4 H) 6.46 (d, *J*=7.98 Hz, 2 H) 7.09–7.26 (m, 2 H).

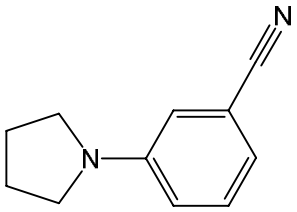

3-(pyrrolidin-1-yl)benzonitrile (15)

The reaction was executed following general method A. The aryl halide used was *m*-bromobenzonitrile, and the amine was pyrrolidine. The reaction came to a halt at 87 % LC-MS

conversion after 15 minutes. The quantitative NMR yield was 78 %. The product was purified with reversed phase flash chromatography (A:NH_4OH/water, B: ACN, gradient 0-100 % eluent B). An issue with the chromatography or the collection of fragments occurred, and therefore no reliable yield for the purified product can be presented. The product was obtained as a white solid.

^{1}H NMR (400 MHz, Chloroform-*d*): 1.98–2.09 (m, 4 H) 3.22–3.33 (m, 4 H) 6.68–6.77 (m, 2 H) 6.89 (dt, *J*=7.49, 1.18 Hz, 1 H) 7.22–7.28 (m, 1 H).

^{13}C NMR: 25.6, 24.7, 112.9, 114.4, 115.9, 118.7, 120.1, 129.9, 147.8.

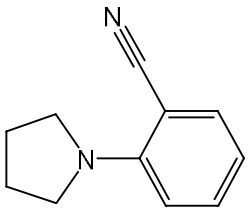

2-(pyrrolidin-1-yl)benzonitrile (16)

The reaction was executed following general method A. The aryl halide used was *o*-bromobenzonitrile, and the amine was pyrrolidine. The reaction came to a halt at 83 % LC-MS conversion after 30 minutes. The quantitative NMR yield was 74 %. The product was purified with reversed phase flash chromatography (A:NH_4OH/water, B: ACN, gradient 0-100 % eluent B). An issue with the chromatography or the collection of fragments occurred, and therefore no reliable yield for the purified product can be presented. The product was obtained as a white solid.

^{1}H NMR (400 MHz, Chloroform-*d*): 1.95–2.06 (m, 4 H) 3.55–3.66 (m, 4 H) 6.59–6.68 (m, 2 H) 7.28–7.36 (m, 1 H) 7.44 (d, *J*=7.63 Hz, 1 H).

^{13}C NMR: 25.9, 50.0, 94.4, 114.4, 116.0, 121.7, 133.6, 135.9, 150.2.

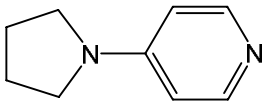

4-(pyrrolidin-1-yl)pyridine (17)

The reaction was executed following general method A. The aryl halide used was 4-bromopyridine HCl, and the amine was pyrrolidine. Because of the HCl salt, the amount of the base was doubled to 1.8 equiv. The reaction came to a halt at 83 % LC-MS conversion after 30 minutes. The quantitative NMR yield was 50 %. The product was purified with reversed phase flash chromatography (A:NH_4OH/water, B: ACN, gradient 0-100 % eluent B). An issue with the chromatography or the collection of fragments occurred, and therefore no reliable yield for the purified product can be presented. The product was obtained as a white solid.

^{1}H NMR (400 MHz, Chloroform-*d*): 2.01–2.12 (m, 4 H) 3.18–3.41 (m, 4 H) 6.44 (d, *J*=5.79 Hz, 2 H) 8.20 (d, *J*=6.54 Hz, 2 H).

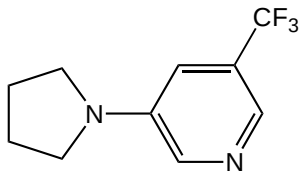

3-(pyrrolidin-1-yl)-5-(trifluoromethyl)pyridine (18)

The reaction was executed following general method A. The aryl halide used was 3-bromo-5-(trifluoromethyl)pyridine, and the amine was pyrrolidine. The reaction reached 100 % LC-MS conversion after 10 minutes. The quantitative NMR yield was 72 %. The product was purified with reversed phase flash chromatography (A:NH_4OH/water, B: ACN, gradient 0-100 % eluent B). An issue with the chromatography or the collection of fragments occurred, and therefore no reliable yield for the purified product can be presented. The product was obtained as a white solid.

^{1}H NMR (400 MHz, Chloroform-*d*): 2.01–2.12 (m, 4 H) 3.29–3.40 (m, 4 H) 6.93 (t, *J*=2.20 Hz, 1 H) 8.11 (d, *J*=2.75 Hz, 1 H) 8.15 (s, 1 H).

^{13}C NMR: 25.6, 47.6, 113.9, 124.2 (q, *J*=272.9 Hz) 126.8 (q, *J*=31.9 Hz) 133.0 (q, *J*=4.3 Hz) 137.44, 143.2.

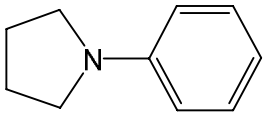

1-phenylpyrrolidine (19)

The reaction was executed following general method C. The aryl halide used was iodobenzene, and the amine was pyrrolidine. The reaction came to a halt at 78 % LC-MS conversion after 30 minutes. The quantitative NMR yield was 73 %. The product was purified with reversed phase flash chromatography (A: NH_4OH/water, B: ACN, gradient 0-100 % eluent B). An issue with the chromatography or the collection of fragments occurred, and therefore no reliable yield for the purified product can be presented. The reaction was conducted first with general method A and a normal phase chromatography purification, but the NMR yield and the purification performed worse than the forementioned method. No purified product was obtained, but the product could be identified from the crude product ^{1}H NMR when compared to literary values[88].

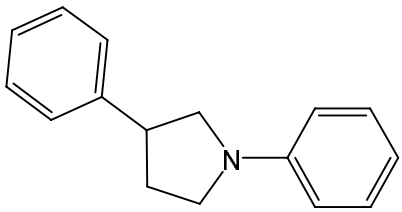

1,3-diphenylpyrrolidine (20)

The reaction was executed following general method A. The aryl halide used was bromobenzene, and the amine was 3-phenylpyrrolidine. The reaction came to a halt at 63 % LC-MS conversion after 60 minutes. The quantitative NMR yield was 23 %. The product was purified with flash chromatography (A: heptane, B: heptane:EtOAc 9:1, gradient 0-100 % eluent B). The product was obtained as a white solid, with a purified yield of 18 %, 0,020 g.

^{1}H NMR (400 MHz, Chloroform-*d*): δ ppm 2.06–2.20 (m, 1 H) 2.36–2.48 (m, 1 H) 3.32–3.57 (m, 4 H) 3.67–3.76 (m, 1 H) 6.56–6.64 (m, 2 H) 6.65–6.73 (m, 1 H) 7.16–7.24 (m, 2 H) 7.26–7.41 (m, 6 H).

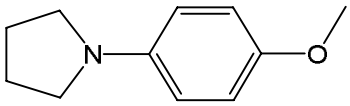

1-(4-methoxyphenyl)pyrrolidine (21)

The reaction was executed following general method C. The aryl halide used was 4-iodoanisole, and the amine was pyrrolidine. The reaction came to a halt at 50 % LC-MS conversion after 60 minutes. The quantitative NMR yield was 49 %. The product was purified with reversed phase flash chromatography (A: NH_4OH/water, B: ACN, gradient 0-100 % eluent B). An issue with the chromatography or the collection of fragments occurred, and therefore no reliable yield for the purified product can be presented. No purified product was obtained, but the product could be identified from the crude product ^1H NMR when compared to literary values.[89]

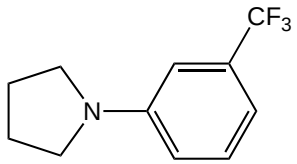

1-(3-(trifluoromethyl)phenyl)pyrrolidine (22)

The reaction was executed following general method C. The aryl halide used was 3-iodobenzotrifluoride, and the amine was pyrrolidine. The reaction came to a halt at 88 % LC-MS conversion after 10 minutes. The quantitative NMR yield was 76 %. The product was purified with reversed phase flash chromatography (A: NH_4OH/water, B: ACN, gradient 0-100 % eluent B). An issue with the chromatography or the collection of fragments occurred, and therefore no reliable yield for the purified product can be presented. No purified product was obtained, but the product could be identified from the crude product ^1H NMR when compared to literary values.[90]

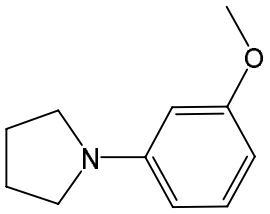

1-(3-methoxyphenyl)pyrrolidine (23)

The reaction was executed following general method C. The aryl halide used was 3-iodoanisole, and the amine was pyrrolidine. The reaction came to a halt at 78 % LC-MS conversion after 20 minutes. The quantitative NMR yield was 70 %. The product was purified with reversed phase flash chromatography (A: NH_4OH/water, B: ACN, gradient 0-100 % eluent B). An issue with the chromatography or the collection of fragments occurred, and therefore no reliable yield for the purified product can be presented. No purified product was obtained, but the product could be identified from the crude product ^1H NMR when compared to literary values.[91]

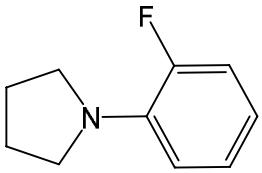

1-(2-fluorophenyl)pyrrolidine (24)

The reaction was executed following general method A. The aryl halide used was1-bromo-2-fluorobenzene, and the amine was pyrrolidine. The reaction came to a halt at 72 % LC-MS conversion after 40 minutes. The quantitative NMR yield was 41 %. The product was purified with reversed phase flash chromatography (A: NH_4OH/water, B: ACN, gradient 0-100 % eluent B). An issue with the chromatography or the collection of fragments occurred, and therefore no reliable yield for the purified product can be presented. No purified product was obtained, but the product could be identified from the crude product ^1H NMR when compared to literary values.[92]

12. References

(1) Bhunia, S.; Pawar, G. G.; Kumar, S. V.; Jiang, Y.; Ma, D. Selected Copper-Based Reactions for C−N, C−O, C−S, and C−C Bond Formation. *Angewandte Chemie International Edition* **2017,** *56* (51), 16136.

(2) Brown, D. G.; Boström, J. Analysis of Past and Present Synthetic Methodologies on Medicinal Chemistry: Where Have All the New Reactions Gone? *Journal of Medicinal Chemistry* **2016,** *59* (10), 4443.

(3) Ley, S. V.; Thomas, A. W. Modern Synthetic Methods for Copper-Mediated C(aryl)-O, C(aryl)-N, and C(aryl)-S Bond Formation. *Angewandte Chemie International Edition* **2003,** *42* (44), 5400.

(4) Beletskaya, I. P.; Cheprakov, A. V. Copper in cross-coupling reactions: The post-Ullmann chemistry. *Coordination Chemistry Reviews* **2004,** *248* (21), 2337.

(5) Cavedon, C.; Seeberger, P. H.; Pieber, B. Photochemical Strategies for Carbon–Heteroatom Bond Formation. *European Journal of Organic Chemistry* **2020,** *2020* (10), 1379.

(6) Shaw, M. H.; Twilton, J.; MacMillan, D. W. C. Photoredox Catalysis in Organic Chemistry. *The Journal of Organic Chemistry* **2016,** *81* (16), 6898.

(7) Bogdos, M. K.; Pinard, E.; Murphy, J. A. Applications of organocatalysed visible-light photoredox reactions for medicinal chemistry. *Beilstein Journal of Organic Chemistry* **2018,** *14*, 2035.

(8) Du, Y.; Pearson, R. M.; Lim, C. H.; Sartor, S. M.; Ryan, M. D.; Yang, H.; Damrauer, N. H.; Miyake, G. M. Strongly Reducing, Visible-Light Organic Photoredox Catalysts as Sustainable Alternatives to Precious Metals. *Chemistry* **2017,** *23* (46), 10962.

(9) Blakemore, D. C.; Castro, L.; Churcher, I.; Rees, D. C.; Thomas, A. W.; Wilson, D. M.; Wood, A. Organic synthesis provides opportunities to transform drug discovery. *Nature Chemistry* **2018,** *10* (4), 383.

(10) Carreira, E. M.; Fessard, T. C. Four-Membered Ring-Containing Spirocycles: Synthetic Strategies and Opportunities. *Chemical Reviews* **2014,** *114* (16), 8257.

(11) Willcox, D.; Chappell, B. G. N.; Hogg, K. F.; Calleja, J.; Smalley, A. P.; Gaunt, M. J. A general catalytic β-C–H carbonylation of aliphatic amines to β-lactams. *Science* **2016,** *354* (6314), 851.

(12) Ruffoni, A.; Julia, F.; Svejstrup, T. D.; McMillan, A. J.; Douglas, J. J.; Leonori, D. Practical and regioselective amination of arenes using alkyl amines. *Nat. Chem.* **2019,** *11* (5), 426.

(13) Tucker, J. W.; Stephenson, C. R. J. Shining Light on Photoredox Catalysis: Theory and Synthetic Applications. *The Journal of Organic Chemistry* **2012,** *77* (4), 1617.

(14) Twilton, J.; Le, C.; Zhang, P.; Shaw, M. H.; Evans, R. W.; MacMillan, D. W. C. The merger of transition metal and photocatalysis. *Nature Reviews Chemistry* **2017,** *1* (7), 52.

(15) Teegardin, K.; Day, J. I.; Chan, J.; Weaver, J. Advances in Photocatalysis: A Microreview of Visible Light Mediated Ruthenium and Iridium Catalyzed Organic Transformations. *Organic Process Research & Development* **2016,** *20* (7), 1156.

(16) McAtee, R. C.; McClain, E. J.; Stephenson, C. R. J. Illuminating Photoredox Catalysis. *Trends in Chemistry* **2019,** *1* (1), 111.

(17) Marzo, L.; Pagire, S. K.; Reiser, O.; Konig, B. Visible-Light Photocatalysis: Does It Make a Difference in Organic Synthesis? *Angew Chem Int Ed Engl* **2018,** *57* (32), 10034.

(18) Miyabe, H. *Organic Reactions Promoted by Metal-Free Organic Dyes Under Visible Light Irradiation, Visible-Light Photocatalysis of Carbon-Based Materials*: IntechOpen, 2017.

(19) Gaya, U. I. In *Heterogeneous Photocatalysis Using Inorganic Semiconductor Solids*; Springer Netherlands: Dordrecht, 2014, DOI:10.1007/978-94-007-7775-0_1 10.1007/978-94-007-7775-0_1.

(20) Wenger, O. S. Photoactive Complexes with Earth-Abundant Metals. *J Am Chem Soc* **2018,** *140* (42), 13522.

(21) Ghosh, I.; Khamrai, J.; Savateev, A.; Shlapakov, N.; Antonietti, M.; König, B. Organic semiconductor photocatalyst can bifunctionalize arenes and heteroarenes. *Science* **2019,** *365* (6451), 360.

(22) Svejstrup, T. D.; Ruffoni, A.; Juliá, F.; Aubert, V. M.; Leonori, D. Synthesis of Arylamines via Aminium Radicals. *Angewandte Chemie International Edition* **2017,** *56* (47), 14948.

(23) Osawa, M.; Nagai, H.; Akita, M. Photo-activation of Pd-catalyzed Sonogashira coupling using a Ru/bipyridine complex as energy transfer agent. *Dalton Transactions* **2007**, DOI:10.1039/B618007H 10.1039/B618007H(8), 827.

(24) McLean, E. B.; Lee, A.-L. Dual copper- and photoredox-catalysed reactions. *Tetrahedron* **2018,** *74* (38), 4881.

(25) Corcoran, E. B.; Pirnot, M. T.; Lin, S.; Dreher, S. D.; DiRocco, D. A.; Davies, I. W.; Buchwald, S. L.; MacMillan, D. W. C. Aryl amination using ligand-free Ni(II) salts and photoredox catalysis. *Science* **2016,** *353* (6296), 279.

(26) Yoo, W.-J.; Tsukamoto, T.; Kobayashi, S. Visible-Light-Mediated Chan–Lam Coupling Reactions of Aryl Boronic Acids and Aniline Derivatives. *Angewandte Chemie International Edition* **2015,** *54* (22), 6587.

(27) Choi, S.; Chatterjee, T.; Choi, W. J.; You, Y.; Cho, E. J. Synthesis of Carbazoles by a Merged Visible Light Photoredox and Palladium-Catalyzed Process. *ACS Catalysis* **2015,** *5* (8), 4796.

(28) An, X.-D.; Yu, S. Photoredox-catalyzed C(sp2)–N coupling reactions. *Tetrahedron Letters* **2018,** *59* (17), 1605.

(29) Stephenson, C. R. J. Y., Tehshik P. MacMillan, David W. C. *Visible Light Photocatalysis in Organic Chemistry - 6.1.2 Classes of Organic Photocatalysts.*; John Wiley & Sons, 2018.

(30) Romero, N. A.; Nicewicz, D. A. Organic Photoredox Catalysis. *Chemical Reviews* **2016,** *116* (17), 10075.

(31) McManus, J. B.; Nicewicz, D. A. Direct C–H Cyanation of Arenes via Organic Photoredox Catalysis. *Journal of the American Chemical Society* **2017,** *139* (8), 2880.

(32) Romero, N. A.; Margrey, K. A.; Tay, N. E.; Nicewicz, D. A. Site-selective arene C-H amination via photoredox catalysis. *Science* **2015,** *349* (6254), 1326.

(33) Friedmann, D.; Hakki, A.; Kim, H.; Choi, W.; Bahnemann, D. Heterogeneous photocatalytic organic synthesis: state-of-the-art and future perspectives. *Green Chemistry* **2016,** *18* (20), 5391.

(34) Liu, Y.-Y.; Liang, D.; Lu, L.-Q.; Xiao, W.-J. Practical heterogeneous photoredox/nickel dual catalysis for C–N and C–O coupling reactions. *Chemical Communications* **2019,** *55* (33), 4853.

(35) Lim, C.-H.; Kudisch, M.; Liu, B.; Miyake, G. M. C–N Cross-Coupling via Photoexcitation of Nickel–Amine Complexes. *Journal of the American Chemical Society* **2018,** *140* (24), 7667.

(36) Kaur, S.; Kumar, M.; Bhalla, V. Supramolecular ensemble of PBI derivative and copper nanoparticles: a light harvesting antenna for photocatalytic C(sp2)–H functionalization. *Green Chemistry* **2016,** *18* (21), 5870.

(37) Zhang, Y.; Zhu, P.; Li, G.; Zhao, T.; Fu, X.; Sun, R.; Zhou, F.; Wong, C.-p. Facile Preparation of Monodisperse, Impurity-Free, and Antioxidation Copper Nanoparticles on a Large Scale for Application in Conductive Ink. *ACS Applied Materials & Interfaces* **2014,** *6* (1), 560.

(38) Brumbaugh, A. D.; Cohen, K. A.; St. Angelo, S. K. Ultrasmall Copper Nanoparticles Synthesized with a Plant Tea Reducing Agent. *ACS Sustainable Chemistry & Engineering* **2014,** *2* (8), 1933.

(39) Wang, B.; Chen, S.; Nie, J.; Zhu, X. Facile method for preparation of superfine copper nanoparticles with high concentration of copper chloride through photoreduction. *RSC Advances* **2014,** *4* (52), 27381.

(40) Liu, L.; Choi, B. G.; Tung, S. O.; Hu, T.; Liu, Y.; Li, T.; Zhao, T.; Kotov, N. A. Low-current field-assisted assembly of copper nanoparticles for current collectors. *Faraday Discussions* **2015,** *181* (0), 383.

(41) Xu, L.; Peng, J.; Srinivasakannan, C.; Zhang, L.; Zhang, D.; Liu, C.; Wang, S.; Shen, A. Q. Synthesis of copper nanoparticles by a T-shaped microfluidic device. *RSC Advances* **2014,** *4* (48), 25155.

(42) Singh, G.; Kumar, M.; Bhalla, V. Ultrafine hybrid Cu2O-Fe2O3 nanoparticles stabilized by hexaphenylbenzene-based supramolecular assemblies: a photocatalytic system for the Ullmann-Goldberg coupling reaction. *Green Chem.* **2018,** *20* (23), 5346.

(43) Park, B. Y.; Pirnot, M. T.; Buchwald, S. L. Visible Light-Mediated (Hetero)aryl Amination Using Ni(II) Salts and Photoredox Catalysis in Flow: A Synthesis of Tetracaine. *The Journal of Organic Chemistry* **2020,** *85* (5), 3234.

(44) Harper, K. C.; Moschetta, E. G.; Bordawekar, S. V.; Wittenberger, S. J. A Laser Driven Flow Chemistry Platform for Scaling Photochemical Reactions with Visible Light. *ACS Cent Sci* **2019,** *5* (1), 109.

(45) Chatterjee, S.; Guidi, M.; Seeberger, P. H.; Gilmore, K. Automated radial synthesis of organic molecules. *Nature* **2020,** *579* (7799), 379.

(46) Masanori, K.; Masayuki, K.; Toshihiko, M. Palladium-catalyzed aromatic amination of aryl bromides with N,N-diethylamino-tributyltin. *Chemistry Letters* **1983,** *12* (6), 927.

(47) Guram, A. S.; Buchwald, S. L. Palladium-Catalyzed Aromatic Aminations with in situ Generated Aminostannanes. *Journal of the American Chemical Society* **1994,** *116* (17), 7901.

(48) Paul, F.; Patt, J.; Hartwig, J. F. Palladium-catalyzed formation of carbon-nitrogen bonds. Reaction intermediates and catalyst improvements in the hetero cross-coupling of aryl halides and tin amides. *Journal of the American Chemical Society* **1994,** *116* (13), 5969.

(49) Guram, A. S.; Rennels, R. A.; Buchwald, S. L. A Simple Catalytic Method for the Conversion of Aryl Bromides to Arylamines. *Angewandte Chemie International Edition in English* **1995,** *34* (12), 1348.

(50) Louie, J.; Hartwig, J. F. Palladium-catalyzed synthesis of arylamines from aryl halides. Mechanistic studies lead to coupling in the absence of tin reagents. *Tetrahedron Letters* **1995,** *36* (21), 3609.

(51) Dorel, R.; Grugel, C. P.; Haydl, A. M. The Buchwald–Hartwig Amination After 25 Years. *Angewandte Chemie International Edition* **2019,** *58* (48), 17118.

(52) Ruiz-Castillo, P.; Buchwald, S. L. Applications of Palladium-Catalyzed C–N Cross-Coupling Reactions. *Chemical Reviews* **2016,** *116* (19), 12564.

(53) Veisi, H.; Safarimehr, P.; Hemmati, S. Buchwald–Hartwig C–N cross coupling reactions catalyzed by palladium nanoparticles immobilized on thio modified-multi walled carbon nanotubes as heterogeneous and recyclable nanocatalyst. *Materials Science and Engineering: C* **2019,** *96*, 310.

(54) Veisi, H.; Sarachegol, P.; Hemmati, S. Palladium(II) anchored on polydopamine coated-magnetic nanoparticles (Fe3O4@PDA@Pd(II)): A heterogeneous and core–shell nanocatalyst in Buchwald–Hartwig C–N cross coupling reactions. *Polyhedron* **2018,** *156*, 64.

(55) Nirmala, M.; Saranya, G.; Viswanathamurthi, P.; Bertani, R.; Sgarbossa, P.; Malecki, J. G. Organonickel complexes encumbering bis-imidazolylidene carbene ligands: Synthesis, X-ray structure and catalytic insights on Buchwald-Hartwig amination reactions. *Journal of Organometallic Chemistry* **2017,** *831*, 1.

(56) Topchiy, M. A.; Asachenko, A. F.; Nechaev, M. S. Solvent-Free Buchwald–Hartwig Reaction of Aryl and Heteroaryl Halides with Secondary Amines. *European Journal of Organic Chemistry* **2014,** *2014* (16), 3319.

(57) Zhou, Y.-P.; Raoufmoghaddam, S.; Szilvási, T.; Driess, M. A Bis(silylene)-Substituted ortho-Carborane as a Superior Ligand in the Nickel-Catalyzed Amination of Arenes. *Angewandte Chemie International Edition* **2016,** *55* (41), 12868.

(58) Moghaddam, F. M.; Tavakoli, G.; Moafi, A.; Saberi, V.; Rezvani, H. R. C□N Bond Formation Using Highly Effective and Reusable Nickel Ferrite Nanoparticles in Water. *ChemCatChem* **2014,** *6* (12), 3474.

(59) Zarnaghash, N.; Panahi, F.; Khalafi-Nezhad, A. Buchwald–Hartwig amination reaction using supported palladium on phosphine-functionalized magnetic nanoparticles. *Journal of the Iranian Chemical Society* **2015,** *12* (11), 2057.

(60) Wheaton, C. A.; Bow, J.-P. J.; Stradiotto, M. New Phosphine-Functionalized NHC Ligands: Discovery of an Effective Catalyst for the Room-Temperature Amination of Aryl Chlorides with Primary and Secondary Amines. *Organometallics* **2013,** *32* (21), 6148.

(61) Prabhu, R. N.; Ramesh, R. Synthesis and structural characterization of palladium(II) thiosemicarbazone complex: application to the Buchwald–Hartwig amination reaction. *Tetrahedron Letters* **2013,** *54* (9), 1120.

(62) Cheng, K.; Zeng, M.; Qi, C. Porous chitosan microspheres supported-palladium catalyst for the C-N cross-coupling of aryl halides with secondary amines. *Journal of Chemical Research* **2013,** *37* (2), 99.

(63) Kim, M.; Shin, T.; Lee, A.; Kim, H. Synergistic Ligand Effect between N-Heterocyclic Carbene (NHC) and Bicyclic Phosphoramidite (Briphos) Ligands in Pd-Catalyzed Amination. *Organometallics* **2018,** *37* (19), 3253.

(64) Sarvestani, M.; Azadi, R. Buchwald-Hartwig amination reaction of aryl halides using heterogeneous catalyst based on Pd nanoparticles decorated on chitosan functionalized graphene oxide. *Applied Organometallic Chemistry* **2018,** *32* (1), e3906.

(65) Subramaniyan, V.; Dutta, B.; Govindaraj, A.; Mani, G. Facile synthesis of Pd(ii) and Ni(ii) pincer carbene complexes by the double C–H bond activation of a new hexahydropyrimidine-based bis(phosphine): catalysis of C–N couplings. *Dalton Transactions* **2019,** *48* (21), 7203.

(66) Fareghi-Alamdari, R.; Haqiqi, M. G.; Zekri, N. Immobilized Pd(0) nanoparticles on phosphine-functionalized graphene as a highly active catalyst for Heck, Suzuki and N-arylation reactions. *New Journal of Chemistry* **2016,** *40* (2), 1287.

(67) Nirmala, M.; Prakash, G.; Ramachandran, R.; Viswanathamurthi, P.; Malecki, J. G.; Linert, W. Nickel(II) complex incorporating methylene bridged tetradentate dicarbene ligand as an efficient catalyst toward CC and CN bond formation reactions. *Journal of Molecular Catalysis A: Chemical* **2015,** *397*, 56.

(68) Huang, P.; Wang, Y.-X.; Yu, H.-F.; Lu, J.-M. N-Heterocyclic Carbene–Palladium(II)–4,5-Dihydrooxazole Complexes: Synthesis and Catalytic Activity toward Amination of Aryl Chlorides. *Organometallics* **2014,** *33* (7), 1587.

(69) Monnier, F.; Taillefer, M. Catalytic C-C, C-N, and C-O Ullmann-Type Coupling Reactions. *Angewandte Chemie International Edition* **2009,** *48* (38), 6954.

(70) Ullmann, F. Ueber eine neue Bildungsweise von Diphenylaminderivaten. *Berichte der deutschen chemischen Gesellschaft* **1903,** *36* (2), 2382.

(71) Goldberg, I. Ueber Phenylirungen bei Gegenwart von Kupfer als Katalysator. *Berichte der deutschen chemischen Gesellschaft* **1906,** *39* (2), 1691.

(72) Wang, Y.; Ling, J.; Zhang, Y.; Zhang, A.; Yao, Q. N-(1-Oxy-2-picolyl)oxalamic Acid as an Efficient Ligand for Copper-Catalyzed Amination of Aryl Iodides at Room Temperature. *European Journal of Organic Chemistry* **2015,** *2015* (19), 4153.

(73) Lo, Q. A.; Sale, D.; Braddock, D. C.; Davies, R. P. New Insights into the Reaction Capabilities of Ionic Organic Bases in Cu-Catalyzed Amination. *European Journal of Organic Chemistry* **2019,** *2019* (9), 1944.

(74) Cano, R.; Ramón, D. J.; Yus, M. Transition-Metal-Free O-, S-, and N-Arylation of Alcohols, Thiols, Amides, Amines, and Related Heterocycles. *The Journal of Organic Chemistry* **2011,** *76* (2), 654.

(75) Jia, X.; Peng, P. N-(4-Thiazolylmethyl)Morpholine N-Oxide as N,O-Bidentate Ligand for Copper-Catalyzed Ullmann-Type N-Arylation of Azoles/Amines with Aryl Halides. *Asian Journal of Organic Chemistry* **2019,** *8* (8), 1548.

(76) Farahat, A. A.; Boykin, D. W. Copper(I) 3-methylsalicylate, an efficient catalyst for N-arylation of heterocycles under moderate reaction conditions. *Tetrahedron Letters* **2014,** *55* (19), 3049.

(77) Zhou, L.; Yin, M.; Jiang, X.; Huang, Q.; Lang, W. Synthesis and characterization of 1,3-diamino-graphene as a heterogeneous ligand for a CuI-catalyzed C–N coupling reaction. *New Journal of Chemistry* **2016,** *40* (2), 1454.

(78) Sung, S.; Braddock, D. C.; Armstrong, A.; Brennan, C.; Sale, D.; White, A. J. P.; Davies, R. P. Synthesis, Characterisation and Reactivity of Copper(I) Amide Complexes and Studies on Their Role in the Modified Ullmann Amination Reaction. *Chemistry – A European Journal* **2015,** *21* (19), 7179.

(79) Nemati, F.; Elhampour, A. Nano-magnetic Fe3O4@TiO2/Cu2O composite: a simple, effective and reusable heterogeneous catalyst for ligand-free N-arylation of amines and nitrogen heterocycles. *Research on Chemical Intermediates* **2016,** *42* (10), 7611.

(80) Deldaele, C.; Evano, G. Room-Temperature Practical Copper-Catalyzed Amination of Aryl Iodides. *ChemCatChem* **2016,** *8* (7), 1319.

(81) Hwang, J. Y.; Ji, A. Y.; Lee, S. H.; Kang, E. J. Redox-Selective Iron Catalysis for α-Amino C–H Bond Functionalization via Aerobic Oxidation. *Organic Letters* **2020,** *22* (1), 16.

(82) Munir, I.; Zahoor, A. F.; Rasool, N.; Naqvi, S. A. R.; Zia, K. M.; Ahmad, R. Synthetic applications and methodology development of Chan–Lam coupling: a review. *Molecular Diversity* **2019,** *23* (1), 215.

(83) Chan, D. M. T.; Monaco, K. L.; Wang, R.-P.; Winters, M. P. New N- and O-arylations with phenylboronic acids and cupric acetate. *Tetrahedron Letters* **1998,** *39* (19), 2933.

(84) Evans, D. A.; Katz, J. L.; West, T. R. Synthesis of diaryl ethers through the copper-promoted arylation of phenols with arylboronic acids. An expedient synthesis of thyroxine. *Tetrahedron Letters* **1998,** *39* (19), 2937.

(85) Lam, P. Y. S.; Clark, C. G.; Saubern, S.; Adams, J.; Winters, M. P.; Chan, D. M. T.; Combs, A. New aryl/heteroaryl C□N bond cross-coupling reactions via arylboronic acid/cupric acetate arylation. *Tetrahedron Letters* **1998,** *39* (19), 2941.

(86) Hardouin Duparc, V.; Bano, G. L.; Schaper, F. Chan–Evans–Lam Couplings with Copper Iminoarylsulfonate Complexes: Scope and Mechanism. *ACS Catalysis* **2018,** *8* (8), 7308.

(87) Hardouin Duparc, V.; Schaper, F. Sulfonato-imino copper(ii) complexes: fast and general Chan–Evans–Lam coupling of amines and anilines. *Dalton Transactions* **2017,** *46* (38), 12766.

(88) Zhou, Y.; Xie, Y.; Yang, L.; Xie, P.; Huang, H. Copper-Catalyzed Aerobic Oxidative Amination of Arylboronic Acid with Aminal under Base-Free Conditions. *Tetrahedron Letters* **2013,** *54* (21), 2713.

(89) Ding, X.; Huang, M.; Yi, Z.; Du, D.; Zhu, X.; Wan, Y. Room-Temperature CuI-Catalyzed Amination of Aryl Iodides and Aryl Bromides. *The Journal of Organic Chemistry* **2017,** *82* (10), 5416.

(90) Xu, L.; Zhu, D.; Wu, F.; Wang, R.; Wan, B. Mild and efficient copper-catalyzed N-arylation of alkylamines and N–H heterocycles using an oxime-phosphine oxide ligand. *Tetrahedron* **2005,** *61* (27), 6553.

(91) La, M. T.; Kang, S.; Kim, H.-K. Metal-Free Synthesis of N-Aryl-Substituted Azacycles from Cyclic Ethers Using POCl3. *The Journal of Organic Chemistry* **2019,** *84* (11), 6689.

(92) Gair, J. J.; Grey, R. L.; Giroux, S.; Brodney, M. A. Palladium Catalyzed Hydrodefluorination of Fluoro-(hetero)arenes. *Organic Letters* **2019,** *21* (7), 2482.

Supporting Spectra

1-(4-(trifluoromethyl)phenyl)pyrrolidine (1)

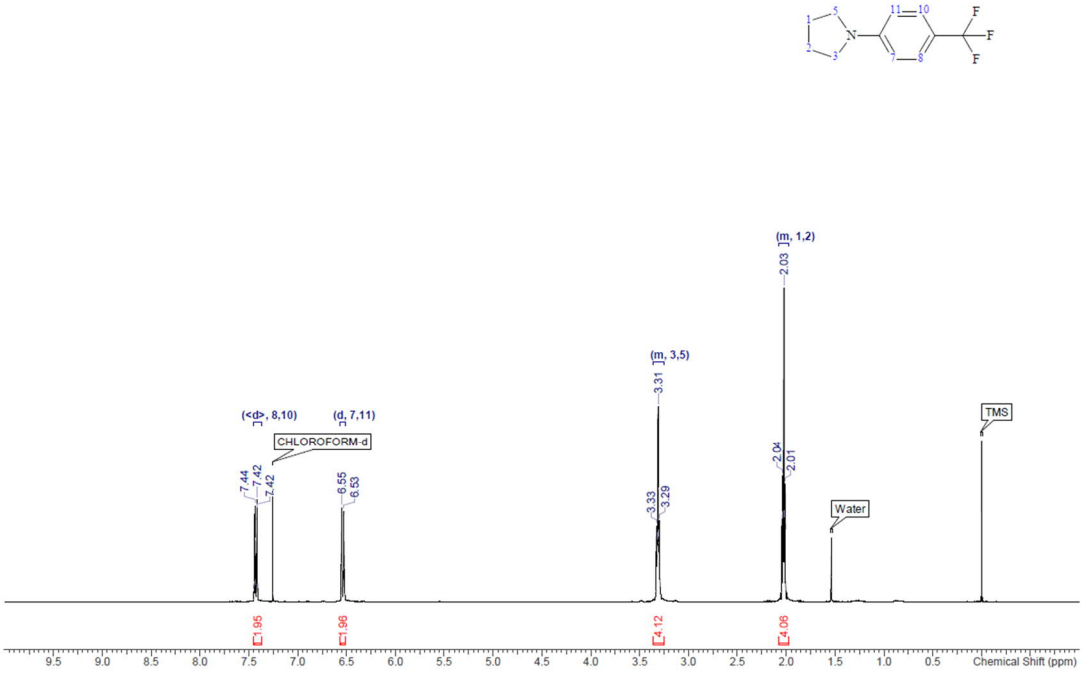

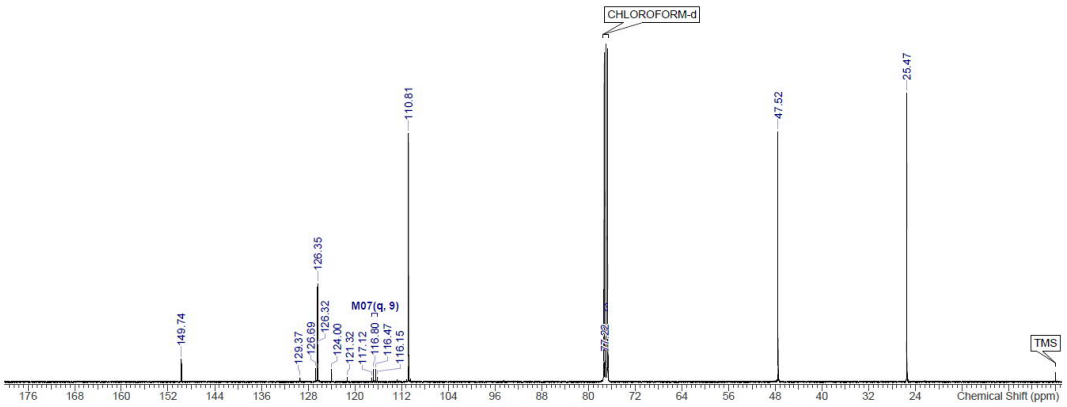

3-benzyl-1-(4-(trifluoromethyl)phenyl)pyrrolidine (2)

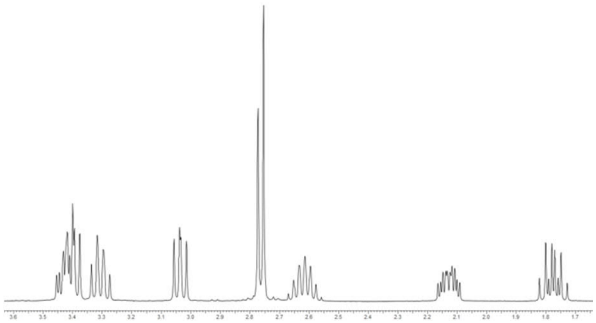

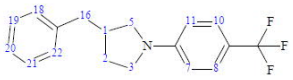

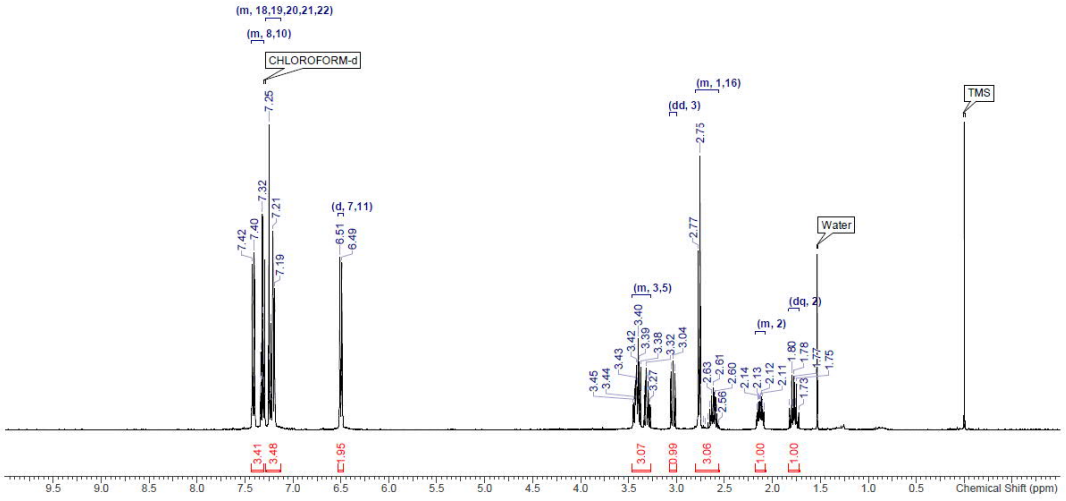

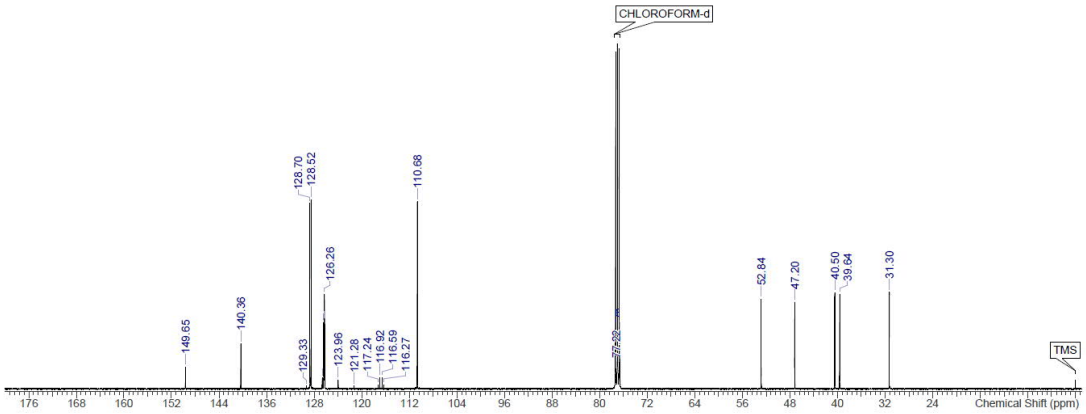

1-(4-(trifluoromethyl)phenyl)pyrrolidin-3-ol (3)

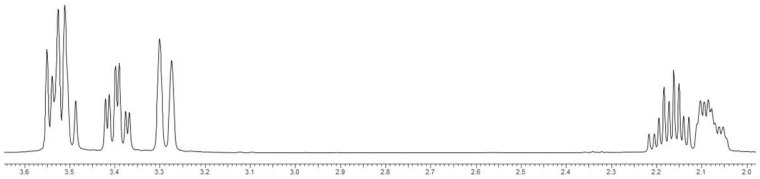

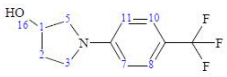

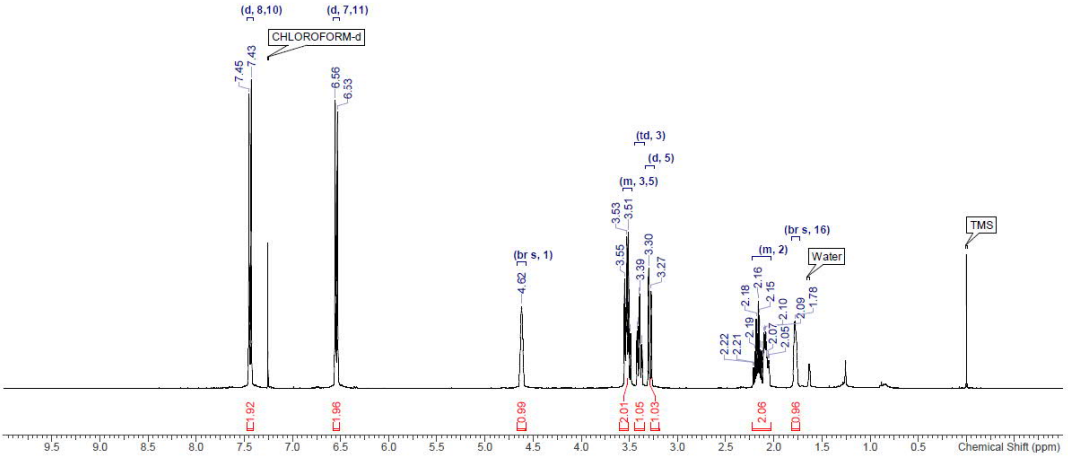

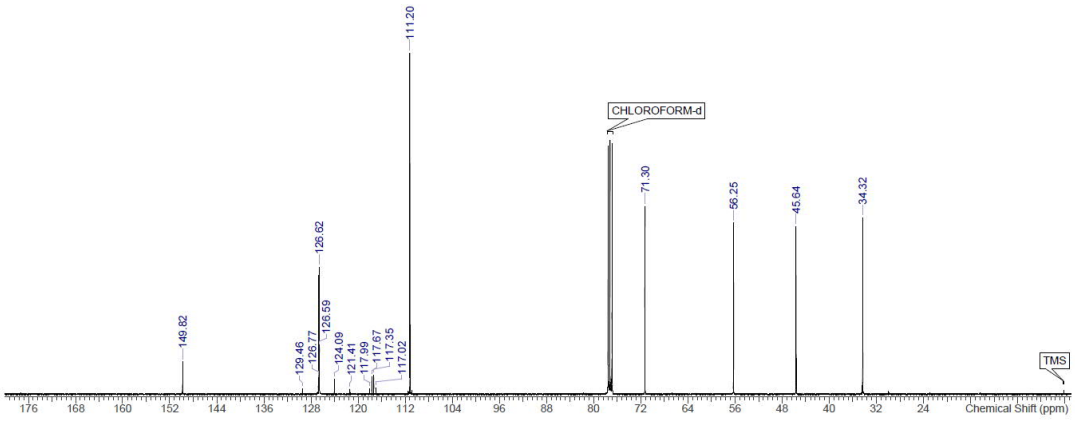

3-methyl-1-(4-(trifluoromethyl)phenyl)pyrrolidine (4)

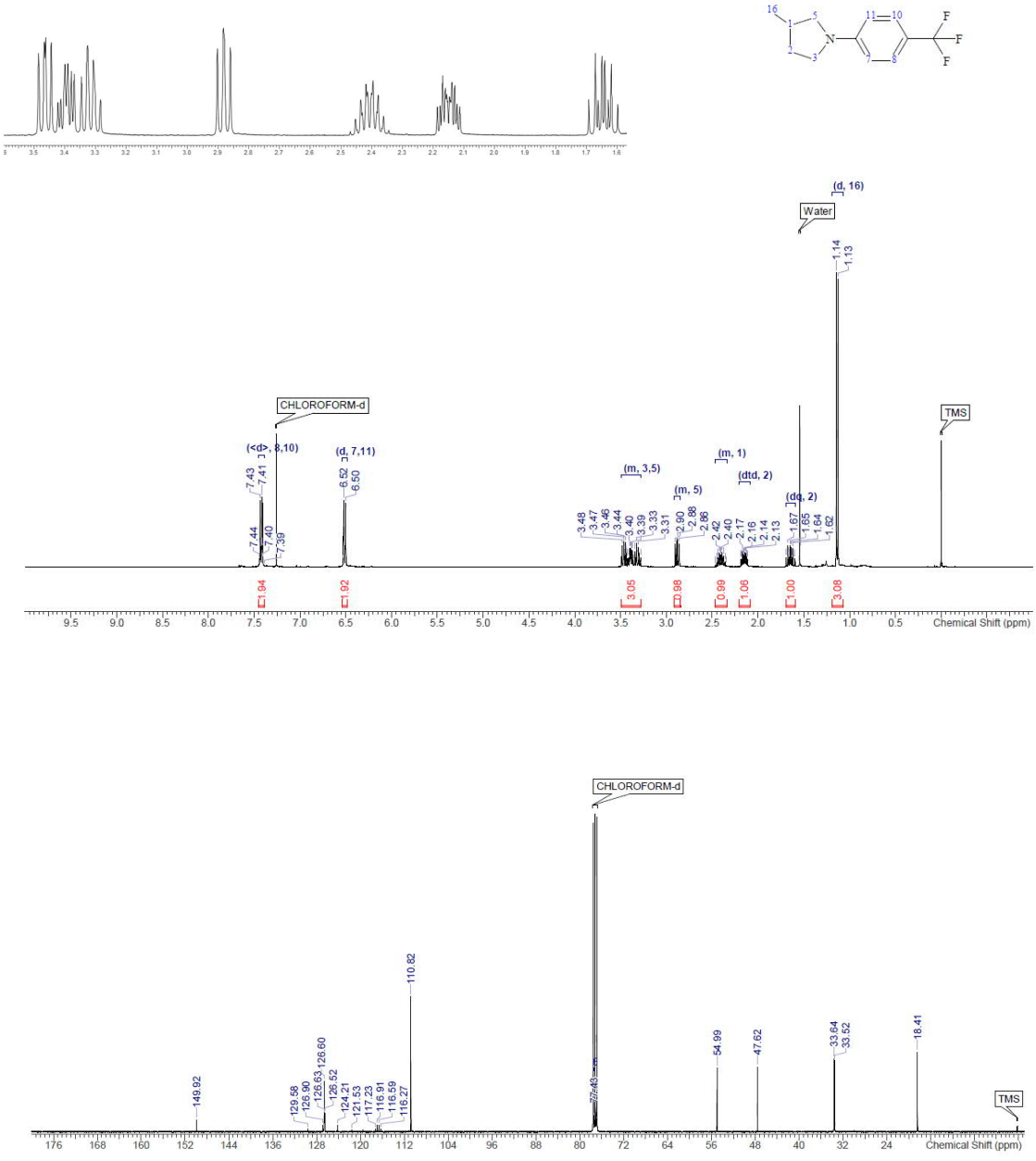

Methyl 1-(4-(trifluoromethyl)phenyl)pyrrolidine-3-carboxylate (5)

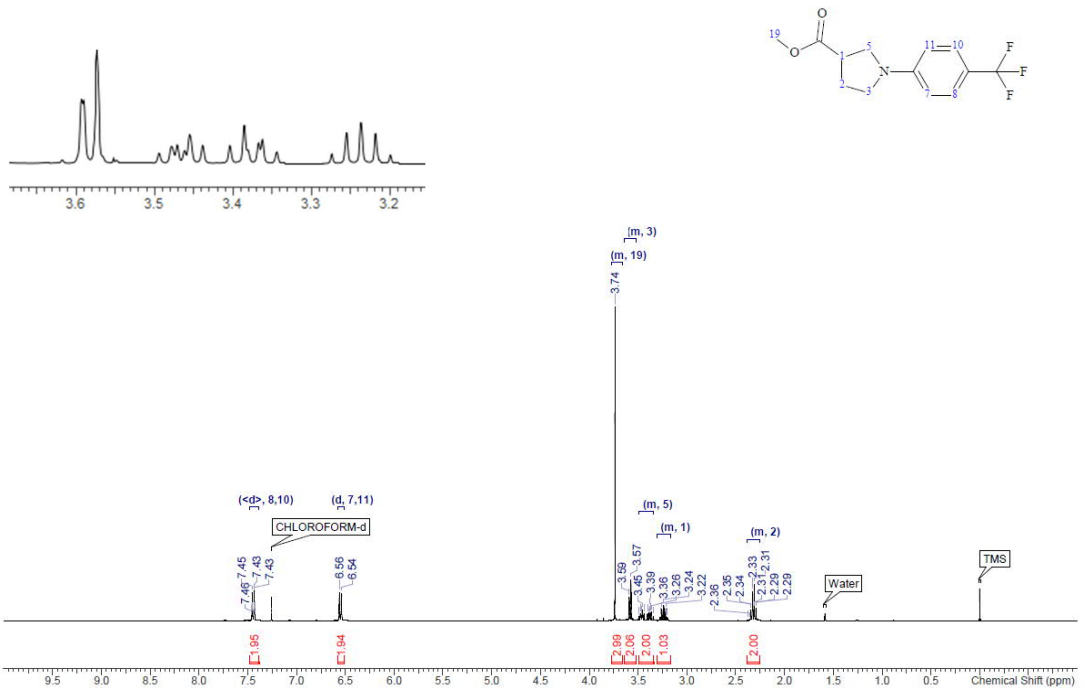

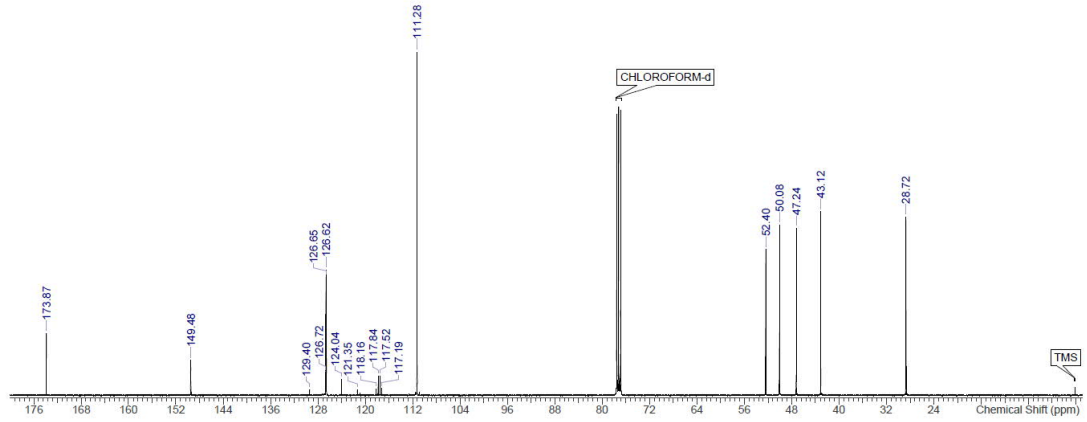

Methyl 1-(4-(trifluoromethyl)phenyl)-4,5-dihydro-1*H*-pyrrole-3-carboxylate (6)

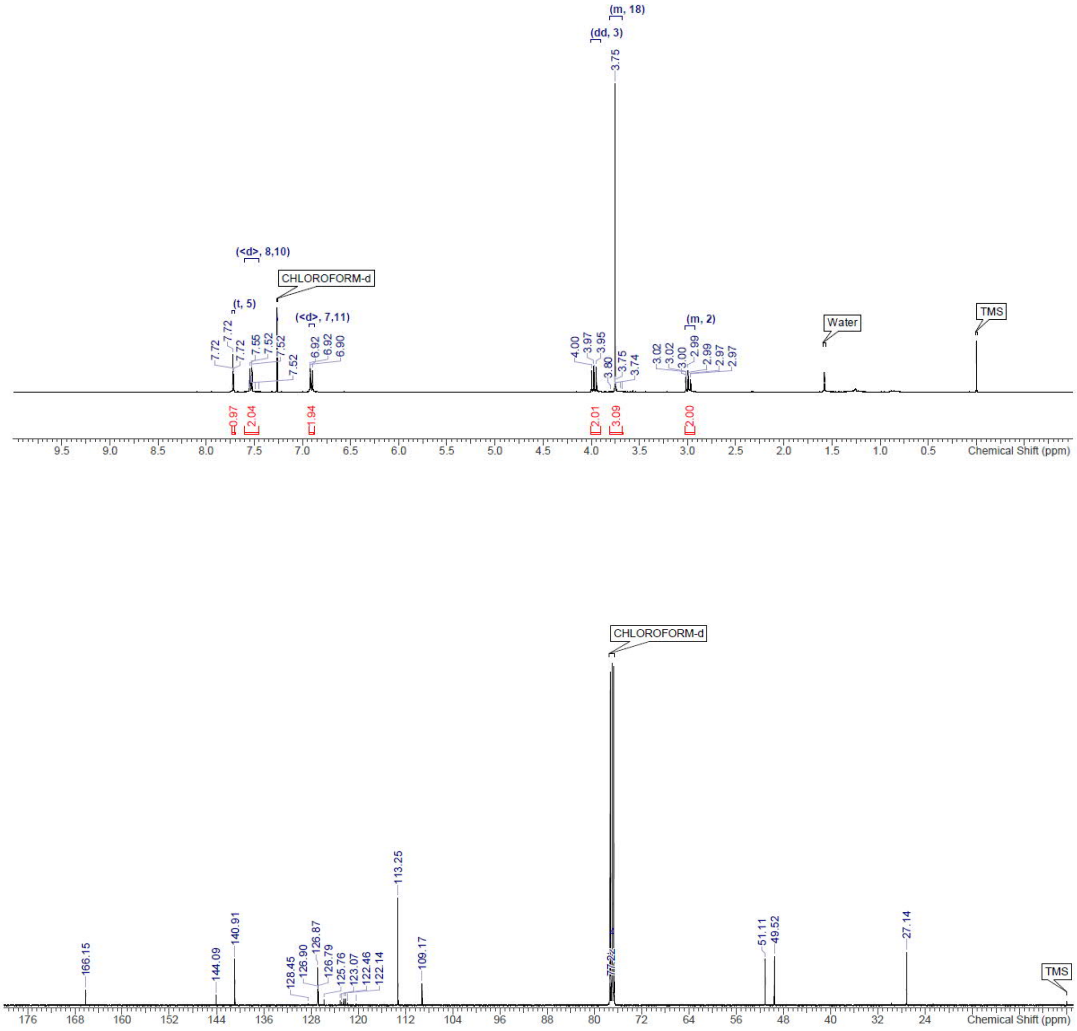

tert-Butyl (1-(4-(trifluoromethyl)phenyl)pyrrolidin-3-yl)carbamate (7)

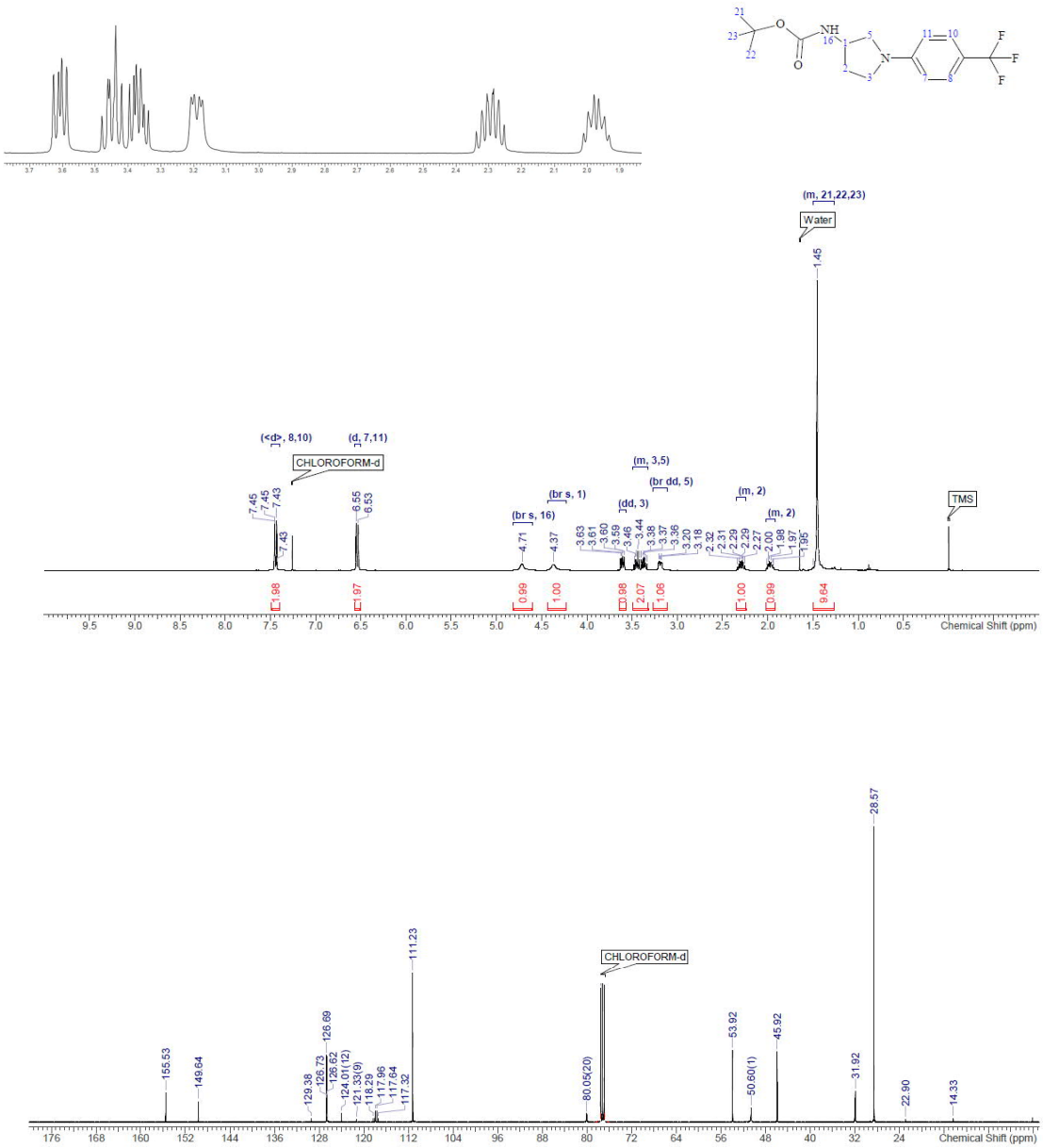

3-methyl-3-phenyl-1-(4-(trifluoromethyl)phenyl)pyrrolidine (8)

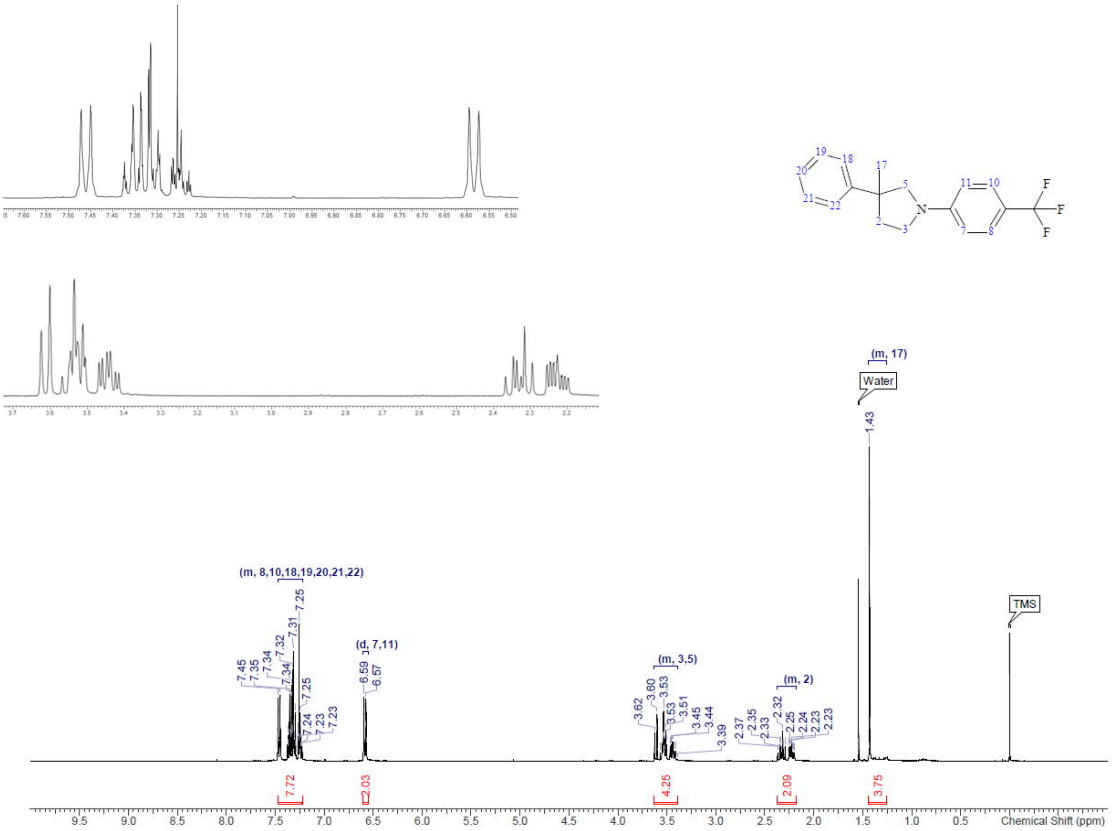

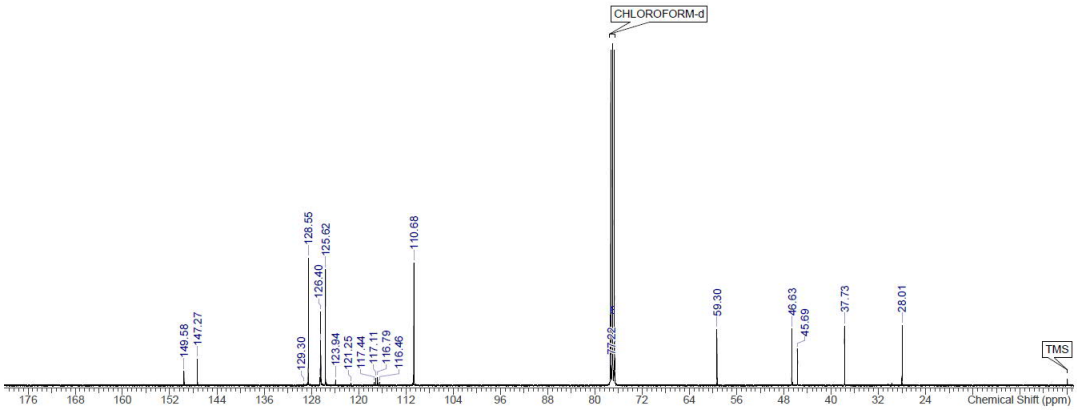

(1-(4-(trifluoromethyl)phenyl)pyrrolidin-3-yl)methanol (9)

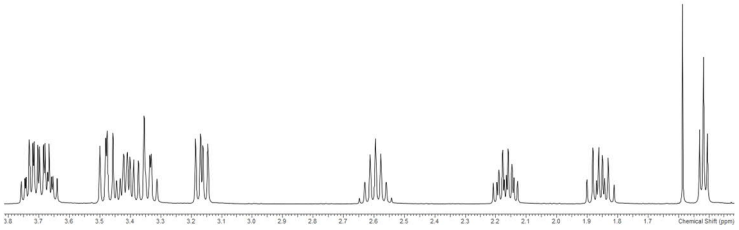

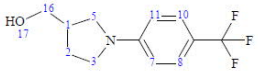

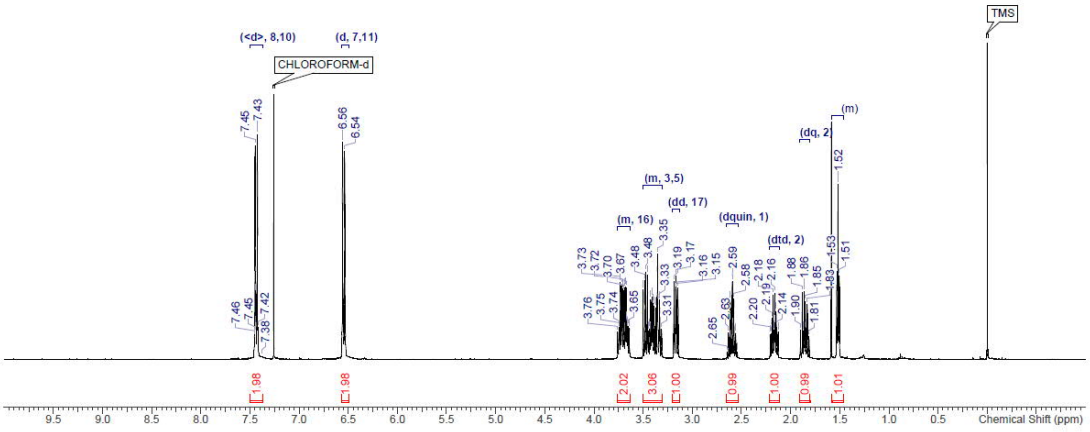

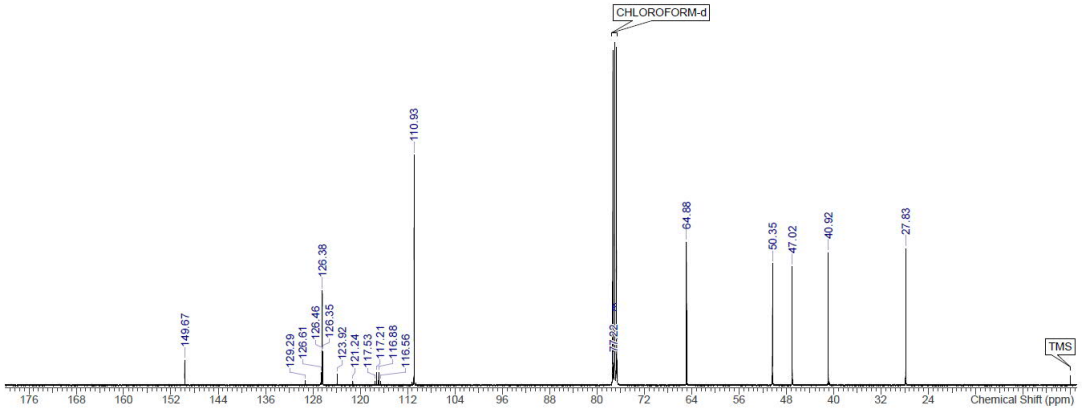

Methyl 2-(1-(4-(trifluoromethyl)phenyl)pyrrolidine-3-yl)acetate (10)

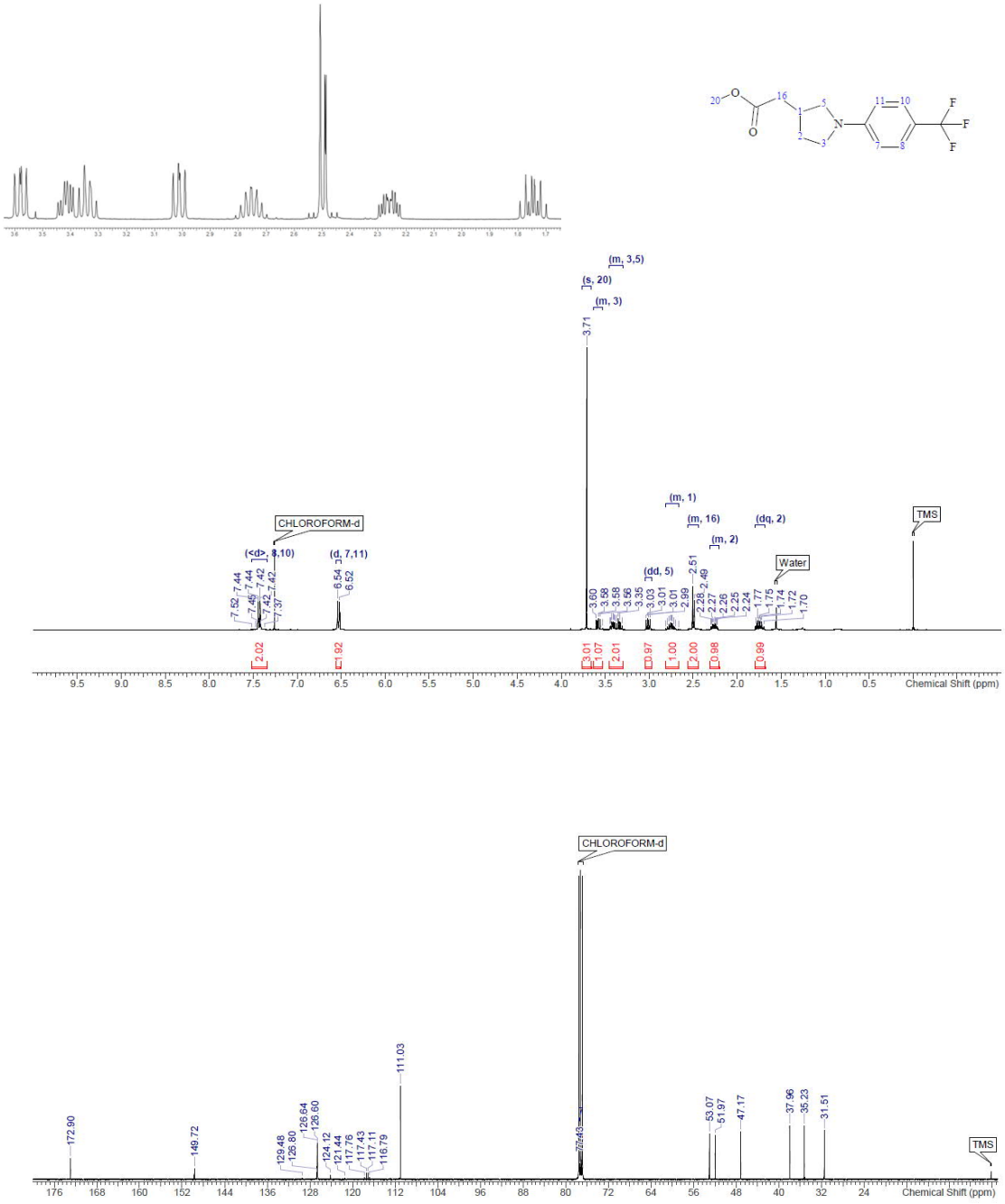

3-phenyl-1-(4-(trifluoromethyl)phenyl)pyrrolidine (11)

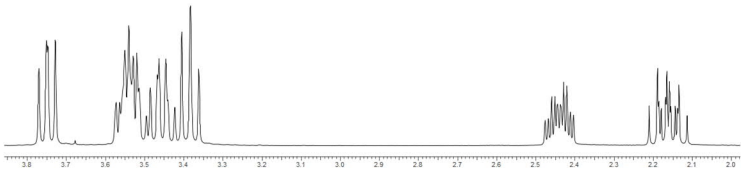

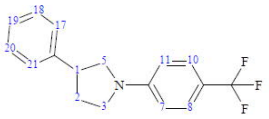

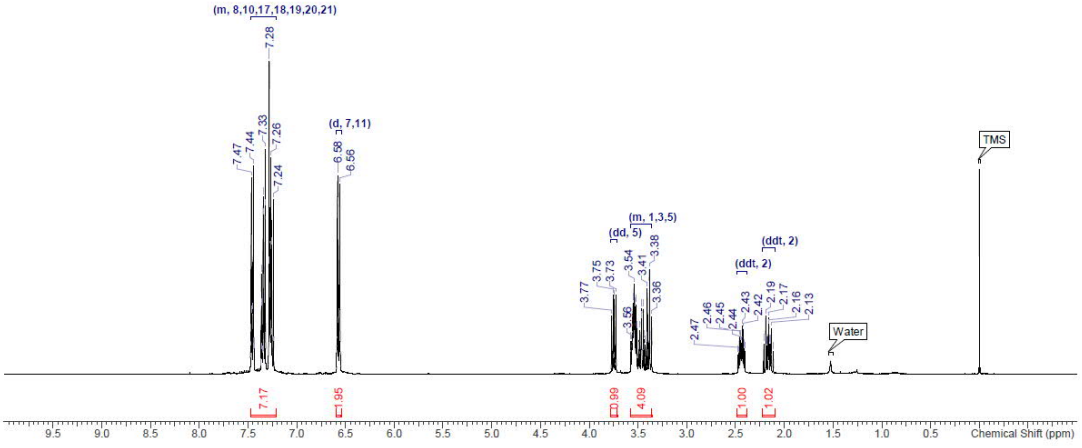

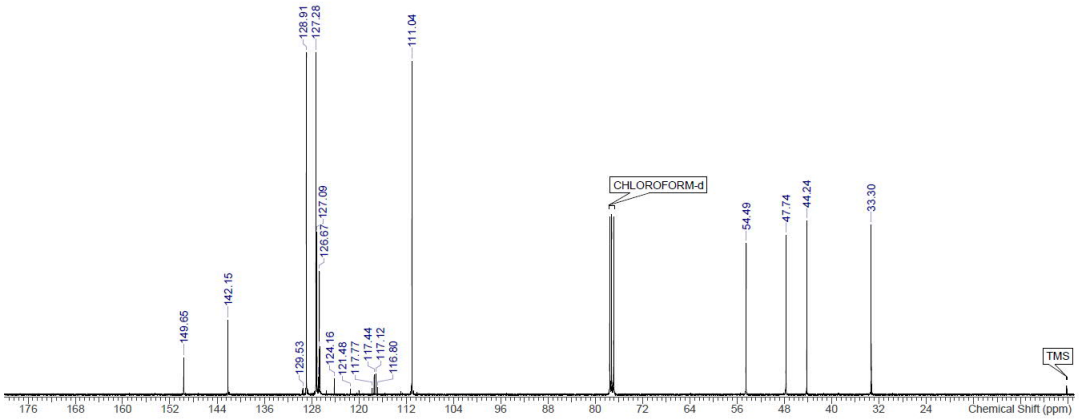

1-(4-(trifluoromethyl)phenyl)pyrrolidine-3-carbonitrile (12)

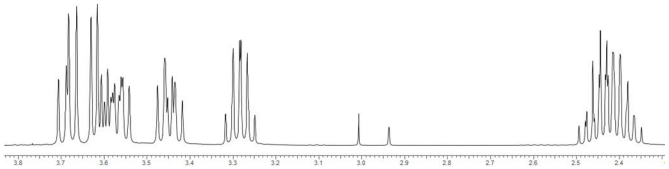

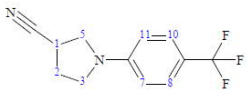

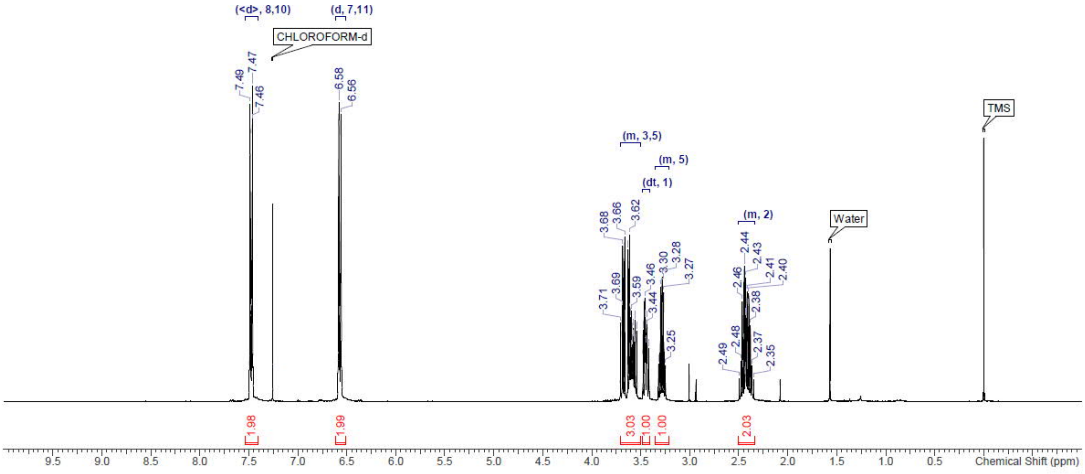

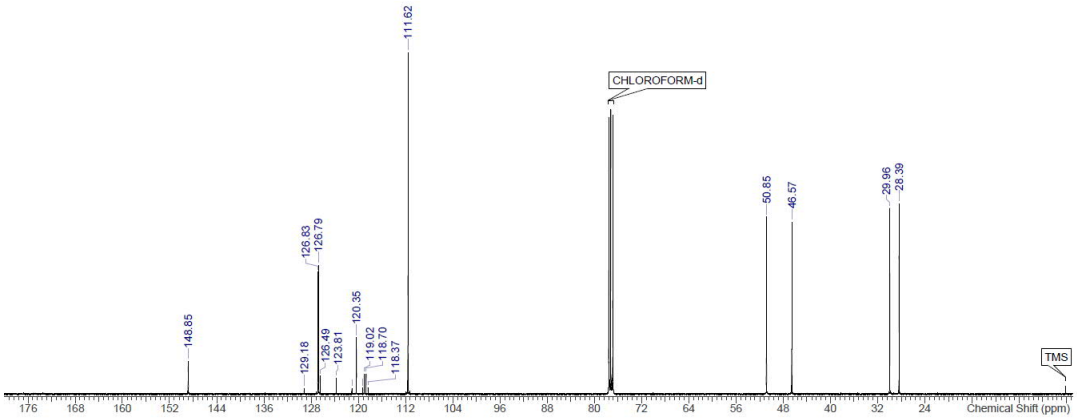

1-(4-chlorophenyl)pyrrolidine-3-carbonitrile (13)

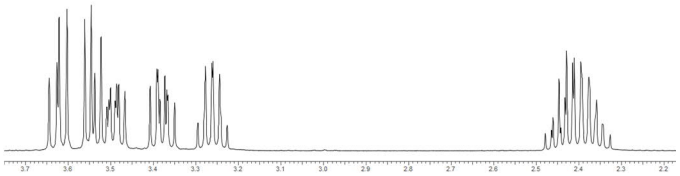

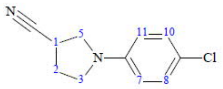

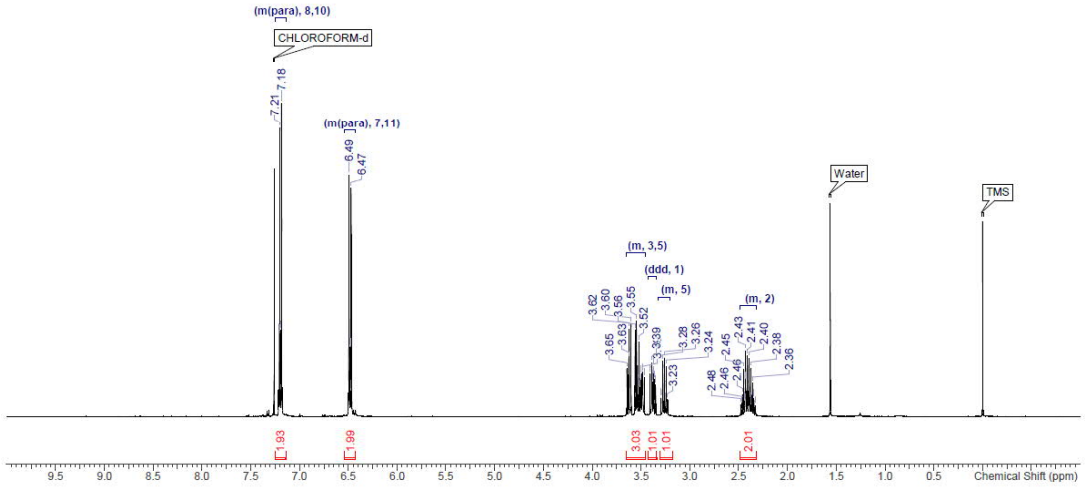

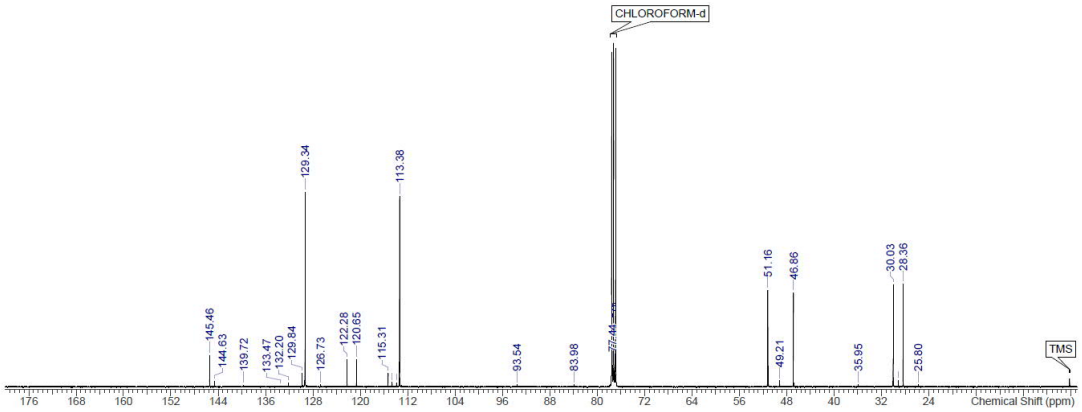

1-(4-chlorophenyl)pyrrolidine (14)

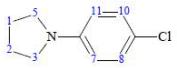

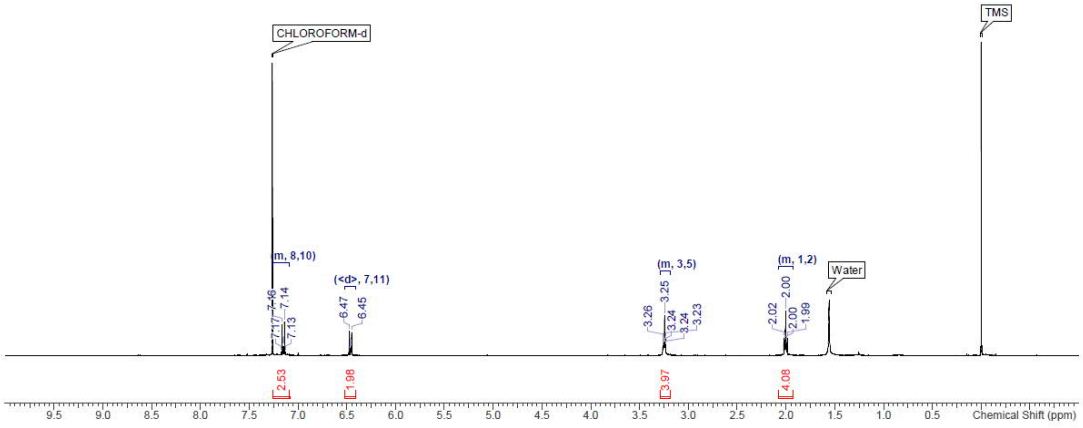

3-(pyrrolidin-1-yl)benzonitrile (15)

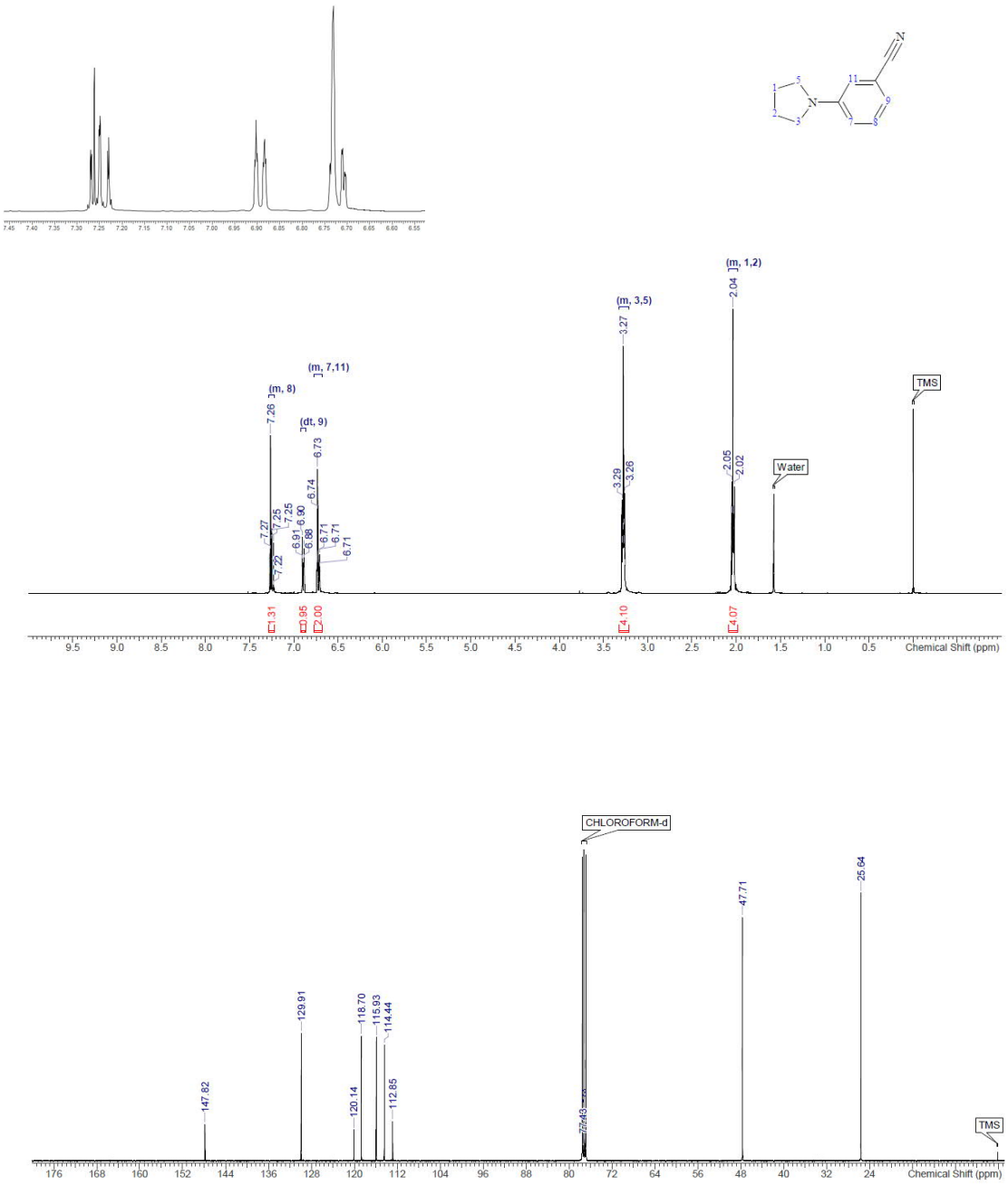

2-(pyrrolidin-1-yl)benzonitrile (16)

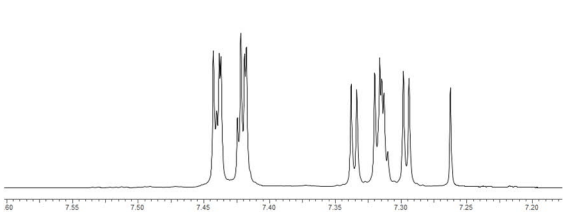

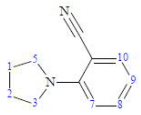

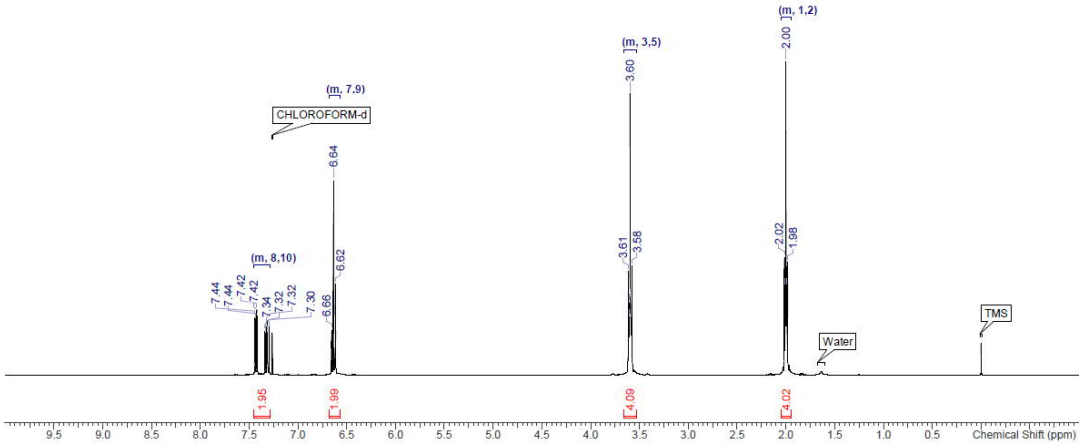

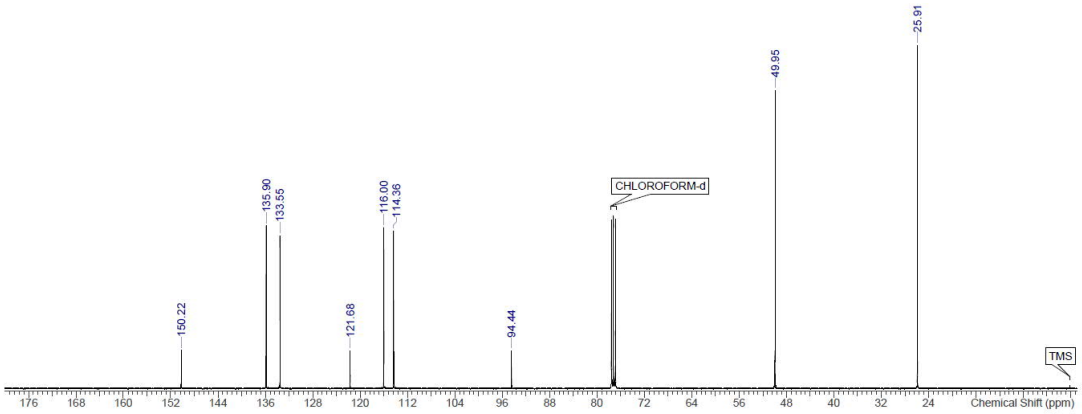

4-(pyrrolidin-1-yl)pyridine (17)

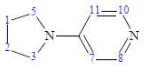

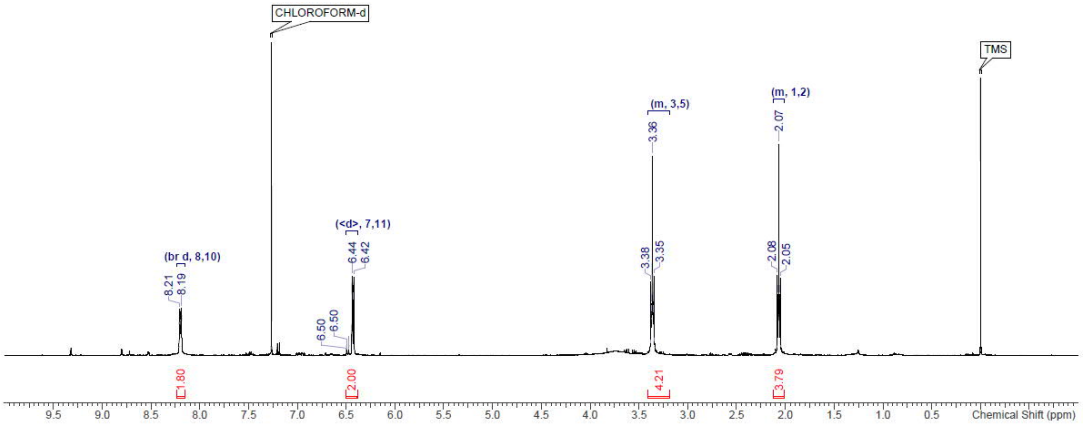

3-(pyrrolidin-1-yl)-5-(trifluoromethyl)pyridine (18)